

Universität
Rostock



Traditio et Innovatio



Universitätsmedizin
Rostock

***In vitro* Studie zur Testung von Etoposid B in
der simultanen Radiochemotherapie anhand der
humanen epithelialen Tumorzelllinien FaDu und
A549**

Kumulative Dissertation

zur

Erlangung des akademischen Grades

doctor rerum naturalium (Dr. rer. nat.)

der Mathematisch-Naturwissenschaftlichen Fakultät

der Universität Rostock

vorgelegt von

Tonja Schröder, geborene Baumgart

geb. am 23.04.1979 in Stendal

aus Rostock

Rostock, den 20.12.2015

Die vorliegende Arbeit wurde an der Klinik und Poliklinik für Strahlentherapie der Universitätsmedizin Rostock angefertigt.

Direktor: Prof. Dr. med. Guido Hildebrandt

Gutachter:

1. Gutachter:

Prof. Dr. Guido Hildebrandt
Klinik und Poliklinik für Strahlentherapie
Universitätsmedizin Rostock

2. Gutachter:

Prof. Dr. Reinhard Schröder
Institut für Biowissenschaften
Universität Rostock

Datum der Einreichung: 23. Dezember 2015

Datum der Verteidigung: 08. April 2016

Inhaltsverzeichnis

Inhaltsverzeichnis	III
Abkürzungsverzeichnis	V
Liste der Publikationen	VI
1 Einleitung.....	1
1.1 Onkologische Erkrankungen.....	1
1.1.1 Entstehung von Tumoren.....	1
1.1.2 Kennzeichen von Tumoren.....	2
1.1.3 Zellzykluskontrollpunkte und Zelltod-Signalwege	3
1.2 Therapie von Tumorerkrankungen.....	4
1.2.1 Therapieoptionen	4
1.2.2 Simultane Radiochemotherapie	4
1.3 Mikrotubuli-interagierende Substanzen.....	6
1.3.1 Die Mikrotubuli-Filamente.....	6
1.3.2 Die Taxane.....	6
1.3.3 Die Etoposide	7
2 Zielstellung	10
3 Publikationen	12
3.1 Publikation 1: Radiosensitizing effect of etoposide B on human epithelial cancer cells	12
3.2 Publikation 2: Effect of etoposide B on cell cycle, metabolic activity, and apoptosis induction on human epithelial cancer cells - under special attention of combined treatment with ionizing radiation	21
3.3 Publikation 3: Investigation of etoposide B-induced cell death mechanisms in human epithelial cancer cells - in consideration of combined treatment with ionizing radiation	33
4 Diskussion	49
4.1 Zytotoxischer Effekt von Etoposid B.....	49
4.1.1 Hemmung der Zellproliferation.....	49
4.1.2 Beeinflussung der metabolischen Aktivität.....	50
4.1.3 Mikrotubuli-stabilisierende Wirkung	50
4.2 Einfluss von Etoposid B auf die Strahlenempfindlichkeit der Tumorzellen ..	51
4.2.1 Strahlensensibilisierender Effekt.....	51
4.2.2 Zellzyklusveränderung.....	53
4.2.3 Reduktion der DNA-Reparaturkapazität	54
4.3 Zelltod durch Apoptose.....	55
4.3.1 Expression von proapoptotischen Proteinen.....	55
4.3.2 Weitere apoptotische Anzeichen	58
4.4 Zelltod durch mitotische Katastrophe	59
4.4.1 Bildung von polyploiden Zellen	59
4.4.2 Einleitung eines Zellzyklusarrestes	59
4.4.3 Expression von G2-Checkpointproteinen.....	60

5	Abschließende Betrachtung	62
6	Zusammenfassung	64
	Literaturverzeichnis	i
	Publikationen und Kongressbeiträge.....	viii
	Danksagung	x

Abkürzungsverzeichnis

7AAD	7-Aminoactinomycin D - Farbstoff
Bax	Bcl2-associated X Protein
Bcl2	B-cell lymphoma 2 - Protein
BRCA1	Breast Cancer 1 - Gen
BRB80	Brinkley reassembly Buffer 80
EZ4U	nicht radioaktiver Zellproliferations- und Zytotoxizitätstest
et al.	und andere
FITC	Fluorescein Isothiocyanate - Farbstoff
G1/2-Phase	Gap (Lücke, Abstand)-Phase (Wachstumsphase im Zellzyklus)
GLOBOCAN	Global Burden of Cancer Study
GTP	Guanosin 5'-triphosphat
H2AFX	H2A Histone Family, Member X - Gen
H2AX	Histongruppe H2A, phosphoryliert
IC ₅₀	Konzentration einer Substanz, die für eine 50 %ige Hemmung notwendig ist
M-Phase	Mitose-Phase (im Zellzyklus)
MDR	Multidrug resistant (Multisubstanzresistent)
p53	Tumorprotein p53
P-gp	Phosphoglycoprotein
PARP	Poly-(Adenosindiphosphat)-Ribose-Polymerase
SDS	Sodium Dodecyl Sulfate (Natriumdodecylsulfat)
SDS-PAGE	SDS-Polyacrylamid-Gelelektrophorese
S-Phase	Synthese-Phase (im Zellzyklus)
TRAIL	Tumor necrosis factor-related apoptosis-inducing ligand

Liste der Publikationen

- Baumgart T, Kriesen S, Neels O, Hildebrandt G, Manda K. (2015) **Investigation of Epothilone B-Induced Cell Death Mechanisms in Human Epithelial Cancer Cells -in Consideration of Combined Treatment With Ionizing Radiation.** Cancer Invest. 33(6):213-224.
- Baumgart T, Kriesen S, Hildebrandt G, Manda K. (2012) **Effect of epothilone B on cell cycle, metabolic activity, and apoptosis induction on human epithelial cancer cells - under special attention of combined treatment with ionizing radiation.** Cancer Invest. 30(8):593-603.
- Baumgart T, Klautke G, Kriesen S, Kuznetsov SA, Weiss DG, Fietkau R, Hildebrandt G, Manda K. (2012) **Radiosensitizing effect of epothilone B on human epithelial cancer cells.** Strahlenther Onkol. 188(2):177-184.

1 Einleitung

Tumorerkrankungen sind neben Herz-Kreislauf- und Infektionskrankheiten eine der häufigsten Todesursachen und werden durch das zunehmende Altern und Wachstum der Bevölkerung in Zukunft zu einer globalen Bürde. Basierend auf den Daten des WHO (World Health Organization) GLOBOCAN Projekts wird geschätzt, dass 2012 weltweit mehr als 14,1 Millionen neuer Tumorerkrankungen und 8,2 Millionen tumorbedingte Todesfälle aufgetreten sind. Dabei war Lungenkrebs die Haupttodesursache bei Männern und nach Brustkrebs die zweithäufigste Todesursache bei Frauen weltweit [TORRE et al., 2015].

1.1 Onkologische Erkrankungen

1.1.1 Entstehung von Tumoren

Die Auslöser einer Tumorerkrankung können vielfältig sein. Hierbei wird zwischen exogenen Einflüssen, wie zum Beispiel Ernährungsgewohnheiten, Lebensstil, physikalischen Agenzien (ionisierende und nicht-ionisierende Strahlung), chemischen (natürliche und synthetische) und biologischen Substanzen (zum Beispiel Viren) sowie endogenen Faktoren, wie beispielsweise chronischen Entzündungen, Störungen des Immunsystems oder genetischer Veranlagung, unterschieden [OLIVEIRA et al. 2007].

Die Entstehung von Tumoren ist ein Mehrstufenprozess, bei dem aufgrund von genetischen Veränderungen zelluläre Signalmechanismen gestört sind. Im Gegensatz zu normalen Zellen, bei denen Wachstum und Differenzierung mittels komplexer intra- und extrazellulärer Regelkreise gesteuert werden, entziehen sich Tumorzellen diesen Kontrollen und vermehren sich auf Kosten des Gesamtorganismus [SCHULTE-HERMANN & PARZEFALL, 2010]. Durch Bonnet und Dick wurde 1997 das Konzept der Tumorstammzellen postuliert [BONNET & DICK, 1997]. Sie wiesen als erste bei einer akuten myeloiden Leukämie Tumorzellen mit Stammzeleigenschaften nach. Die Theorie besagt, dass eine kleine Subpopulation von Tumorstammzellen für die Entstehung von Tumorerkrankungen, Rezidiven und sogar für die Resistenz gegen Radio- und Chemotherapie verantwortlich

sind. Seitdem konnten bei einer Vielzahl weiterer Krebserkrankungen, wie Tumore der Kopf- und Halsregion, Tumorstammzellen isoliert werden [ALLEGRA & TRAPASSO, 2012]. Der Prozess der Tumorentstehung wird in die drei Stufen Initiation, Promotion und Progression eingeteilt. Während der Initiation erfolgt eine irreversible Mutation eines wachstumsregulierenden Genes. In der folgenden Promotionsphase kommt es zum anormalen Wachstum der initiierten Zelle durch unkontrollierte Vermehrung und weitere Mutationen häufen sich an. In der Progressionsphase erfolgt die Umwandlung der präneoplastischen Zellen in einen malignen Tumor, was durch das Auswandern von Tumorzellen in andere Organe und Bildung von Metastasen gekennzeichnet ist [DEVI, 2004].

1.1.2 Kennzeichen von Tumoren

Zellen erwerben während der schrittweisen Tumorentstehung bestimmte vorteilhafte phänotypische Eigenschaften, die als „Hallmarks of Cancer“ durch Hanahan und Weinberg postuliert wurden [HANAHAHAN & WEINBERG, 2000]. Die im Jahr 2000 veröffentlichten Kennzeichen von Tumorzellen sind demnach die Eigenversorgung mit wachstumsfördernden Signalen, die Blockierung wachstumshemmender Signalwege, die Aktivierung der replikativen Immortalität, das Entgehen des programmierten Zelltodes (Apoptose), die Induktion von Angiogenese sowie die Aktivierung der Invasion und Metastasierung. Ergänzend veröffentlichten sie 2011 weitere Eigenschaften von Tumorzellen, wie die Veränderung des Energiehaushaltes sowie der Zerstörung durch das Immunsystem zu entgehen. Grundlagen für die Tumorentstehung sind u. a. das Auftreten von inflammatorischen Prozessen, welche in der Mikroumgebung von Tumorzellen entstehen können, und die genomische Instabilität [HANAHAHAN & WEINBERG, 2011].

Aufgrund der genomischen Instabilität kommt es durch verschiedene genetische Veränderungen, wie Punktmutationen, Chromosomenverlust oder Chromosomentranslokationen, zu einer Anhäufung von Mutationen in den Onkogenen und Tumorsuppressorgenen [HANAHAHAN & WEINBERG, 2011]. Dabei beeinflusst beispielsweise das Tumorsuppressorprotein p53 eine Vielzahl von wichtigen zellulären Funktionen, wie zum Beispiel Zelltod-Kontrolle, Zellzyklusarrest, genomische Stabilität, Differenzierung, DNA-Reparatur, Seneszenz und Angiogenese [MAY & MAY, 1999]. Interessanterweise liegt bei fast 50% aller Tumoren eine Mutation dieses p53 Proteins vor [WELLER, 1998].

Durch verschiedene körpereigene Mechanismen, wie die Aktivierung von Zellzykluskontrollpunkten oder auch die Einleitung von Zelltod-Signalwegen, kann der Entstehung von Tumorzellen entgegengewirkt werden.

1.1.3 Zellzykluskontrollpunkte und Zelltod-Signalwege

Der Zellzyklus wird durch mehrere Kontrollpunkte (Checkpoints) reguliert, so dass der Proteinstatus, die Zellgröße oder die DNA auf Schäden überprüft werden können. Die Einteilung der Zellzykluskontrollpunkte erfolgt in zwei Gruppen. Dies ist einerseits der Kontrollpunkt während der Metaphase, in der die erfolgreiche Spindelbildung für die Trennung der Chromosomen kontrolliert wird. Dem gegenüber stehen die beiden Kontrollpunkte während der G1- und G2-Phase, in der DNA-Schäden erkannt und repariert werden können [Alberts et al., 2004].

An den Kontrollpunkten besteht die Möglichkeit zur Arretierung des Zellzyklus, so dass durch Reparaturmechanismen die aufgetretenen Schäden, zum Beispiel an der DNA, beseitigt werden können. Zur Beseitigung von DNA-Schäden stehen verschiedene Reparatursysteme zur Verfügung, wie z. B. die homologe Rekombination und das non-homologe end joining, die Verknüpfung nichthomologer DNA-Enden. Bei nicht reparablen Schäden erfolgt allerdings ein irreversibler Wachstumsstillstand oder die Einleitung des Zelltodes zum Beispiel durch Apoptose [PAWLIK & KEYOMARSI, 2004].

Bei der Behandlung von Tumorerkrankungen ist die Einleitung des Zelltodes ein wichtiger therapeutischer Endpunkt, wobei neben der Apoptose weitere Zelltod-Signalwege, wie zum Beispiel die Nekrose, die mitotische Katastrophe, die Autophagie und die Seneszenz bekannt sind. Neben der Apoptose ist die mitotische Katastrophe ein häufig ausgelöster Zelltod nach strahleninduzierten DNA-Schäden oder nach einer Behandlung mit Mikrotubuli-interagierenden Substanzen, besonders wenn die Zellen Defekte in den Zellzykluskontrollpunkten oder in den DNA-Reparatursystemen aufweisen [PORTUGAL et al., 2009]. Zellen, die durch eine mitotische Katastrophe zugrunde gehen, können noch für einige Mitosen überleben, in einen permanenten Wachstumsstillstand übertreten (Seneszenz) oder Sterben mittels einer verzögert ablaufenden Apoptose oder Nekrose bzw. Nekroptosis [ERIKSSON & STIGBRAND, 2010].

1.2 Therapie von Tumorerkrankungen

1.2.1 Therapieoptionen

Zur Behandlung von Tumorerkrankungen stehen verschiedene Therapiemöglichkeiten zur Verfügung; die Chirurgie, die Strahlen- oder Radiotherapie und die Chemotherapie. Für eine Vielzahl von Tumorerkrankungen wird allerdings eine multimodale Behandlung eingesetzt, also eine gezielte Kombination der einzelnen Therapieformen [DUNST et al., 1997]. Die lokal wirkenden Behandlungsmethoden, wie die Chirurgie und die Radiotherapie, können heilen, wenn das Tumorleiden noch auf seinen Ausgangsort begrenzt ist. Dagegen wird bei einer fortgeschrittenen, metastasierenden Tumorerkrankung in der Regel der Einsatz einer medikamentösen Behandlung erfolgen, da sich bei dieser Therapie die tumorschädigende Wirkung im gesamten Organismus zeigt [SAUER, 2010].

Bei der lokal wirkenden Radiotherapie wird ionisierende Strahlung, wie zum Beispiel Gamma-Strahlung, eingesetzt, wodurch Strahlenschäden an den Zellbestandteilen, wie der DNA, hervorgerufen werden. Die Schädigung der DNA führt zu einer Aktivierung von komplexen Regelkreisen durch Signalkaskaden, der sogenannten „DNA Damage Response“, und abhängig vom Ausmaß des Schadens kommt es zu einem vorübergehenden oder permanenten Zellzyklusarrest und/oder zum Zelltod [LAUBER et al., 2012]. Die strahlenbiologische Wirkung von ionisierender Strahlung mit einem niedrigen linearen Energietransfer ist in euoxischen Zellen durch den Sauerstoffeffekt zwei- bis viermal höher als in hypoxischen Zellen [PÖTTER et al., 2012].

Die Chemotherapie ist dagegen eine medikamentöse Systemtherapie, bei der der gesamte Körper beeinflusst wird. Hierbei wird zwischen Zytostatika, die die Zellproliferation hemmen ohne den Zelltod herbeizuführen und zytotoxisch wirkenden Substanzen, welche eine Wachstumsverzögerung des Tumors durch ein Absterben der Zellen hervorrufen, unterschieden [TWENTYMAN, 1980].

1.2.2 Simultane Radiochemotherapie

Durch eine Kombination von Chemo- und Bestrahlungstherapie, speziell wenn sie simultan durchgeführt werden, soll eine verbesserte lokoregionale Kontrolle des Tumors

im Bestrahlungsfeld erreicht werden, wodurch es zu einer Prognose-Verbesserung für den Patienten kommt. Die Anwendung einer simultanen Radiochemotherapie hat somit zum Ziel, im Bereich der bestrahlten Region eine lokale Wirkungsverstärkung sowie bei ausreichender Verabreichung des Chemotherapeutikums eine Verbesserung der systemischen Kontrolle, also die Mitbehandlung von eventuell vorhandenen Metastasen, zu erreichen [FIETKAU, 2012].

Damit sich eine Substanz als Medikament in der simultanen Radiochemotherapie eignet, sollte es den nach Peckham und Steel eingeführten Prinzipien entsprechen [STEEL & PECKHAM, 1979]. Demnach sind für eine effektive Medikamenten-Bestrahlungsinteraktion, adaptiert nach Bentzen und Kollegen, fünf biologische Grundsätze zu erfüllen. Dies wären die räumliche Kooperation, die Erhöhung der Zytotoxizität, die biologische Kooperation, die zeitliche Modulation und der Schutz des umliegenden normalen Gewebes [BENTZEN et al., 2007].

Die Vorteile der simultanen Radiochemotherapie gegenüber den einzeln angewandten Behandlungsformen sind somit zurückzuführen auf die strahlenbiologische Wirkungsweise der kombinierten Therapieformen [DUNST et al., 1997]. Die Interaktionen zwischen Bestrahlung und Medikamenten sollen demzufolge nicht nur eine additive Antitumorwirkung erzielen, also eine Addition der Einzeleffekte beider Therapien, sondern einen supraadditiven oder synergistischen radiosensibilisierenden Effekt. Dabei ist die strahlenbiologische Wirkung der kombinierten Behandlung größer als die Summe beider Einzeltherapien. Demgegenüber ist ebenfalls eine Verminderung der biologischen Wirkung möglich, welches als subadditiver oder radioprotektiver Effekt beschrieben wird [WILSON et al., 2006].

Bei der Behandlung von Tumorerkrankungen findet die Anwendung von Medikamenten, die bestimmte Strukturen des Zytoskeletts, die Mikrotubuli, beeinträchtigen, eine besondere Beachtung.

1.3 Mikrotubuli-interagierende Substanzen

1.3.1 Die Mikrotubuli-Filamente

Die Mikrotubuli-Filamente unterliegen durch ihre dynamische Instabilität einem ständigen Auf- und Abbau und sind an der Ausführung wichtiger Zellfunktionen beteiligt, wie zum Beispiel dem Vesikel-Transport, dem Zell-Signaling, bei der Zellbewegung und bei der Mitose [DOWNING & NOGALES, 1998].

Die Mikrotubuli-beeinflussenden Substanzen werden entsprechend ihrer Wirkungsweise in zwei Gruppen eingeteilt. Während Mikrotubuli-destabilisierende Substanzen den Aufbau von Tubulin-Filamenten aus α - und β -Untereinheiten hemmen, verhindern Mikrotubuli-Stabilisatoren den Abbau bzw. die Verkürzung von Mikrotubuli-Heterodimeren [BODE et al., 2002]. Die Anwendung von Mikrotubuli-stabilisierenden Substanzen führt somit zu einer Akkumulation von polymerisierten Mikrotubuli-Bündeln und letztendlich zu einer Störung der mitotischen Spindelfunktion, welche bei sich schnell teilenden Tumorzellen zum Zelltod führt [PEREZ, 2009]. Die bekanntesten Vertreter dieser Wirkstoffklasse sind die Taxane. Aber auch die neue Substanzklasse der Epothilone zeigt vielversprechende zytotoxische Eigenschaften.

1.3.2 Die Taxane

Die Taxane wurden bereits in den 1960er Jahren aus der pazifischen Eibe isoliert und durch Wani und Kollegen als Antitumorwirkstoff klassifiziert [WANI et al., 1971]. Später wurde durch Schiff und Mitarbeiter ihre biologische Wirkungsweise beschrieben [SCHIFF et al., 1979; SCHIFF & HORWITZ, 1980]. Die Naturstoffe werden seit mehr als 20 Jahren als Medikamente Paclitaxel (Taxol[®]) und Docetaxel (Taxotere[®]) erfolgreich für ein breites klinisches Spektrum angewendet [KINGSTON, 2009]. Durch ihre strahlensensibilisierenden Eigenschaften finden sie ebenfalls in der simultanen Radiochemotherapie Anwendung [LIEBMANN et al., 1994; TISHLER et al., 1999; AGRAWAL et al., 2003; CHOE et al., 2010]. Der klinische Einsatz der Taxane wird jedoch durch eine Vielzahl von Einschränkungen begleitet, wie die Entwicklung von Resistenzen der Tumore und die hohe Anzahl an Nebenwirkungen [DONEHOWER & ROWINSKY, 1993; PICCART, 2003]. Die Suche nach

alternativen Substanzen führte zur Entdeckung neuer Naturstoffklassen, wie den Epothilonen.

1.3.3 Die Epothilone

Die Arbeitsgruppen um Reichenbach und Höfle von der Gesellschaft für Biotechnologische Forschung in Braunschweig isolierten aus dem Myxobakterium *Sorangium cellulosum* sekundäre Metabolite, die als Epothilone bezeichnet wurden [GERTH et al., 1996]. Ihren Namen erhielten die 16-gliedrigen, makrozyklischen Polyketide durch die markanten Strukturelemente Epoxid, Thiazol und Keton. Während der Fermentation von *Sorangium cellulosum* werden die Epothilone A und B (Abb. 1), neben einer Vielzahl weiterer Epothilone, in den höchsten Konzentrationen gebildet [ALTMANN et al., 2007].

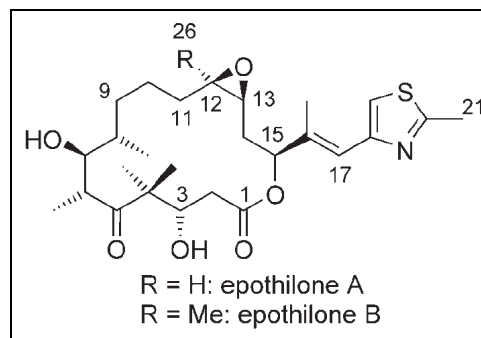


Abb. 1: Epothilone A und Epothilone B, die sich nur durch eine Methylgruppe an C12 unterscheiden [ALTMANN et al., 2007].

Vorteile der Epothilone

Obwohl die Epothilone strukturell nicht mit den Taxanen verwandt sind, weisen sie eine taxan-ähnliche Wirkungsweise auf und können sogar Taxanmoleküle von den Mikrotubuli-Bündeln verdrängen [BOLLAG et al., 1995; KOWALSKI et al., 1997]. Durch bildgebende Verfahren konnte nachgewiesen werden, dass sich beide Naturstoffe die gleiche beziehungsweise zumindest eine überlappende Nucleotid-Bindungsdomäne auf dem β -Tubulin-Filament der Mikrotubuli teilen [NETTLES et al., 2004]. Vorklinische Forschungen offenbarten, dass Epothilone gegen eine Vielzahl von verschiedenen Tumorarten, inklusive taxan- und multimedikamentenresistenten Tumorzellen, wachstumshemmend wirken

[FUMOLEAU et al., 2007]. Außerdem wurden strahlensensibilisierende Einflüsse beschrieben [KIM et al., 2003; HOFSTETTER et al., 2005].

Die antiproliferative Wirkung in taxan- bzw. multisubstanzresistenten Tumorzellen kann mit Hilfe der nicht-taxoiden Struktur der Epothilone erklärt werden. Diese Tumorzellen weisen eine Überexpression an MDR1/Phosphoglycoprotein 170 (P-gp) Efflux-Pumpen auf, durch die die Taxanmoleküle aus den Zellen transportiert werden. Die Epothilonmoleküle sind dagegen keine Substrate für diese Pumpen und verbleiben in den Tumorzellen [ALTMANN et al., 2007]. Daneben weisen die Epothilone weitere Vorteile auf. Durch die bessere Wasserlöslichkeit der Epothilone kann auf die Verwendung toxischer Lösungsvermittler, wie CremophorEL[®] verzichtet werden, welches unter anderem bei Paclitaxel für Nebenwirkungen wie schwere Überempfindlichkeitsreaktionen verantwortlich ist [WESSJOHANN, 1997]. Außerdem konnte für die Epothilone mittels *in vitro*-Versuchen eine 5- bis 26-fache höhere Mikrotubuli-stabilisierende Wirkung als die der Taxane bestimmt werden, wobei dem in dieser Arbeit untersuchten Epothilon B die größte Polymerisationsfähigkeit zugesprochen wird [FLÖRSHEIMER & ALTMANN, 2001]. Desweiteren ist die Gewinnung der Epothilone mittels Fermentation und durch synthetische Herstellung möglich und neben den natürlich vorkommenden Epothilonen konnten eine Vielzahl von semi- und vollsynthetischen Epothilon-Analoga entwickelt werden [ALTMANN et al., 2007].

Anwendung von Epothilon B

Epothilon B (Patupilone, EPO906) wird durch den Pharmakonzern Novartis entwickelt [GALMARINI & DUMONTET, 2003] und ist neben Ixabepilon, dem Laktam-Analogen von Epothilon B, die am weitesten untersuchte Substanz dieser Naturstoffklasse [ARGYRIOU et al., 2011]. Epothilon B konnte bereits in klinischen Studien gegen verschiedene solide Tumorarten, inklusive Paclitaxel-resistente Tumore, positiv getestet werden [ROTHERMEL et al., 2003; LARKIN, 2007]. Aktuell wird Epothilon B in klinischen Studien zur Behandlung von Lungen- [EDELMAN & SHVARTSBEYN, 2012], Kolon- [MELICHAR et al., 2011] und Prostatakarzinomen [KONG et al., 2010] sowie bei Erkrankungen des Zentralnervensystems [FOGH et al., 2010; OEHLER et al., 2012], eingesetzt. Neben unseren Studien wurden weitere Untersuchungen zur kombinierten Anwendung von Epothilon B und Bestrahlung durchgeführt [HOFSTETTER et al., 2005; ROHRER BLEY et al., 2009; KONG et al., 2010; OEHLER et al., 2011].

Der kombinierte Einsatz von Bestrahlung und Chemotherapeutika bietet gegenüber den Monotherapien viele Vorteile, wie die Potenzierung der Einzeleffekte, und stellt zudem eine günstige Behandlungsoption dar, wenn die Organ- und Funktionserhaltung in sensiblen anatomischen Regionen unterstützt werden soll, wie beispielsweise bei Kopf- und Halstumoren [TISHLER et al., 1999].

2 Zielstellung

Verschiedene Epothilone befinden sich derzeit in klinischen Studien zur Vorbereitung auf die Markteinführung oder konnten bereits erfolgreich als Chemotherapeutikum, wie das Epothilon B-Derivat Ixabepilon (Ixempra[®]), zugelassen werden [FORLI, 2014]. Das in dieser Arbeit untersuchte Epothilon B wurde an Patientinnen mit fortgeschrittenem oder rezidivierenden Eierstockkrebs bis zur klinischen Phase III getestet, zeigte aber in der abschließenden Studie gegenüber der Vergleichsbehandlung keine signifikante Überlebensverlängerung, so dass eine Zulassung nicht beantragt wurde [COLOMBO et al., 2012]. Epothilon B befindet sich jedoch weiterhin in klinischen Studien für andere Tumorarten, wie beispielsweise bei Erkrankungen des ZNS, Lungen-, Kolon- oder Prostatakarzinomen.

Die in dieser Arbeit untersuchten humanen epithelialen Tumorzelllinien sind die FaDu-Zellen aus einem Plattenepithelkarzinom des Hypopharynx und die A549-Zellen aus einem Plattenepithelkarzinom der Lunge. Die simultane Radiochemotherapie mit Epothilon B gilt für diese Tumorarten als neue Therapieoption, da diese Krebserkrankungen mit mäßigen Behandlungsmöglichkeiten und geringem Therapieerfolg assoziiert sind [KRIESEN, 2013].

Das Ziel dieser Arbeit bestand darin, im Rahmen vorklinischer Studien einen Beitrag zur Etablierung des Wirkstoffes Epothilon B in der simultanen Radiochemotherapie zur Behandlung von Tumoren epithelialen Ursprungs, im besonderen von Plattenepithelkarzinomen, zu leisten.

Dabei stellten sich folgende Fragen:

- Hat der Wirkstoff Epothilon B einen zytotoxischen Effekt auf die beiden epithelialen Tumorzelllinien?
- Beeinflusst der Wirkstoff Epothilon B die Strahlenempfindlichkeit der untersuchten Tumorzellen?
- Welche Wirkungsmechanismen von Epothilon B sind verantwortlich für die Effekte auf die Tumorzellen:
 1. Welche Mechanismen sind für die strahlensensibilisierende Wirkung von Epothilon B verantwortlich?
 2. Welche Zelltod-Signalwege werden durch die Anwendung von Epothilon B allein und in Kombination mit ionisierender Strahlung eingeleitet?

Zur Untersuchung dieser Fragen wurden verschiedene zell- und molekularbiologische Methoden angewendet. Dies waren vor allem Zytotoxizitätstests, wie Wachstumsversuche und EZ4U-Proliferationsassays, Koloniebildungstests, fluoreszenzmikroskopische und durchflusszytometrische Untersuchungen, DNA-Reparaturtests, Western Blot Experimente sowie Versuche zur Tubulin-Polymerisation.

3 Publikationen

3.1 Publikation 1: Radiosensitizing effect of epothilone B on human epithelial cancer cells

T. Baumgart, G. Klautke, S.Kriesen, S.A. Kuznetsov, D.G. Weiss, R. Fietkau, G. Hildebrandt, K. Manda

Strahlenther Onkol. 2012 Feb;188(2):177-184.

Kurze Zusammenfassung:

In dieser Studie wurde die Wirkung von Epothilon B, allein und kombiniert mit ionisierender Strahlung, auf zwei epitheliale Tumorzelllinien (FaDu- und A549-Zellen) getestet. Durch verschiedene *in vitro*-Experimente konnte gezeigt werden, dass Epothilon B eine zytotoxische Wirkung auf die Tumorzellen zeigt, wobei die IC₅₀-Werte im nanomolaren Bereich lagen. Eine durch Epothilon B hervorgerufene Strahlensensibilisierung der beiden Tumorzelllinien konnte ebenfalls nachgewiesen werden, wobei der strahlensensibilisierende Effekt durch eine Epothilon B-bedingte verminderte Fähigkeit der Zellen zur DNA-Reparatur induziert werden kann. Desweiteren konnte demonstriert werden, dass Epothilon B eine um den Faktor 1,49 stärkere Fähigkeit zur Polymerisation von Mikrotubuli-Bündeln aufweist als das klinisch etablierte Chemotherapeutikum Paclitaxel.

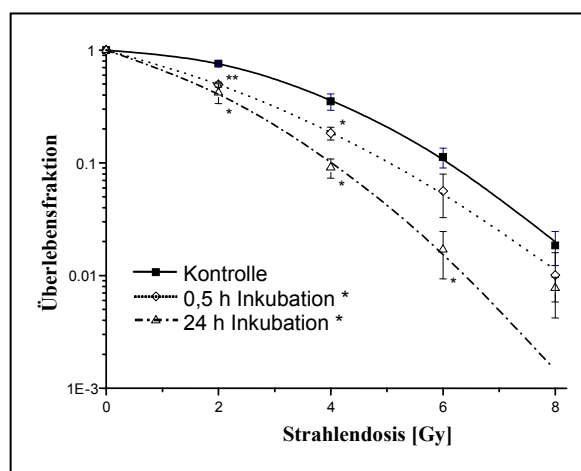


Abb. 2: Zeitabhängiger Einfluss von Epothilon B auf das klonogene Überleben der FaDu-Zellen [Baumgart et al., 2012]. * Inkubation mit Epothilon B vor der Bestrahlung

Radiosensitizing effect of epothilone B on human epithelial cancer cells

Concurrent chemoradiotherapy is a standard treatment for a majority of locally advanced tumor entities [10, 12, 38, 43]. In anticancer therapies, a great deal of attention has been focused on drugs that inhibit the mitotic spindle function, such as the clinically validated drug paclitaxel [1].

The mechanism of paclitaxel derives from its ability to promote formation and stabilization of microtubules, which leads to an accumulation of cells in the most radiosensitive phase of the cell cycle, the G2/M phase [37]. This results in an inhibition of cell proliferation and cell death via apoptosis or necrosis [48]. Paclitaxel is a validated radiosensitizer [17, 28, 44] and is used in a number of clinical sites [22, 26, 36]. However, the clinical use of taxanes has several significant limitations, including multidrug resistance [36].

Screening for alternative drug therapies has led to the discovery of the epothilones [5, 15]. They act similarly to taxanes [5, 23], but are structurally unrelated to them. Both drugs occupy the same nucleotide-binding site on β -tubulin [30]. In preclinical studies, anticancer activities and radiosensitization properties have been demonstrated against several cancer types including models that are paclitaxel-resistant [18, 19]. Several further advantages compared with taxanes have been discovered:

- the epothilones are 5–25 times more potent than paclitaxel *in vitro* and
- they are clearly more water soluble, resulting in the use of fewer toxic excipients and fewer side effects [3, 13].

Epothilone B (Patupilone, EPO906) is one of six epothilones that have been evaluated in different clinical trials for the treatment of several solid cancer types, including paclitaxel-resistant tumors [20]. Although in a now completed phase III trial epothilone B does not achieve the effectiveness of pegylated liposomal doxorubicin against refractory or relapsed ovarian cancer, it is still in clinical development for other cancers (e.g., central nervous system malignancies [6]), even in combination with radiotherapy [13, 32].

In the present study, we examined the natural product epothilone B and its effect on two human epithelial tumor cell lines, the FaDu squamous cell line and the A549 lung cancer cells. It is well known that chromosomal instability is widely spread even in squamous carcinomas [33] and in the A549 lung cancer cells [41] and a high degree of chromosomal instability is associated with paclitaxel-resistant tumors. We showed that epothilone B has high cytotoxic activity and is a potential radiosensitizer in the cancer cell lines used.

Methods and materials

Cell lines and drug preparation

Human FaDu and A549 cells were cultured in Dulbecco's modified Eagle's medium (DMEM) containing 10% fetal bovine serum and 1% penicillin/streptomycin at 37 °C and 5% CO₂. The FaDu cells were additionally incubated with 2% HEPES buffer solution, 1% sodium py-

ruvate, and 1% nonessential amino acids. Epothilone B was ordered from Sigma-Aldrich (Taufkirchen, Germany) and dissolved in dimethyl sulfoxide (DMSO, Merck KGaA, Darmstadt, Germany) to generate a 10 μ M stock solution. DMEM was used for dilution.

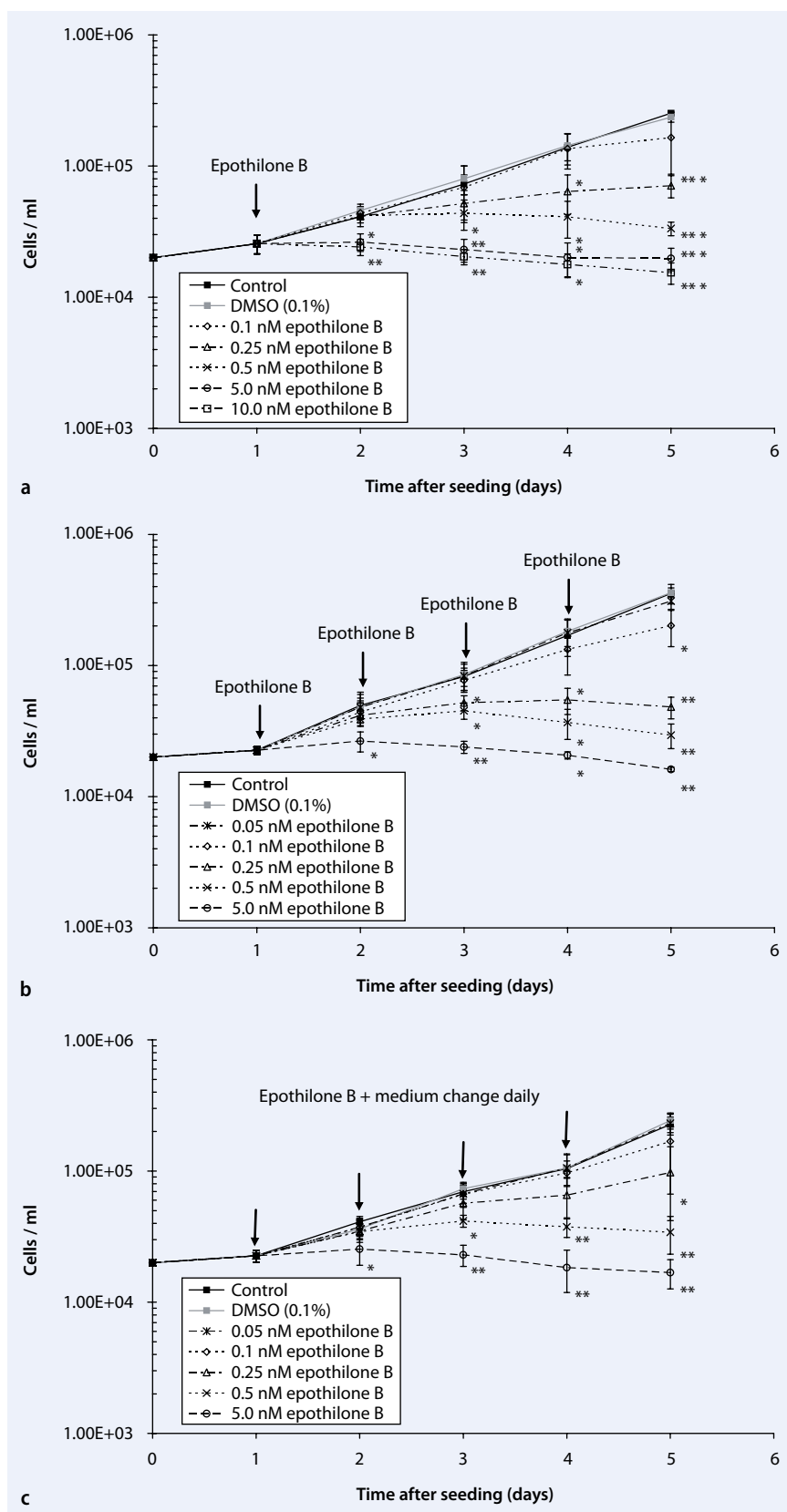
Proliferation assay

The cancer cells were seeded in 24-well plates and, after attaching for 24 h, treated with various epothilone B concentrations. The cell numbers were counted daily using a Coulter Counter (Beckman Coulter GmbH, Krefeld, Germany). Analysis of data and determination of IC₅₀ values were evaluated with Microsoft Excel software (Microsoft, Redmond, WA, USA).

Parts of the results were presented at the 15th Annual Conference of the DEGRO Bremen, Germany, 11–14 June 2009.

Tab. 1 Inhibitory effect of epothilone B on growth of cancer cells. Cells were seeded (day 0) and epothilone B was added after a 24 h cell adhesion period. IC₅₀ values were calculated after 24 h treatment of epothilone B

Cell line (cell sowing density)	IC ₅₀ values of epothilone B
FaDu (2 × 10 ³)	3.00 nM
FaDu (2 × 10 ⁴)	13.29 nM
A549 (2 × 10 ⁴)	11.77 nM



Colony-forming assay

We used exponentially growing cells pre-treated 24 and 0.5 h before irradiation with three drug concentrations (0.05 nM, 0.075 nM, and 0.1 nM). Higher epothilone B concentrations had led to a strong decrease in the plating efficiencies so that no data evaluation was possible. The cells were allowed to grow for 14 days. Colonies were stained with crystal violet and counted manually by scoring only colonies with a minimum of 50 cells. Analysis of data and determination of plating efficiencies and surviving fractions were evaluated with Microsoft Excel.

Irradiation

Irradiation was administered at room temperature utilizing a Siemens Oncor linear accelerator (Siemens, Erlangen, Germany) at 2 Gy/min (energy 6 MeV). The irradiation doses used were 2, 4, 6, and 8, and 0 Gy as a control.

γ H2AX foci assay

The DNA double-strand breaks (DSB) were detected by immunofluorescence of γ H2AX foci as described in detail previously [45]. Cells (2×10^4) were seeded on glass slides, incubated with 1.0 nM epothilone B for 24 h and irradiated. The first samples were fixed 1 h after irradiation and the last samples were incubated for 24 h to allow repair of ionizing radiation-induced DSB. Cells were labeled first with the anti-phospho-histone H2AX antibody (Millipore, Schwalbach, Germa-

Fig. 1 ◀ Inhibitory effect of increasing concentrations of epothilone B on proliferation of FaDu cells. The cells were seeded on day 0. **a** Epothilone B was added once without medium change after a 24-h cell adhesion period. **b** Epothilone B was added daily without medium change after a 24-h cell adhesion period. **c** Epothilone B was added daily with previous medium change after a 24-h cell adhesion period. Error bars indicate the standard deviation for three independent experiments; wells were assayed in triplicate in each of the different experiments. * $p < 0.05$, ** $p < 0.003$, *** $p < 0.0001$

T. Baumgart · G. Klautke · S. Kriesen · S.A. Kuznetsov · D.G. Weiss · R. Fietkau · G. Hildebrandt · K. Manda
Radiosensitizing effect of epothilone B on human epithelial cancer cells**Abstract**

Background. A combined modality treatment employing radiation and chemotherapy plays a central role in the management of solid tumors. In our study, we examined the cytotoxic and radiosensitive effect of the microtubule stabilizer epothilone B on two human epithelial tumor cell lines in vitro and its influence on the microtubule assembly.

Methods. Cancer cells were treated with epothilone B in proliferation assays and in combination with radiation in colony-forming assays. For the analysis of ionizing radiation-induced DNA damage and the influence of the drug on its repair a γ H2AX foci assay was used. To determine the effect of epothilone B on the microtubule assembly in cells and on purified tubulin, immunofluorescence staining and tu-

bulin polymerization assay, respectively, were conducted.

Results. Epothilone B induced a concentration- and application-dependent antiproliferative effect on the cells, with IC_{50} values in the low nanomolar range. Colony forming assays showed a synergistic radiosensitive effect on both cell lines which was dependent on incubation time and applied concentration of epothilone B. The γ H2AX assays demonstrated that ionizing radiation combined with the drug resulted in a concentration-dependent increase in the number of double-strand breaks and suggested a reduction in DNA repair capacity. Epothilone B produced enhanced microtubule bundling and abnormal spindle formation as revealed by immunofluo-

rescence microscopy and caused microtubule formation from purified tubulin.

Conclusion. The results of this study showed that epothilone B displays cytotoxic antitumor activity at low nanomolar concentrations and also enhances the radiation response in the tumor cells tested; this may be induced by a reduced DNA repair capacity triggered by epothilone B. It was also demonstrated that epothilone B in fact targets microtubules in a more effective manner than paclitaxel.

Keywords

Epothilone B · Irradiation · Cancer cells · DNA breaks · Microtubules

Strahlensensibilisierender Effekt von Epothilon B auf humane epitheliale Tumorzellen**Zusammenfassung**

Hintergrund. Die simultane Strahlenchemotherapie ist ein wichtiger Bestandteil in der Behandlung von soliden Tumoren. In der vorliegenden Arbeit wurden die zytotoxischen und strahlensensibilisierenden Effekte des Spindelgifts Epothilon B anhand zweier humaner Tumorzelllinien in verschiedenen In-vitro-Experimenten untersucht.

Material und Methoden. Die Tumorzellen wurden in Proliferationstests mit Epothilon B allein inkubiert und in Koloniebildungstests kombiniert mit Bestrahlung exponiert. Um die durch ionisierende Strahlung induzierten DNA-Schäden und den Einfluss des Wirkstoffs auf die DNA-Reparaturkapazität der Zellen zu analysieren, wurde der γ H2AX-Test durchgeführt. Der Effekt von Epothilon B auf die Mikrotubulstruktur der Zellen wurde mittels Immunfluoreszenz, die Wirkung auf reines Tubulin anhand des Tubulin-Polymerisations-Assays nachgewiesen.

Ergebnisse. Die Gabe von Epothilon B induzierte eine konzentrationsabhängige Hemmung des Wachstums der Zellen (Fig. 1, 2), wobei die IC_{50} -Werte im niedrigen nanomolaren Bereich lagen (Tab. 1). Anhand von Koloniebildungstests konnte ein synergistischer Effekt von Epothilon B und ionisierender Strahlung auf beide Tumorzelllinien nachgewiesen werden. Dieser war sowohl von der Inkubationszeit als auch von der verwendeten Wirkstoffkonzentration abhängig (Fig. 3, 4). Die γ H2AX-Analyse zeigte, dass die kombinierte Behandlung der Zellen mit ionisierender Strahlung und Epothilon B einen Anstieg von Doppelstrangbrüchen hervorruft (Fig. 5), was auf eine reduzierte DNA-Reparaturkapazität hindeutet. Außerdem wurde nachgewiesen, dass durch Epothilon B verstärkt Mikrotubulibündel und abnormale Spindelformationen in

den behandelten Zellen generiert werden (Fig. 6) sowie ein Mikrotubuliumaufbau aus gereinigtem Tubulin verursacht werden kann (Fig. 7).

Zusammenfassung. Die Ergebnisse zeigen, dass Epothilon B eine zytotoxische Aktivität im nanomolaren Bereich gegenüber Tumorzellen aufweist und eine Strahlensensibilisierung in den untersuchten Tumorzellen hervorruft, welche durch eine Epothilon-B-bedingte reduzierte DNA-Reparaturkapazität induziert werden kann. Zudem konnte anhand dieser Studie demonstriert werden, dass Epothilon B eine Polymerisation der Mikrotubuli hervorruft, die effektiver ist als unter Einfluss von Paclitaxel.

Schlüsselwörter

Epothilon B · Bestrahlung · Tumorzellen · DNA-Brüche · Mikrotubuli

ny). The second antibody was Alexa Fluor 495 goat anti-mouse IgG (Molecular Probes, Karlsruhe, Germany). To stain the DNA the cells were covered with DAPI/antifade (Appligene Oncor, Eschwege, Germany). The number of foci were counted using an Eclipse TE300 inverted microscope (Nikon, Tokyo, Japan) with a magnification of 1000 diameters. Fifty cells were scored per glass slide.

Immunofluorescence staining of cellular microtubules

For the experiments, 1×10^4 cells were grown on glass coverslips. After attaching for 24 h, 10 nM epothilone B was added to the cells and the samples were incubated with the drug for 24 h. The process of cell fixation and staining has been described previously [2, 21]. Cells were labeled with mouse monoclonal anti- α -tubulin anti-

body (Sigma, Taufkirchen, Germany), followed by incubation with Alexa Fluor 488 goat anti-mouse IgG (Molecular Probes, Karlsruhe, Germany). Finally, the DNA was stained with Hoechst 33258 (Sigma, Taufkirchen, Germany). Images of the cells at a magnification of 600 were acquired with a Nikon Diaphote 300 inverted microscope (Nikon GmbH, Düsseldorf, Germany).

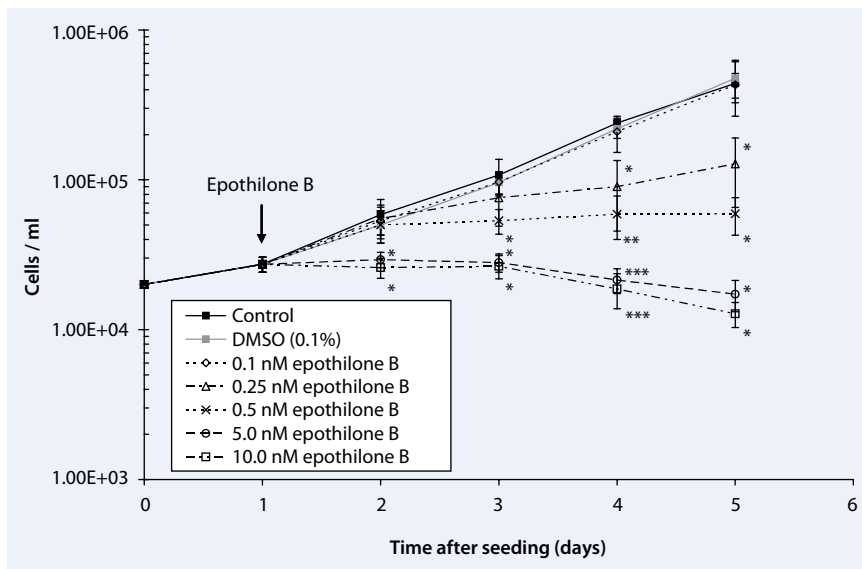


Fig. 2 ▲ Inhibitory effect of increasing concentrations of epothilone B on proliferation of A549 cells. The cells were seeded on day 0 and epothilone B was added once without medium change after a 24-h cell adhesion period. Error bars indicate the standard deviation for three independent experiments; wells were assayed in triplicate in each of the different experiments. * $p < 0.05$, ** $p < 0.003$, *** $p < 0.0001$

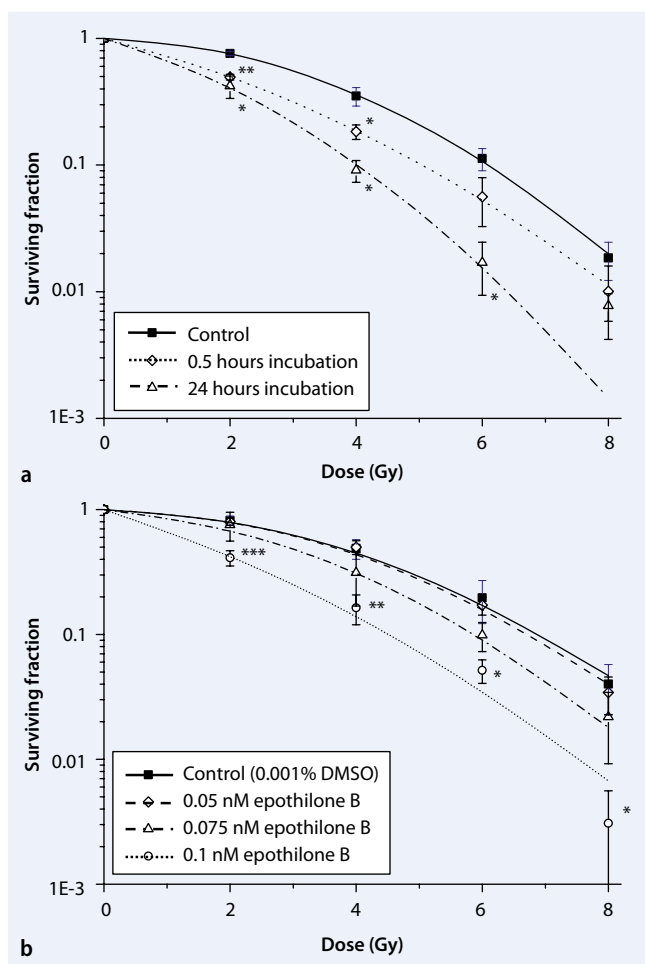


Fig. 3 ▲ **a** Time-dependent effect of 0.075 nM epothilone B on clonogenic survival of FaDu cells, when pretreated different periods before irradiation. **b** Concentration-dependent effect of epothilone B on surviving fraction of FaDu cells, addition of epothilone B 0.5 h prior to irradiation. Error bars indicate the standard deviation for three separate experiments, cell sowing density of 2000 cells/25 cm² culture flask. * $p < 0.05$, ** $p < 0.003$, *** $p < 0.0001$

Tubulin polymerization and sedimentation assay

To determine if epothilone B is able to cause tubulin polymerization, samples of purified tubulin monomers were isolated from bovine brain as described previously [24]. The tubulin was mixed with BRB80 buffer (80 mM PIPES, pH 6.8, 1 mM MgCl₂, 1 mM EGTA) at a concentration of 1 mg/ml and polymerization was initialized by adding 0.5 mM GTP. Tubulin solutions were incubated for 1 h at 37 °C with 10 μM epothilone B or with 10 μM paclitaxel (Sigma-Aldrich, Taufkirchen, Germany) as a positive control. Negative controls were treated with DMSO or only with tubulin and GTP. The microtubule assembly was analyzed by the video-enhanced contrast light microscopy (VEC-DIC microscopy) as described previously [21]. Subsequently a sedimentation assay of tubulin pellets [34] including SDS-PAGE followed and analysis of the relative amount of tubulin in the sediments was performed using the software Fujifilm Science Lab Image Gauge (Fujifilm Photo Film Co. Ltd., Tokyo, Japan).

Statistical analysis

The significance of treatments with various amounts of epothilone B for different time periods was determined with Student's t-test. A significant difference was presumed to exist when $p < 0.05$.

Results

Inhibition of cell proliferation

Growth inhibitory assays were used to estimate the IC₅₀ values (■ **Tab. 1**). Epothilone B has an antiproliferative effect at low nanomolar concentrations on both cell lines. The A549 cells are, however, slightly more sensitive than the FaDu cells.

Continuative studies showed that epothilone B affected the proliferation of FaDu cells in a concentration-dependent manner with a significant antiproliferative effect, starting at 0.25 nM epothilone B (■ **Fig. 1a**). The cytotoxic effect depended on the seeded cell number (■ **Tab. 1**). The IC₅₀ value decreased with the cell number.

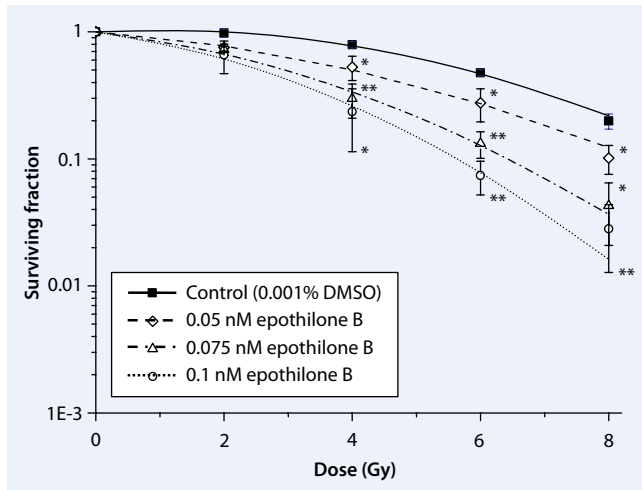


Fig. 4 ◀ Concentration-dependent effect of epothilone B on surviving fraction of A549 cells, addition of epothilone B 0.5 h prior to irradiation. Error bars indicate the standard deviation for three separate experiments, duplicate flasks in each experiment, cell sowing density of 2000 cells/25 cm² culture flask. **p* < 0.05, ***p* < 0.003

To investigate whether the epothilone B molecules are existent in the medium or accumulated in the cells, different application procedures are used. Repeated drug treatment without medium change pronounced the cytotoxic effect of epothilone B (■ Fig. 1b) with an inhibitory effect beginning at 0.1 nM epothilone B. Daily application of epothilone B with a previous medium change resulted in a lower cytotoxicity with an initiating significant inhibitory effect at a concentration of 0.25 nM (■ Fig. 1c). This is comparable with the results from the experiments with the one-time addition of epothilone B and demonstrates that the epothilone B molecules linger mainly in the medium.

The toxic effect of epothilone B on A549 cells is shown in ■ Fig. 2. The proliferation inhibition began at 0.25 nM epothilone B, which illustrates that both cell lines were equally sensitive to epothilone B.

Further experiments required different cell sowing densities so that the epothilone B concentrations had to be adapted.

Radiosensitizing effect of epothilone B

Combined treatment of epothilone B and irradiation resulted in a concentration- and time-dependent loss of the colony-forming ability. The time-dependent effect of 0.075 nM epothilone B on the radiosensitivity of FaDu cells is shown in ■ Fig. 3a. As seen in the figure, the incubation of epothilone B for 0.5 h led to

a distinct radiosensitivity of FaDu cells which was more pronounced after an incubation time of 24 h.

The effect of three different epothilone B concentrations and ionizing radiation on FaDu and A549 cells, respectively, are demonstrated in ■ Fig. 3b and ■ Fig. 4. The FaDu colony-forming assays showed a radiosensitive effect beginning at 0.075 nM epothilone B and a significant effect at 0.1 nM epothilone B. In contrast, 0.05 nM epothilone B already resulted in an enhanced radiosensitivity on A549 cells, which was more pronounced at 0.075 nM.

Thus, epothilone B is able to induce a synergistic radiosensitive effect on FaDu and A549 cells, which is more distinct by addition of the drug 24 h prior to radiation and by using higher concentrations.

Reduction of DSB repair capacity

The influence of epothilone B on the number of residual DSB for FaDu cells via the formation of γ H2AX foci is demonstrated in ■ Fig. 5a. Incubation with epothilone B alone did not result in additional γ H2AX foci, as can be seen from the equal number of counted foci present at 0 Gy. After a repair time of 1 h, the values only marginally differ between 0 nM and 1 nM epothilone B. However, after 24 h the number of γ H2AX foci was enhanced when 1 nM epothilone B was combined with radiation. The statistical analysis of the experiments showed no significance but a tendency toward a concentration-dependent increase in the

number of γ H2AX foci, thus, suggesting a reduction of DSB repair capacity. This effect can be seen in ■ Fig. 5b for A549 cells which display a sensitivity to the induction of γ H2AX foci similar to the FaDu cells. Assays with higher epothilone B concentrations showed a great number of multinucleated cells, so that no analysis was possible.

Destruction of microtubule arrays in cells

The cells without drug treatment showed characteristic cytoplasmatic microtubules (■ Fig. 6a, b). In interphase cells, the microtubules are seen radiating outwards from the microtubule organizing center, the centrosome, to the plasma membrane. In contrast, cells incubated with epothilone B displayed compact microtubule bundling and abnormal spindle formations as a tight network distributed homogeneously in the cytoplasm so that the centrosome is masked (■ Fig. 6c).

Stimulation of microtubule assembly in vitro

The study showed that epothilone B was able to promote microtubule polymerization from purified tubulin (■ Fig. 7a). As can be seen, epothilone B is several times more potent than paclitaxel at the same concentration for the induction of microtubule formation. In ■ Fig. 7a it can also be seen that DMSO is not able to cause tubulin polymerization.

In addition, a sedimentation assay including SDS-PAGE of tubulin pellets disclosed the relative amount of microtubules in the sediments. As seen in ■ Fig. 7b, epothilone B showed the highest ability to promote tubulin aggregation with a relative amount of 149 compared with paclitaxel, whose polymerization ability is set as 100 (positive control).

Discussion

Microtubules are promising targets for chemotherapeutic drugs [16] aimed at disturbing mitosis and inducing cell death in frequently dividing tumor cells. Epothilones are naturally occurring products produced by myxobacteria, which stabi-

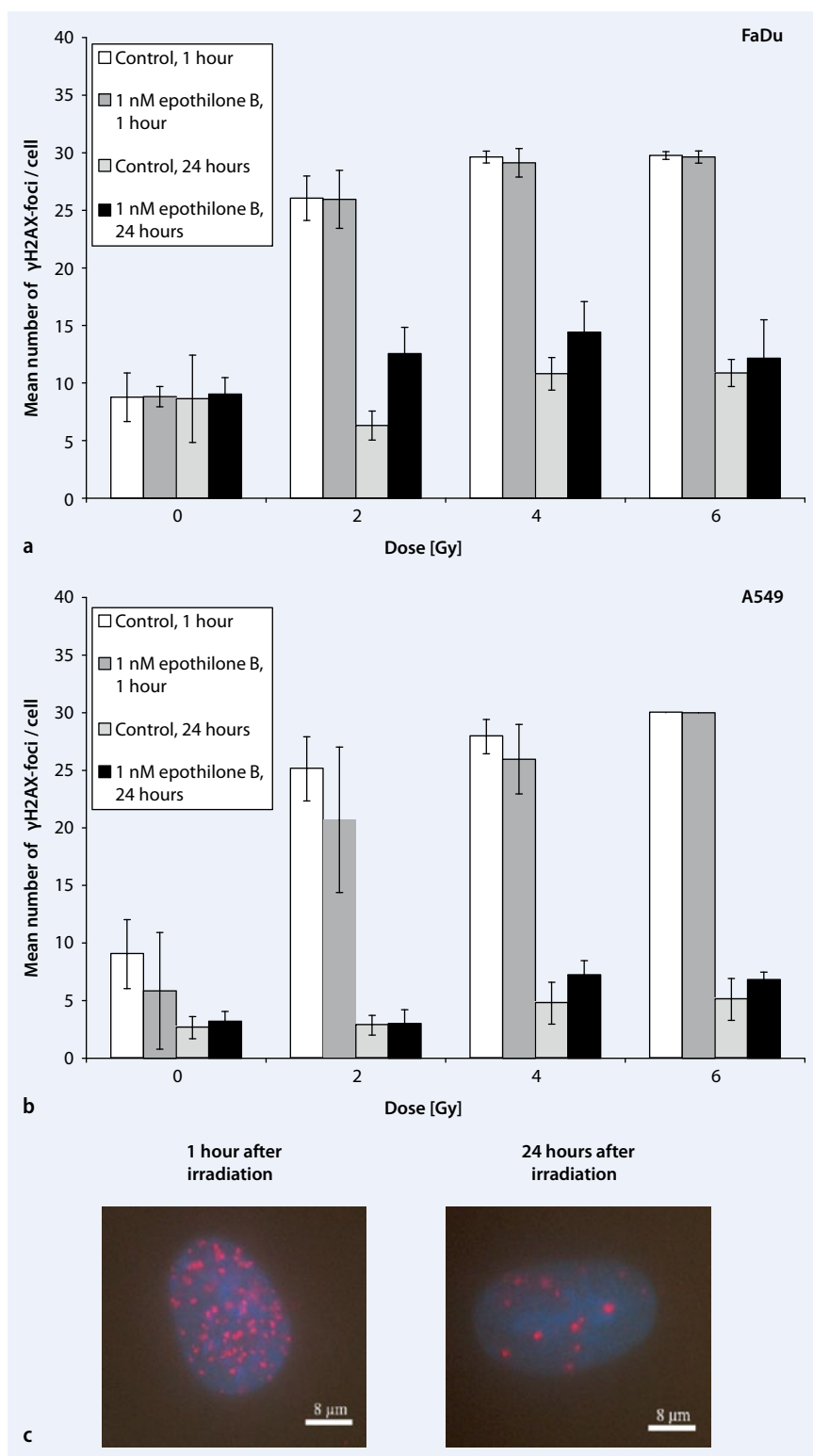


Fig. 5 ▲ Effect of epothilone B on DNA DSB repair capacity of **a** FaDu cells and **b** A549 cells after a repair time of 1 h and 24 h. Error bars indicate the standard deviation for three independent experiments. **c** Immunofluorescence microscopy of FaDu cells after irradiation with 4 Gy (red γ H2AX foci, blue cell nuclei)

lize microtubules with a paclitaxel-like mechanism of action.

In this study, we examine epothilone B alone and in combination with ionizing radiation. The tumor cells were exposed to epothilone B concentrations between 10 nM and 0.05 nM, which are used in a clinically achievable range of drug concentrations [47]. The 10 nM epothilone B treatment yields drug concentrations in the plasma equivalent to the maximum tolerable doses (MTD) [40].

We demonstrated first that epothilone B is able to induce growth inhibition in our two tested cell lines, the FaDu and the A549 cells. Consistent with previous reports [4, 14, 23], epothilone B has an antiproliferative effect at low nanomolar concentrations. We showed that the cytotoxic effect of epothilone B depends on several factors like the seeded cell number and different application approaches.

Second, it was shown that epothilone B in combination with radiation has the ability to operate as a radiosensitizer. Colony-forming assays presented a statistically significant synergistic radiosensitive effect on both cell lines, which was dependent on pre-incubation time and applied concentration of epothilone B. Therapy schedule-dependent effects are also known for many other drugs from published reports [7, 29, 31]. Our results are in contrast to the observations made by Rohrer Bley et al. [35], who discovered only an additive effect of epothilone B in the A549 cell line after an addition of epothilone B 18 h prior to irradiation. On the other hand, Hofstetter et al. [18] observed that epothilone B induced a synergistic radiosensitive influence in the human colon adenocarcinoma cell line SW480 and in p53-null MEF cells. Kim et al. [19] demonstrated this effect for the semi-synthetic epothilone B derivative Ixabepilone (BMS-247550) on the human H460 lung cancer cell line.

Third, the present study demonstrated that epothilone B had an influence on the number of residual DSB in cancer cells after irradiation. First, γ H2AX foci assays showed that ionizing radiation combined with epothilone B resulted in a concentration-dependent increase of the number of double-strand breaks which suggests a reduction in DNA repair capacity.

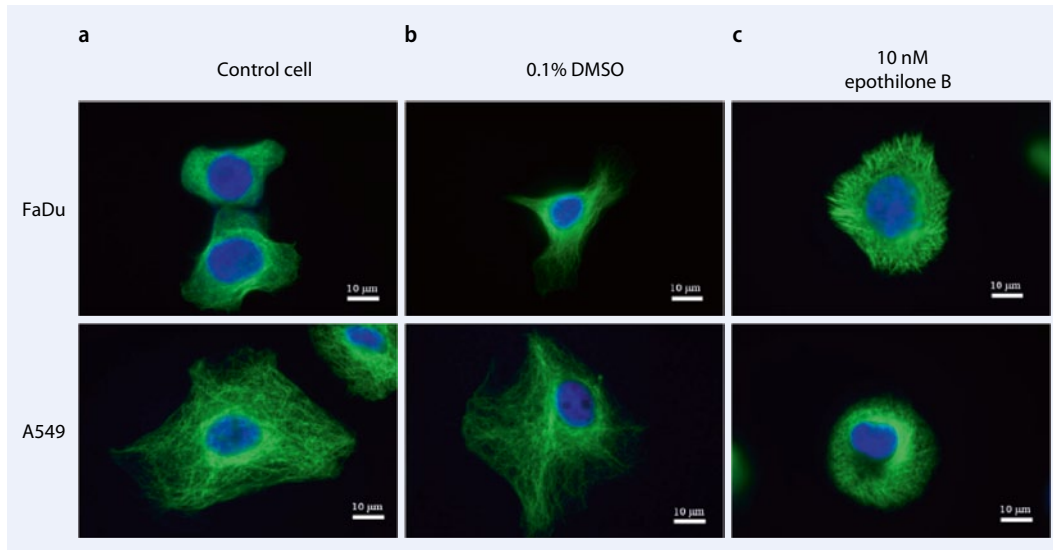


Fig. 6 ◀ Effect of epothilone B on the microtubule network (green cytoskeleton, blue cell nuclei) in FaDu and A549 cells, analyzed by immunofluorescence microscopy

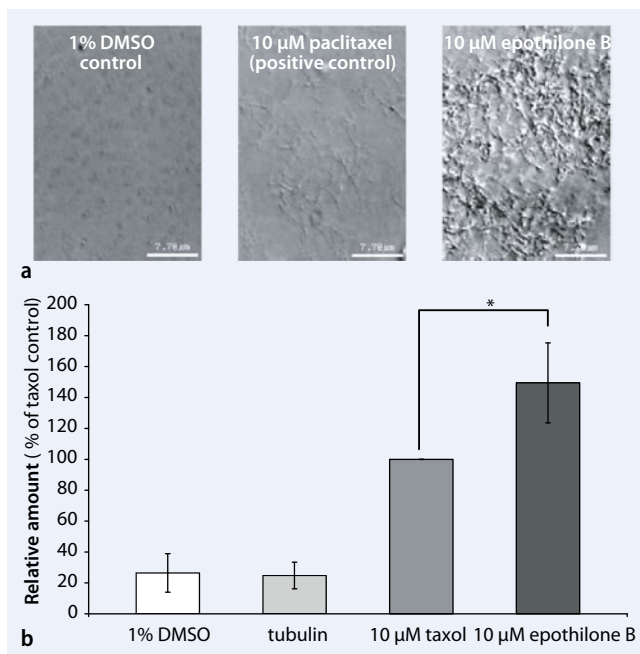


Fig. 7 ◀ Sedimentation analysis of the polymerized microtubules after incubation with the test compounds. **a** Effect on purified tubulin analyzed by VEC-DIC microscopy. **b** Evaluation of the relative amount of tubulin in the sediments. Error bars indicate the standard deviation for three independent experiments. * $p \leq 0.05$

Lichtner et al. [27] published their observation of a strong accumulation of epothilone B in the cell nucleus, more precisely in the fraction of nuclear proteins. This indicates an inhibition of proteins like the nuclear tubulin isotype [27] which, thus, results in a possible DNA-damaging effect of epothilone B [9]. Swanton et al. [41] emphasized that the effect of microtubule-stabilizing agents is based on the repression of genes which play a role in DNA repair (e.g., BRCA1, H2AFX). They also suggested that downregulation of these genes could not start efficient mismatch repair or homologous recombination. Although the rate of γ H2AX loss is cell-

type dependent, Taneja et al. [42] showed that γ H2AX foci persist longer after irradiation exposure in radiosensitive cells than in radioresistant cell lines. To underline our observations, further studies using methods like the micronucleus or the equivalent chromosome aberration technique [46] are necessary in order to analyze radiation-induced DNA damage and the influence of epothilone B on its repair.

Fourth, using immunofluorescence microscopy we showed a distinct influence of epothilone B on the microtubule assembly compared with cells cultured normally. Consistent with previous reports [8, 23, 39], we determined that ep-

othilone B produces enhanced microtubule bundling and abnormal spindle formation. Although we used lower epothilone B concentrations, our observations confirm those of Bollag et al. [5] who published that 5×10^{-9} to 1×10^{-6} M epothilone B mainly affect mitotic microtubules by building multipolar spindles.

Fifth, by studying the interaction of epothilone B with purified α - and β -tubulin, this study confirmed that epothilone B really targets microtubules. The comparison of epothilone B with paclitaxel demonstrated that epothilone B is able to induce tubulin polymerization 1.49-fold more potently than paclitaxel. Our findings supported previous observations [5, 25] that epothilone B promotes microtubule aggregation more effectively than several epothilone derivatives and paclitaxel. Kowalski et al. [23] also published that epothilone B is able to induce tubulin assembly in the absence of either GTP or microtubule-associated proteins (MAPs).

Our results demonstrate that epothilone B shows direct tumor-cytotoxic action and a high clonogenic potential. These findings, combined with the fact that epothilone B can influence the tumor microenvironment through vascular disruptive effects [11] or by blocking tumor angiogenesis [4], highlight the strong antitumor activities of the drug.

Conclusion

This study verifies the antiproliferative and radiosensitive effects of epothilone B.

The drug causes a significant increase in the radiation response in the cells; this may be mediated by a reduction of their DNA repair capacity. We also demonstrate that epothilone B targets microtubules in a more effective way than paclitaxel. This finding gives crucial evidence of the high potential of epothilone B for use in radiotherapy in the future.

Corresponding address

K. Manda

Department of Radiotherapy and Radiation Oncology, University of Rostock
Südring 75, 18059 Rostock
Germany
katrin.manda@uni-rostock.de

Conflict of interest. The corresponding author states that there are no conflicts of interest.

References

- Agrawal NR, Ganapathi R, Mekhail T (2003) Tubulin interacting agents: novel taxanes and epothilones. *Curr Oncol Rep* 5:89–98
- Al-Haddad A, Shonn MA, Redlich B et al (2001) Myosin Va bound to phagosomes binds to F-actin and delays microtubule-dependent motility. *Mol Biol Cell* 12:2742–2775
- Altmann KH, Wartmann M, O'Reilly T (2000) Epothilones and related structures – a new class of microtubule inhibitors with potent in vivo antitumor activity. *Biochim Biophys Acta* 1470:M79–91
- Bocci G, Nicolaou KC, Kerbel RS (2002) Protracted low-dose effects on human endothelial cell proliferation and survival in vitro reveal a selective antiangiogenic window for various chemotherapeutic drugs. *Cancer Res* 62:6938–6943
- Bollag DM, McQueney PA, Zhu J et al (1995) Epothilones, a new class of microtubule-stabilizing agents with a taxol-like mechanism of action. *Cancer Res* 55:2325–2333
- Bystricky B, Chau I (2011) Patupilone in cancer treatment. *Expert Opin Investig Drugs* 20:107–117
- Chalmers AJ, Ruff EM, Martindale C et al (2009) Cytotoxic effects of temozolomide and radiation are additive- and schedule-dependent. *Int J Radiat Oncol Biol Phys* 75:1511–1519
- Chen JG, Horwitz SB (2002) Differential mitotic responses to microtubule-stabilizing and -destabilizing drugs. *Cancer Res* 62:1935–1938
- Chen JG, Yang CPH, Cammer M et al (2003) Gene expression and mitotic exit induced by microtubule-stabilizing drugs. *Cancer Res* 63:7891–7899
- Vos FY de, Bos AM, Gietema JA et al (2004) Paclitaxel and carboplatin concurrent with radiotherapy for primary cervical cancer. *Anticancer Res* 24:345–348
- Ferretti S, Allegrini PR, O'Reilly T et al (2005) Patupilone induced vascular disruption in orthotopic rodent tumor models detected by magnetic resonance imaging and interstitial fluid pressure. *Clin Cancer Res* 11:7773–7784
- Fietkau R, Semrau S (2010) Stage III: definitive chemoradiotherapy. *Front Radiat Ther Oncol* 42:122–134
- Fogh S, Machtay M, Werner-Wasik M et al (2010) Phase I trial using patupilone (epothilone B) and concurrent radiotherapy for central nervous system malignancies. *Int J Radiat Oncol Biol Phys* 77:1009–1016
- Fumoleau P, Coudert B, Isambert N et al (2007) Novel tubulin-targeting agents: anticancer activity and pharmacologic profile of epothilones and related analogues. *Ann Oncol* 18(Suppl 5):v9–15
- Gerth K, Bedorf N, Höfle G et al (1996) Epothilons A and B: antifungal and cytotoxic compounds from *Sorangium cellulosum* (Myxobacteria). Production, physico-chemical and biological properties. *J Antibiot (Tokyo)* 49:560–563
- Hait WN, Rubin E, Alli E et al (2007) Tubulin targeting agents. *Update Cancer Ther* 2:1–18
- Hei TK, Piao CQ, Geard CR et al (1994) Taxol and ionizing radiation: interaction and mechanisms. *Int J Radiat Oncol Biol Phys* 29:267–271
- Hofstetter B, Voung V, Broggin-Tenzer A et al (2005) Patupilone acts as radiosensitizing agent in multidrug-resistant cancer cells in vitro and in vivo. *Clin Cancer Res* 11:1588–1596
- Kim JC, Kim JS, Saha D et al (2003) Potential radiation-sensitizing effect of semisynthetic epothilone B in human lung cancer cells. *Radiother Oncol* 68:305–313
- Kingston DG (2009) Tubulin-interactive natural products as anticancer agents. *J Nat Prod* 72:507–515
- Kiselyov AS, Semenova MN, Chernyshova NB et al (2010) Novel derivatives of 1,3,4-oxadiazoles are potent mitostatic agents featuring strong microtubule depolymerizing activity in the sea urchin embryo and cell culture assays. *Eur J Med Chem* 45:1683–1697
- Klautke G, Foitzik T, Ludwig K et al (2004) Neoadjuvant radiochemotherapy in locally advanced gastric carcinoma. *Strahlenther Onkol* 180:695–700
- Kowalski RJ, Giannakakou P, Hamel E (1997) Activities of the microtubule-stabilizing agents epothilones A and B with purified tubulin and in cells resistant to paclitaxel (Taxol). *J Biol Chem* 272:2534–2541
- Kuznetsov SA, Rodionov VI, Bershinsky AD et al (1980) High molecular weight protein MAP 2 promoting microtubule assembly in vitro is associated with microtubules in cells. *Cell Biol Int Rep* 4:1017–1024
- Lee FY, Borzilleri R, Fairchild CR et al (2001) BMS-247550: a novel epothilone analog with a mode of action similar to paclitaxel but possessing superior antitumor efficacy. *Clin Cancer Res* 7:1429–1437
- Leibl BJ, Vitz S, Schäfer W et al (2011) Adenocarcinoma of the esophagogastric junction: Neoadjuvant radiochemotherapy and radical surgery: early results and toxicity. *Strahlenther Onkol* 187:231–237
- Lichtner RB, Rotgeri A, Bunte T et al (2001) Subcellular distribution of epothilones in human tumor cells. *Proc Natl Acad Sci U S A* 98:11743–11748
- Liebmann J, Cook JA, Fisher J et al (1994) In vitro studies of taxol as a radiation sensitizer in human tumor cells. *J Natl Cancer Inst* 86(6):441–446
- Manda K, Kriesen S, Hildebrandt G et al (2011) Omega-3 fatty acid supplementation in cancer therapy: does eicosapentaenoic acid influence the radiosensitivity of tumor cells? *Strahlenther Onkol* 187:127–134
- Nettles JH, Li H, Cornett B et al (2004) The binding mode of epothilone A on alpha, beta-tubulin by electron crystallography. *Science* 305:866–869
- Niero A, Emiliani E, Monti G et al (1999) Paclitaxel and radiotherapy: sequence-dependent efficacy – a preclinical model. *Clin Cancer Res* 5:2213–2222
- Oehler C, Bueren AO von, Furmanova P et al (2011) The microtubule stabilizer patupilone (epothilone B) is a potent radiosensitizer in medulloblastoma cells. *Neuro Oncol* 13(9):1000–1010
- Pentenero M, Donadini A, Di Nallo E et al (2011) Distinctive chromosomal instability patterns in oral verrucous and squamous cell carcinomas detected by high-resolution DNA flow cytometry. *Cancer* 117:5052–5057
- Rodionov VI, Gyoeva FK, Kashina AS et al (1990) Microtubule-associated proteins and microtubule-based translocators have different binding sites on tubulin molecule. *J Biol Chem* 265:5702–5707
- Rohrer Bley C, Jochum S, Orłowski K et al (2009) Role of the microenvironment for radiosensitization by patupilone. *Clin Cancer Res* 15:1335–1342
- Rowinsky EK, Donehower RC (1995) Paclitaxel (taxol). *N Engl J Med* 332:1004–1014
- Schiff PB, Horwitz SB (1980) Taxol stabilizes microtubules in mouse fibroblast cells. *Proc Natl Acad Sci U S A* 77:1561–1565
- Semrau S, Waldfahrer F, Lell M et al (2011) Feasibility, toxicity, and efficacy of short induction chemotherapy of docetaxel plus cisplatin or carboplatin (TP) followed by concurrent chemoradiotherapy for organ preservation in advanced cancer of the hypopharynx, larynx, and base of tongue. Early results. *Strahlenther Onkol* 187:15–22
- Sepp-Lorenzino L, Balog A, Su DS et al (1999) The microtubule-stabilizing agents epothilones A and B and their desoxy-derivatives induce mitotic arrest and apoptosis in human prostate cancer cells. *Prostate Cancer Prostatic Dis* 2:41–52
- Stalder MW, Anthony CT, Woltering EA (2011) Metronomic dosing enhances the anti-angiogenic effect of epothilone B. *J Surg Res* 169:247–256
- Swanton C, Nicke B, Schuett M et al (2009) Chromosomal instability determines taxane response. *Proc Natl Acad Sci U S A* 106:8671–8676
- Taneja N, Davis M, Choy JS et al (2004) Histone H2AX phosphorylation as a predictor of radiosensitivity and target for radiotherapy. *J Biol Chem* 279:2273–2280
- Tishler RB, Busse PM, Norris CM Jr et al (1992) An initial experience using concurrent paclitaxel and radiation in the treatment of head and neck malignancies. *Cancer Res* 52:3495–3497
- Tishler RB, Geard CR, Hall EJ et al (1999) Taxol sensitizes human astrocytoma cells to radiation. *Int J Radiat Oncol Biol Phys* 43:1001–1008
- Toulany M, Kasten-Pisula U, Brammer I et al (2006) Blockage of epidermal growth factor receptor-phosphatidylinositol 3-kinase-AKT signaling increases radiosensitivity of K-RAS mutated human tumor cells in vitro by affecting DNA repair. *Clin Cancer Res* 12:4119–4126
- Wolff HA, Hennes S, Hermann MKA et al (2011) Comparison of the micronucleus and chromosome aberration techniques for the documentation of cytogenetic damage in radiochemotherapy-treated patients with rectal cancer. *Strahlenther Onkol* 187:52–58
- Woltering EA, Lewis JM, Maxwell PJ 4th et al (2003) Development of a novel in vitro human tissue-based angiogenesis assay to evaluate the effect of antiangiogenic drugs. *Ann Surg* 237:790–800
- Yeung TK, Germond C, Chen X et al (1999) The mode of action of taxol: apoptosis at low concentration and necrosis at high concentration. *Biochem Biophys Res Commun* 263:398–404

3.2 Publikation 2: Effect of epothilone B on cell cycle, metabolic activity, and apoptosis induction on human epithelial cancer cells - under special attention of combined treatment with ionizing radiation

T. Baumgart, S. Kriesen, G. Hildebrandt, K. Manda

Cancer Invest. 2012 Oct;30(8):593-603.

Kurze Zusammenfassung:

Ziel dieser Studie war es, die in der ersten Publikation nachgewiesene zytotoxische und strahlensensibilisierende Wirkungsweise von Epothilon B auf die beiden epithelialen Tumorzelllinien (FaDu- und A549-Zellen) genauer zu untersuchen. Dabei konnte mit Hilfe von durchflusszytometrischen Messungen festgestellt werden, dass durch Epothilon B eine Anhäufung der Tumorzellen in der strahlensensiblen G2/M-Phase des Zellzyklus hervorgerufen wird, womit die Epothilon B-induzierte Radiosensibilisierung erklärt werden konnte. Weitere Experimente bewiesen, dass die zytotoxische Wirkung von Epothilon B zum apoptotischen Absterben von Tumorzellen führt sowie die Bildung von multinukleären Zellen hervorruft. Desweiteren konnte eine verminderte metabolische Aktivität der Tumorzellen durch die Epothilon B-Gabe nachgewiesen werden.

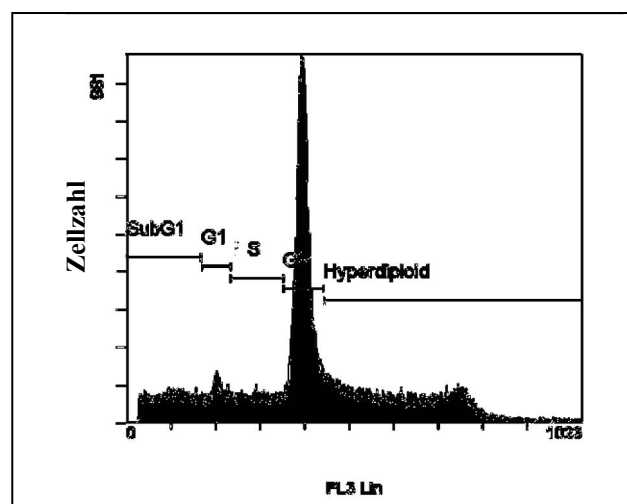


Abb. 3: Analyse eines DNA Histogramms der FaDu-Zellen nach einer 24-stündigen Inkubation mit 10 nM Epothilon B [Baumgart et al., 2012].

ORIGINAL ARTICLE

Effect of Etoposide B on Cell Cycle, Metabolic Activity, and Apoptosis Induction on Human Epithelial Cancer Cells—Under Special Attention of Combined Treatment With Ionizing Radiation

Tonja Baumgart, Stephan Kriesen, Guido Hildebrandt, and Katrin Manda

Department of Radiotherapy and Radiation Oncology, University of Rostock, Rostock, Germany

In recent studies, etoposide B was shown to have a cytotoxic and radiosensitizing effect on cells. The aim of our investigation was to explain this impact by examining the mode of action of etoposide B on FaDu and A549 tumor cells. Flow cytometry was used for cell cycle distribution and for the evaluation of apoptosis. Metabolic activity was studied by proliferation assay. Influence on nuclei morphology was investigated by DNA-staining. We showed that etoposide B-induced G2/M accumulation is the main rationale for drug-induced radiosensitivity. The cytotoxic effect resulted in apoptotic cell death, decreased metabolic activity, and formation of multinucleated cells.

Keywords Etoposide B, Irradiation, Cell cycle, Apoptosis, Multinuclear cells

INTRODUCTION

Recent studies showed that etoposide B, which is known to stabilize microtubules, has a cytotoxic and radiosensitizing effect on cancer cells (1, 2). Microtubules are built up of α - and β -tubulin monomers and they are involved in diverse cellular processes, including vesicular transport, signaling, cell movement, and mitosis (3). For this reason, tubulin polymers are promising targets for chemotherapeutic agents aimed at blocking the mitotic spindle function and inducing cell death in frequently dividing cancer cells (4). Especially in combined chemoradiotherapy for solid tumors a great deal of attention has been focused on microtubule-interfering drugs, like the clinically validated radiosensitizer paclitaxel (5–8). Paclitaxel stabilizes microtubules, which leads to an accumulation of cells in the G2/M phase, the most radiosensitive phase of the cell cycle (9), and cell death via apoptosis or necrosis (10). However, its clinical use is limited by the development of chemoresistance (11) and a high rate of toxicities (12, 13).

The etoposides, an interesting family of microtubule stabilizing agents, act in a way similar to paclitaxel (14, 15). Etoposides as naturally occurring products were first

isolated as secondary metabolites from the myxobacterium *Sorangium cellulosum* (16). They were soon recognized as potent cytotoxic drugs against eukaryotic cells (16), but only a decade later was their mode of action published (14, 15). The etoposides are structurally unrelated to paclitaxel, but they occupy the same nucleotide-binding site on β -tubulin (17). Various preclinical studies revealed an antiproliferative effect of etoposides on several cancer types, including models that are paclitaxel-resistant, with IC₅₀ values at a low nanomolar range. Furthermore, the radiosensitizing effect of etoposide B has been demonstrated (18–20). The application of etoposides showed further advantages: for instance, good water solubility, which leads to the use of less toxic solubilizer and the observation of fewer side effects (21, 22).

Etoposide B (Etoposide, EPO906) was developed by Novartis pharma GmbH and is along with Ixabepilone, a semisynthetic etoposide derivative, the most widely investigated agent of this new microtubule stabilizing class (23). Etoposide B has been evaluated in different clinical trials for the treatment of several solid carcinomas, including paclitaxel-resistant tumors (24, 25). Currently, it is under development for the treatment of cancers such as central nervous system malignancies (26), even in combination with radiotherapy (1, 22). We previously showed by clonogenic assays that etoposide B enhances radiation response in FaDu and A549 tumor cell lines, and that this may be induced by a reduced DNA repair capacity triggered by the drug (2).

In the present study, we investigated the mode of action of etoposide B on two human epithelial cancer cell lines, the FaDu squamous cell line and the A549 lung cancer cells. It is well known that chromosomal instability is widely spread even in squamous carcinomas (27) and in the A549 lung cancer cells (28) and a high degree of chromosomal instability is connected with paclitaxel resistance. We showed that etoposide B has a great effect on the metabolic activity of the cells as well as its influence on cell cycle distribution and on the type of cell death after combined treatment with irradiation.

METHODS AND MATERIALS

Materials

Dulbecco's modified Eagle's medium (DMEM), fetal bovine serum (FBS), penicillin/streptomycin (P/S), HEPES buffer solution, phosphate buffered saline (PBS), and trypsin/EDTA (0.05%) were obtained from PAA Laboratories GmbH (Cölbe, Germany). Sodium pyruvate and nonessential amino acids (NEA) were purchased from Biochrom AG seromed® (Berlin, Germany). Epothilone B, nocodazole, RNase (Ribonuclease A, from bovine pancreas), propidium iodide, and bisbenzimidazole (Hoechst 33258) were ordered from Sigma-Aldrich Fine Chemicals (Taufkirchen, Germany). Dimethyl sulfoxide (DMSO), sodium chloride, and methanol were provided from Merck KGaA (Darmstadt, Germany) and 70% ethanol was obtained from Apomix (Halle/Saale, Germany).

Drug preparation

Drugs were both dissolved in DMSO to generate stock solutions (epothilone B: 10 μ M; nocodazole: 1 mM). The stock solutions were diluted with DMEM for the experiments. The final concentration of DMSO in the experiments was 0.1% or less, a concentration that had no effect on the control cells.

Cell culture conditions

FaDu cells were cultured in DMEM supplemented with 10% FBS, 2% HEPES buffer solution, 1% sodium pyruvate, 1% NEA, and 1% P/S at 37°C under a 5% CO₂ humidified atmosphere. The A549 cells were grown in DMEM containing 10% FBS and 1% P/S at 37°C and 5% CO₂.

Flow cytometry analysis

Experimental design for flow cytometry studies

Confluent cells (0.75×10^6) were plated in T75-flasks. Different time points, between 24 hr before irradiation until 48 hr after irradiation, were investigated. Irradiation followed 48 hr after cell seeding. Ten nanomolar epothilone B was added 24 hr or, additionally for the cell cycle analysis, 0.5 hr prior to irradiation. Control cells were incubated free of drugs.

Propidium iodide staining for the analysis of cell cycle distribution

Media with detached cells and trypsinized adherent cells were collected in the same tube. Cell number was counted to adjust 1×10^6 cells/sample. After centrifugation, the pellet was resuspended in 70% ethanol at -20°C for fixation. For measurement, the cells were centrifuged to eliminate ethanol and then incubated for 15 min at 37°C with 1 mg/ml RNase in HBS-buffer (4 mM HEPES, 154 mM sodium chloride, pH 7.4). After repeated centrifugation, the pellet was resuspended in propidium iodide (100 μ g/ml in HBS buffer) and DNA content was measured.

The flow cytometer Cytomics FC500 (Beckman Coulter GmbH, Krefeld, Germany) with an argon laser and an excitation wavelength of 488 nm was used for the experiments. Data acquisition and analysis of histograms and dot plots were performed by the Beckman Coulter CXP Analysis software. For the cell cycle analysis, the DNA content

of propidium iodide stained cells were measured with a wavelength of 620 nm. Apoptotic cells were characterized by a decreased DNA content and thereby discriminable from intact cells (sub-G1 peak).

AnnexinV-FITC and 7-AAD labeling for examination of apoptosis and necrosis

Cells were collected as described above. The AnnexinV-FITC/7-AAD Kit (PN IM3614) from Beckman Coulter GmbH was used according to the manufacturer's instructions. To ensure that the cancer cells are able to undergo apoptosis, a positive control was generated using 1 μ M nocodazole (29, 30).

The flow cytometer Cytomics FC500 was used for the experiments. Data acquisition and analysis of dot plots were performed by the Beckman Coulter CXP Analysis software.

For the apoptosis assay, the AnnexinV-FITC binding of the cells was detected with a wavelength of 525 nm. The 7-AAD uptake was measured with a wavelength of 675 nm. AnnexinV binds to phosphatidylserine on the membrane of early apoptotic cells. In contrast, late apoptotic or necrotic cells were double stained by AnnexinV and by the cell nucleus dye 7-AAD because of their permeabilized cell membrane. For data interpretation, the density dot plots were analyzed by defining polygonal regions marking distinct populations. Four populations could be described, the viable (AnnexinV⁻/7-AAD⁻), the early apoptotic (AnnexinV⁺/7-AAD⁻), and the late apoptotic/necrotic cells (AnnexinV⁺/7-AAD⁺), as well as cell nuclei fragments (AnnexinV⁻/7-AAD⁺).

Cell proliferation assay for metabolic activity

To determine the metabolic activity in drug-treated cells, the EZ4U cell proliferation assay (Biomedica, Wien, Austria) was used according to the manufacturer's instruction. The cells were plated into 96-well plates and after a 24-hr cell adhesion period, different epothilone B concentrations between 0.05 nM and 10 nM were added. As controls, cells with DMEM or cells with media containing 0.1% DMSO were used. The first measurement was done 1 hr after drug addition. The second test was analyzed after a 24-hr epothilone B treatment. For the second experiment, the cultures were incubated with the drug and irradiated with 6 Gy (control 0 Gy) 24 hr later. One hour after irradiation, the XTT-test substance was added for 2.5 hr to detect metabolically formed formazan crystals using a zenyth microplate spectrophotometer (anthos Mikrosysteme GmbH, Krefeld, Germany). Each reaction was carried out in at least five replicates.

Irradiation

Irradiation was performed at room temperature utilizing a Siemens Oncor linear accelerator (Siemens, Erlangen, Germany) at a dose rate of 3.7 Gy/min (photons 6 MV). The irradiation doses used were 6 Gy and 0 Gy as a control.

Immunofluorescence staining of cellular nuclei

Cells (0.75×10^5) were grown on glass slides in 24-well plates. After attaching for 24 hr, 1 nM epothilone B was

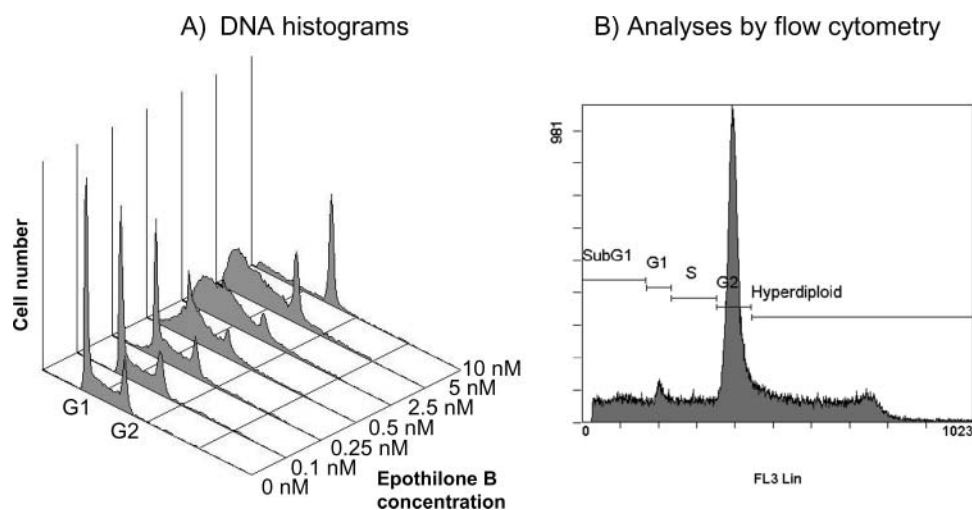


Figure 1. Analysis of the cell cycle distribution of FaDu cells using flow cytometry. (a) DNA histograms of cell cycle distribution after a 24-hr incubation with different epothilone B concentrations. (b) Analysis of a DNA histogram of FaDu cells after a 24-hr incubation with 10 nM epothilone B.

added and the samples were incubated with the drug for 24 hr. The negative control was drug-free. Cells were fixed with -20°C methanol for 20 min and DNA was stained with bis-benzimide ($1\ \mu\text{g}/\text{ml}$). Images of the cells at a magnification of 1000x were acquired with an Eclipse TE300 inverted microscope (Nikon, Tokyo, Japan). Two hundred cells were scored per glass slide and each approach was done in duplicate.

Statistical analysis

All error bars indicate the standard deviation of the mean for three independent experiments in the figures. The significance of treatments with the drugs was determined with Student's *t*-tests. *P*-values originate from two-sided tests; significant differences were presumed when $p < .05$. A student's *t*-test was also used in the cell cycle experiment for the statistical analysis of the G2/M phase and in the Annexin V/7-AAD assay for the analysis of the apoptotic fractions.

RESULTS

Cell cycle distribution

To analyze the effect of epothilone B alone on cell cycle progression, first the cell cycle distribution after 24 hr of treatment with different epothilone B concentrations was determined (Figure 1(a)). Incubation of FaDu cells with low concentrations of epothilone B (0.1 and 0.25 nM) resulted in minor differences in the cell cycle progression in the cells. However, treatment with higher drug concentrations (0.5–10 nM) showed a dose-dependent accumulation of cells at the G2/M stage at the expense of cells in the G0/G1 phase.

For all further investigations of the cell cycle distribution with radiation exposure, 10 nM epothilone B was chosen as a result of the observed G2/M accumulation. The effect of this drug concentration was analyzed after different treatment periods using the example of 6 Gy based on the formerly done colony-forming assays and the significant radiosensitive effect discovered by this irradiation dose (2).

Figure 1(b) illustrates an exemplarily analysis of a DNA histogram of FaDu cells after 24 hr of drug incubation. Five regions could be distinguished in the histograms, the sub-G1 peak, the G0/G1 phase, the synthesis phase, the G2/Mitosis phase, and the hyperdiploid cells.

The impact of 10 nM epothilone B on the cell cycle distribution of FaDu cells is demonstrated in Figure 2 (see also Tables 1 and 2). In Figure 2(a) (see also Table 1), the drug was added 0.5 hr prior to irradiation. Eight hours after irradiation (Epo B, 8.5 hr), epothilone B induced a significant accumulation of cells in the G2/M phase (33%) compared with only 19% of the control cells. The combined treatment of epothilone B and irradiation increased the G2/M arrest significantly to 41%. The high percentages of the cells in the G2/M block led to the loss of cells in the G0/G1 phase, which 8 hr after irradiation was only 18–20% of the cells. G2/M accumulation decreased over the observed time period. Dissolution of the G2/M block was accompanied by an increase in the percentage of cells in sub-G1 phase as well as a rise of hyperdiploid cells. Almost 24 hr after irradiation (Epo B, 24.5 hr), for instance, there were still 16% of the cells in the G2/M block, 25% hyperdiploid cells and 28% dead cells were counted in the sub-G1 area.

Figure 2(b) (see also Table 2) displays a significant time-dependent cell cycle G2/M arrest induced by 10 nM epothilone B on the FaDu cells. The drug was added 24 hr before irradiation. The highest concentration of cells in the G2/M phase was found to occur between 8 hr (43%) and 24 hr (44%) after drug addition. The massive accumulation of cells in the G2/M phase was beneficial for the irradiation time point, so that a high percentage of cells were arrested in the most radiosensitive G2/M cell cycle phase during radiation exposure. The escape from the cell cycle block was characterized by an increased content of dead cells (sub-G1 peak) and an enormous rise in the hyperdiploid cell population. Figure 2 (see also Tables 1 and 2) also shows the FaDu-controls without epothilone B treatment for 0 Gy and 6 Gy

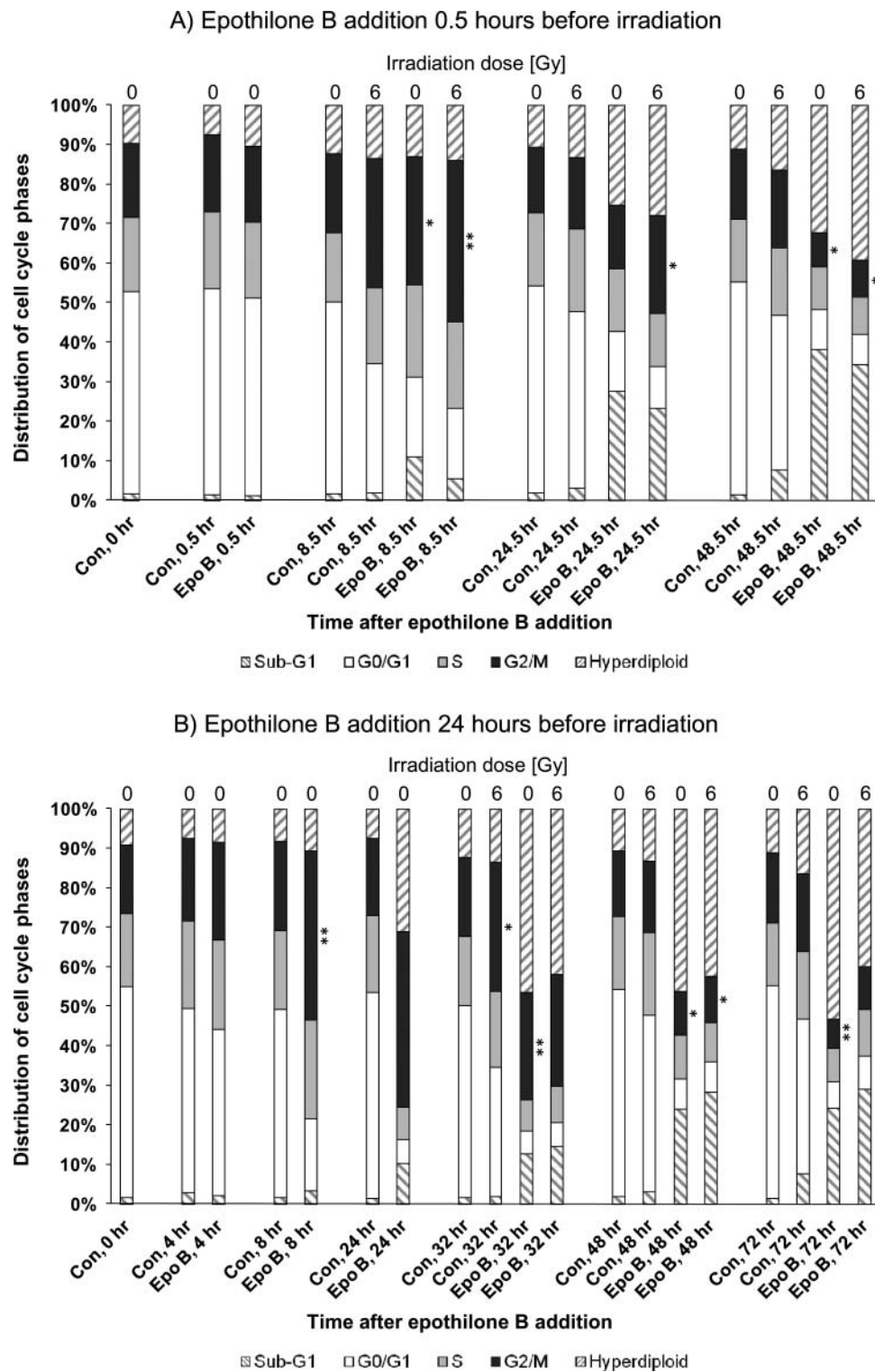


Figure 2. Analysis of the cell cycle distribution of FaDu cells using flow cytometry. Cell cycle analysis following treatment with 10 nM epothilone B. The drug was added 0.5 hr (a) or 24 hr (b) prior to irradiation (0 Gy or 6 Gy). Cells were harvested and analyzed at different time points after irradiation. Asterisks illustrate significance: * $p < .05$, ** $p < .003$. Abbr. Con = control, Epo B = epothilone B.

at the time points observed. There were only small changes in cell cycle distribution between the controls. For instance in Figure 2(b) (see also Table 2), ionizing radiation caused a small G2/M block of the cells, whose biggest size was reached 8 hr after irradiation. In the nonirradiated controls, most of cells were in the G0/G1 phase (47–54%), whereas only

17–23% of the cells were in the G2/M stage and 16–22% in the S-phase.

The effect of epothilone B on the A549 cell cycle distribution is shown in Figure 3 (see also Table 3). The cell cycle arrest in the radiosensitive G2/M phase was stronger and more long-lasting in comparison to the G2/M accumulation

Table 1. Analysis of the Cell Cycle Distribution of FaDu Cells Using Flow Cytometry

Sample	Gy	Sub-G1 (%)	G0/G1 (%)	S (%)	G2/M (%)	Hyperdiploid (%)
Con, 0 hr	0	1.6 ± 0.6	51.2 ± 1.6	18.8 ± 0.8	18.8 ± 1.5	9.7 ± 0.7
Con, 0.5 hr	0	1.3 ± 0.1	52.3 ± 0.9	19.4 ± 1.1	19.6 ± 1.1	7.5 ± 1.0
Epo B, 0.5 hr	0	1.2 ± 0.3	49.9 ± 1.9	19.3 ± 0.1	19.3 ± 1.0	10.3 ± 0.9
Con, 8.5 hr	0	1.5 ± 0.4	48.7 ± 3.0	17.4 ± 1.1	20.0 ± 1.0	12.4 ± 2.8
Con, 8.5 hr	6	1.8 ± 0.5	32.7 ± 3.6	19.1 ± 1.4	32.7 ± 2.7	13.7 ± 3.4
Epo B, 8.5 hr	0	11.0 ± 2.5	20.3 ± 2.7	23.2 ± 0.8	32.5 ± 3.7	13.1 ± 1.4
Epo B, 8.5 hr	6	5.3 ± 1.8	17.8 ± 0.6	22.0 ± 1.4	41.0 ± 4.2	13.9 ± 0.9
Con, 24.5 hr	0	1.7 ± 1.0	52.6 ± 3.4	18.5 ± 0.6	16.6 ± 3.1	10.6 ± 2.1
Con, 24.5 hr	6	3.0 ± 0.9	44.7 ± 3.7	21.0 ± 1.2	18.0 ± 2.7	13.2 ± 1.3
Epo B, 24.5 hr	0	27.6 ± 3.4	15.1 ± 1.5	15.8 ± 1.7	16.2 ± 1.3	25.4 ± 5.1
Epo B, 24.5 hr	6	23.2 ± 4.6	10.6 ± 0.2	13.4 ± 0.5	24.7 ± 2.5	28.0 ± 3.1
Con, 48.5 hr	0	1.3 ± 0.4	54.0 ± 3.1	15.6 ± 0.2	17.9 ± 0.5	11.2 ± 2.6
Con, 48.5 hr	6	7.5 ± 3.2	39.4 ± 1.2	17.0 ± 0.2	19.6 ± 2.1	16.5 ± 0.8
Epo B, 48.5 hr	0	38.1 ± 9.6	10.1 ± 1.0	10.8 ± 1.7	8.7 ± 2.3	32.3 ± 5.5
Epo B, 48.5 hr	6	34.2 ± 11.5	7.9 ± 0.7	9.3 ± 1.2	9.4 ± 2.5	39.2 ± 9.7

Cell cycle analysis following treatment with 10 nM epothilone B. The drug was added 0.5 hr prior to irradiation (0 Gy or 6 Gy). Cells were harvested and analyzed at different time points after irradiation.

of the FaDu cells. The biggest extent of the G2/M block (66%) was observed after 24 hr of drug treatment (Epo B, 24 hr) and, therefore, this time point should be a favorable working point for the irradiation. The high percentage of the cells in the G2/M stage was existent over the entire observation with only a marginal increase of cells in the hyperdiploid population, in contrast to the rise of the cells in the sub-G1 area.

Induction of apoptosis

Density scatter-plots with distributions of AnnexinV-FITC and 7-AAD-labeled cultures which were used for the determination of distinct populations are illustrated in Figure 4. The viable, unstained population is shown in the lower left quadrant. Early apoptotic cells, stained only with AnnexinV-FITC, appear in the lower right quadrant of the density plots. The necrotic and late apoptotic cells emerge in the upper right quadrant because they are double labeled with

AnnexinV-FITC and 7-AAD. The cell nuclei fragments only marked by 7-AAD staining are shown in the upper left field.

The associated dot plots of the forward and side scatter properties are illustrated beneath the density dot plots. Figure 4(a) (bottom) demonstrates that the 7-AAD positive and AnnexinV-FITC negative cells are nuclei with reduced forward scatter.

On the basis of density plots, further analysis could be done by gating distinct populations. Figure 5 demonstrates the time-dependent increase of the early apoptotic population as well as the growth of the late apoptotic/necrotic fraction induced by 10 nM epothilone B. Four hours after the addition of epothilone B, the content of early apoptotic cells was 1%, and after 48 hr the percentage rose significantly to 12%. In contrast, the late apoptotic or necrotic population grew only slightly from 6% (Epo B, 4 hr) to 8% (Epo B, 72 hr). Additionally, there were only minor differences between the nonirradiated and the 6 Gy irradiated cells. These differed

Table 2. Analysis of the Cell Cycle Distribution of FaDu Cells Using Flow Cytometry

Sample	Gy	Sub-G1 (%)	G0/G1 (%)	S (%)	G2/M (%)	Hyperdiploid (%)
Con, 0 hr	0	1.5 ± 0.5	53.5 ± 1.6	18.5 ± 0.4	17.5 ± 1.5	9.2 ± 0.4
Con, 4 hr	0	2.8 ± 1.3	46.6 ± 4.2	22.1 ± 0.7	20.9 ± 4.5	7.6 ± 1.2
Epo B, 4 hr	0	1.9 ± 0.7	42.1 ± 6.8	22.7 ± 1.3	24.8 ± 3.8	8.5 ± 2.1
Con, 8 hr	0	1.5 ± 0.4	47.6 ± 1.2	19.9 ± 0.4	22.6 ± 1.7	8.4 ± 2.0
Epo B, 8 hr	0	3.2 ± 1.2	18.3 ± 1.7	25.1 ± 1.4	42.7 ± 3.7	10.7 ± 0.9
Con, 24 hr	0	1.3 ± 0.1	52.3 ± 0.9	19.4 ± 1.1	19.6 ± 1.1	7.5 ± 1.0
Epo B, 24 hr	0	10.2 ± 2.2	6.0 ± 0.5	8.3 ± 0.6	44.5 ± 3.4	31.0 ± 3.5
Con, 32 hr	0	1.5 ± 0.4	48.7 ± 3.0	17.4 ± 1.1	20.0 ± 1.0	12.4 ± 2.8
Con, 32 hr	6	1.8 ± 0.5	32.7 ± 3.6	19.1 ± 1.4	32.7 ± 2.7	13.7 ± 3.4
Epo B, 32 hr	0	12.7 ± 5.4	5.7 ± 1.4	8.1 ± 0.6	27.0 ± 4.6	46.6 ± 10.5
Epo B, 32 hr	6	14.4 ± 5.7	6.1 ± 1.0	9.1 ± 0.6	28.4 ± 6.1	41.9 ± 9.5
Con, 48 hr	0	1.7 ± 1.0	52.6 ± 3.4	18.5 ± 0.6	16.6 ± 3.1	10.6 ± 2.1
Con, 48 hr	6	3.0 ± 0.9	44.7 ± 3.7	21.0 ± 1.2	18.0 ± 2.7	13.2 ± 1.3
Epo B, 48 hr	0	24.0 ± 8.7	7.7 ± 1.1	11.0 ± 1.1	11.2 ± 1.3	46.2 ± 9.4
Epo B, 48 hr	6	28.2 ± 3.7	7.6 ± 0.8	10.1 ± 2.0	11.6 ± 0.6	42.5 ± 4.6
Con, 72 hr	0	1.3 ± 0.4	54.0 ± 3.1	15.6 ± 0.2	17.9 ± 0.5	11.2 ± 2.6
Con, 72 hr	6	7.5 ± 3.2	39.4 ± 1.2	17.0 ± 0.2	19.6 ± 2.1	16.5 ± 0.8
Epo B, 72 hr	0	24.1 ± 9.7	6.8 ± 1.2	8.5 ± 1.2	7.4 ± 0.7	53.2 ± 9.8
Epo B, 72 hr	6	28.9 ± 2.6	8.5 ± 2.3	11.9 ± 3.5	10.7 ± 3.3	40.1 ± 10.6

Cell cycle analysis following treatment with 10 nM epothilone B. The drug was added 24 hr prior to irradiation (0 Gy or 6 Gy). Cells were harvested and analyzed at different time points after irradiation.

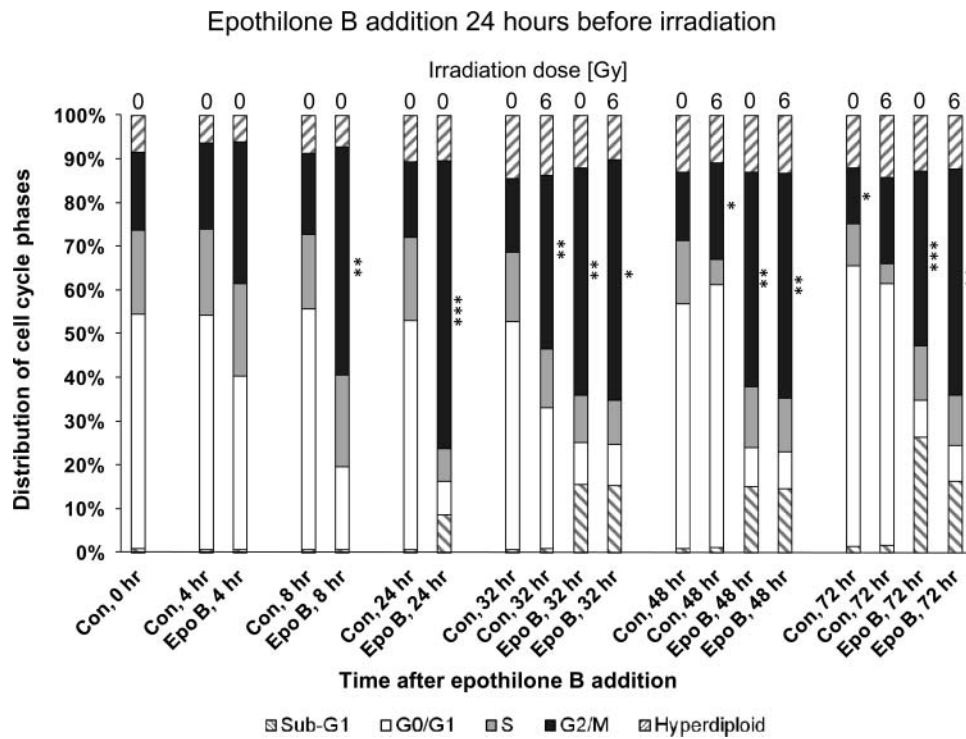


Figure 3. Cell cycle analysis of A549 cells using flow cytometry following treatment with 10 nM epothilone B. The drug was added 24 hr prior to irradiation (0 Gy or 6 Gy). Asterisks illustrate significance: * $p < .05$, ** $p < .003$, and *** $p < .0001$. Abbr. Con = control, Epo B = epothilone B.

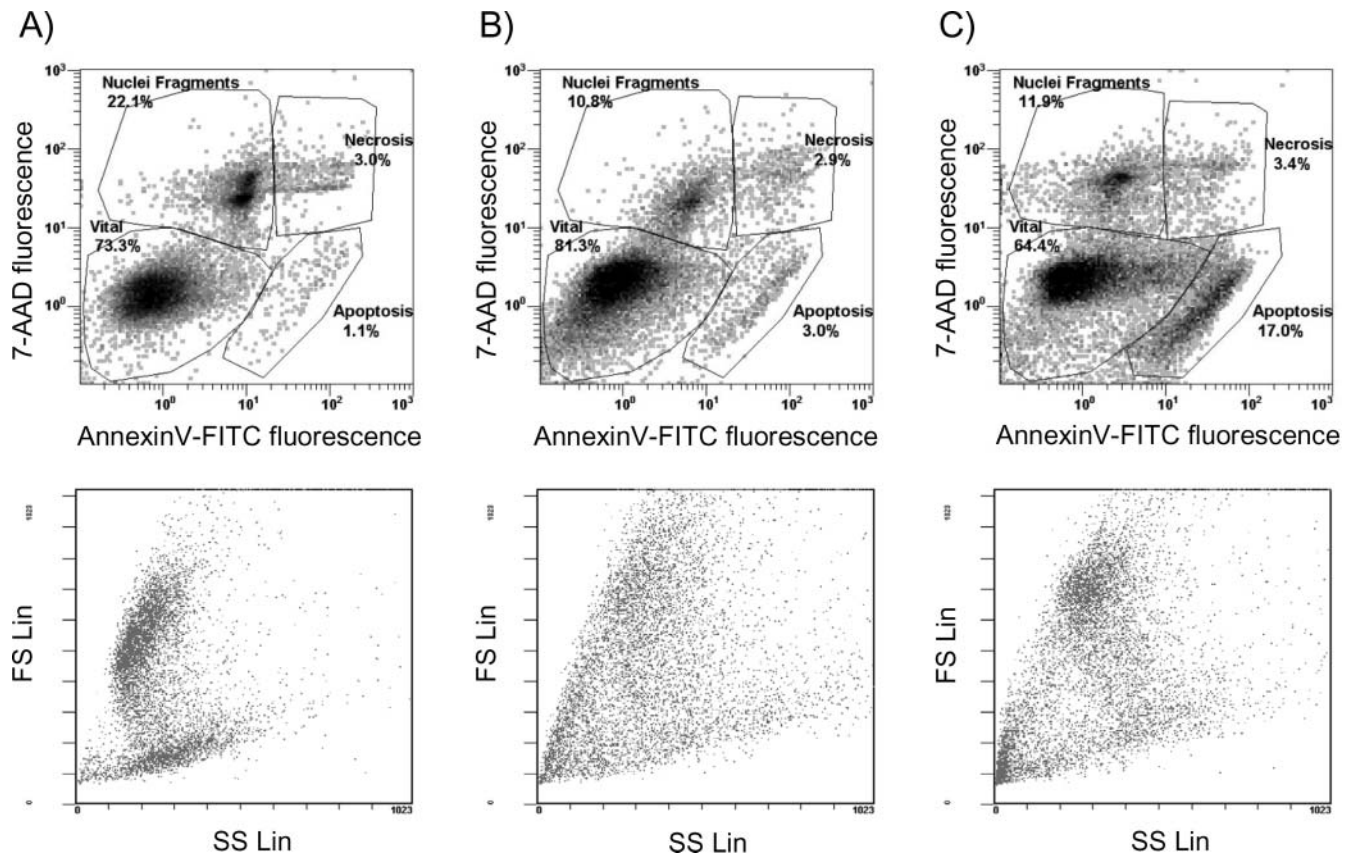


Figure 4. Three representative density plots display the distribution of 7-AAD and AnnexinV-FITC labeled FaDu cells and beneath the associated dot plots of the forward and side scatter. FaDu cells were analyzed by flow cytometry 32 hr after epothilone B addition. (a) Untreated control cells. (b) Cells treated with 10 nM epothilone B. (c) Cells incubated with 1 μ M nocodazole, used as a positive control for induction of apoptotic cell death.

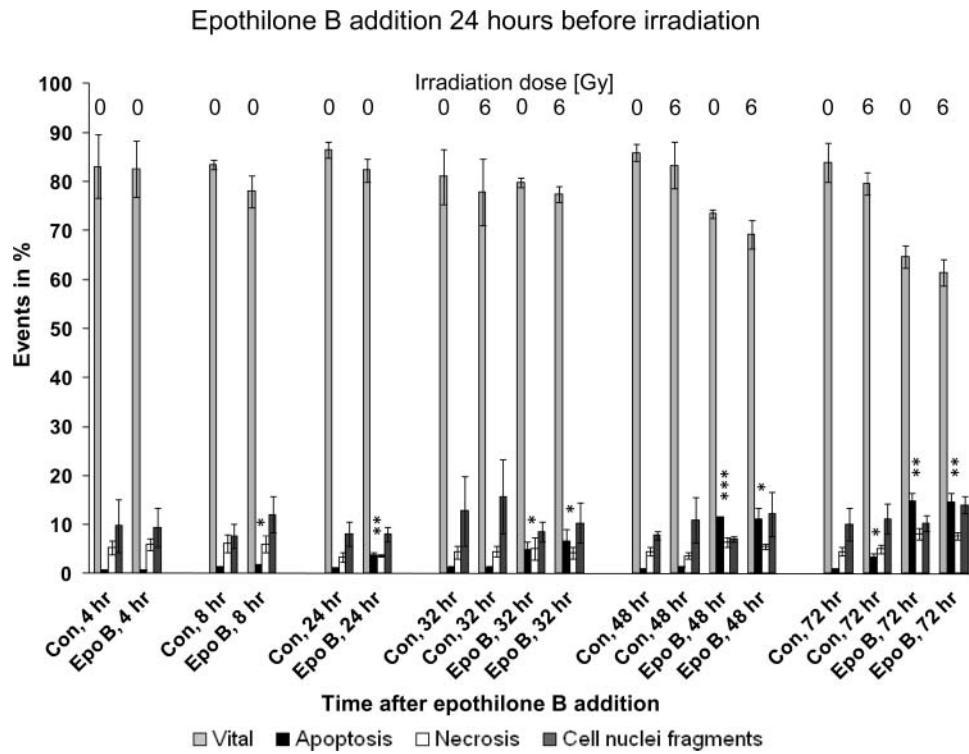


Figure 5. Quantitative analysis of FaDu cells of apoptotic, necrotic, and viable cell populations using flow cytometry. The cells were stained and measured following a 10 nM epothilone B treatment at different time points. The drug was added 24 hr prior to irradiation (0 Gy or 6 Gy). Asterisks illustrate significance: * $p < .05$, ** $p < .003$, and *** $p < .0001$. The calculated significances refer to the apoptotic fraction of the untreated control. Abbr. Con = control, Epo B = epothilone B.

mostly in regard to the fractions of the viable cells and the cell nuclei fragments. For example, 48 hr after drug addition, the nonirradiated 7-AAD stained population (cell nuclei fraction) was 7% and the irradiated 7-AAD positive population was 12%, whereas the unstained, living population was 73% (nonirradiated) and 69% (irradiated), respectively. Figure 5 shows nonirradiated and 6 Gy irradiated controls without any

epothilone B treatment of the FaDu cells. The percentages of the vital populations changed only marginally and the apoptotic cells increased slightly from 1% to 3%, 72 hr after drug adding. The late apoptotic or necrotic cell fraction was almost identical at 5–6% during all time points measured. Only the cell nuclei fragments differed, ranging between 8% and 16%.

Table 3. Analysis of the Cell Cycle Distribution of A549 Cells Using Flow Cytometry

Sample	Gy	Sub-G1 (%)	G0/G1 (%)	S (%)	G2/M (%)	Hyperdiploid (%)
Con, 0 hr	0	0.8 ± 0.2	53.7 ± 2.4	19.1 ± 1.7	17.8 ± 1.8	8.6 ± 3.5
Con, 4 hr	0	0.7 ± 0.2	53.5 ± 0.7	19.7 ± 1.3	19.9 ± 1.0	6.3 ± 2.5
Epo B, 4 hr	0	0.7 ± 0.3	39.7 ± 2.4	21.1 ± 0.9	32.5 ± 2.0	6.1 ± 0.2
Con, 8 hr	0	0.6 ± 0.3	55.1 ± 0.9	17.0 ± 1.8	18.3 ± 0.2	8.9 ± 1.4
Epo B, 8 hr	0	0.7 ± 0.3	18.9 ± 2.5	20.8 ± 0.7	52.4 ± 2.0	7.2 ± 0.9
Con, 24 hr	0	0.5 ± 0.3	52.4 ± 1.0	19.0 ± 1.4	17.3 ± 1.2	10.8 ± 1.5
Epo B, 24 hr	0	8.6 ± 4.2	7.6 ± 0.5	7.5 ± 1.9	66.0 ± 5.4	10.3 ± 1.4
Con, 32 hr	0	0.6 ± 0.2	52.1 ± 0.4	16.0 ± 1.3	16.7 ± 0.5	14.6 ± 1.7
Con, 32 hr	6	0.8 ± 0.1	32.3 ± 2.4	13.3 ± 0.5	39.7 ± 2.8	13.8 ± 2.0
Epo B, 32 hr	0	15.4 ± 5.6	9.7 ± 2.5	10.7 ± 0.3	51.9 ± 10.8	12.2 ± 2.8
Epo B, 32 hr	6	15.2 ± 5.0	9.4 ± 0.6	10.1 ± 2.1	55.2 ± 4.3	10.2 ± 1.4
Con, 48 hr	0	0.1 ± 0.0	56.0 ± 2.1	14.2 ± 0.8	15.7 ± 0.6	13.1 ± 1.1
Con, 48 hr	6	1.0 ± 0.4	60.1 ± 1.6	5.9 ± 0.8	22.0 ± 1.0	11.0 ± 2.1
Epo B, 48 hr	0	15.0 ± 4.4	9.0 ± 1.4	13.9 ± 0.3	49.1 ± 4.2	13.0 ± 1.1
Epo B, 48 hr	6	14.5 ± 1.9	8.5 ± 0.7	12.4 ± 0.8	51.3 ± 0.9	13.4 ± 1.9
Con, 72 hr	0	1.2 ± 0.2	64.2 ± 1.9	9.7 ± 0.6	12.7 ± 0.4	12.2 ± 1.2
Con, 72 hr	6	1.5 ± 0.6	60.0 ± 1.2	4.5 ± 0.1	19.8 ± 1.8	14.2 ± 0.3
Epo B, 72 hr	0	26.4 ± 19.4	8.4 ± 1.7	12.5 ± 0.9	39.9 ± 15.7	12.9 ± 4.5
Epo B, 72 hr	6	16.2 ± 5.4	8.3 ± 0.9	11.4 ± 0.3	51.8 ± 5.0	12.4 ± 0.6

Cell cycle analysis following treatment with 10 nM epothilone B. The drug was added 24 hr prior to irradiation (0 Gy or 6 Gy). Cells were harvested and analyzed at different time points after irradiation.

To classify the apoptosis-inducing potential of 10 nM epothilone B in both tested cell lines, two selected time points were chosen for comparison (Figure 6). At first, the figures show the ability of both cell lines to undergo apoptosis, induced by the positive control nocodazole. Figure 6(a) demonstrates that, for FaDu cells, 24 hr after addition of 1 μ M nocodazole, 15% of the cells underwent apoptosis and the percentages increased significantly to 30% after 48 hr of drug incubation. These results underline the fact that the FaDu cells are able to die by apoptosis. Figure 6(b) demonstrates these findings for the A549 cells as well, where the apoptotic cell population increased from 5% 24 hr after drug addition to 38% after a 48 hr incubation time.

Under treatment with epothilone B, the FaDu and A549 cells showed only minor changes in the distribution of the four populations analyzed. For instance, in the A549 cells, the epothilone B-induced formation of apoptotic cells increased from 3% 24 hr after addition of epothilone B to 13% 48 hr after drug addition (Figure 6(b)). Likewise, the late apoptotic/necrotic cell population grew from 3% (Epo B, 24 hr) to 7% (Epo B, 48 hr); accordingly the viable population decreased from 81% to 71%. The controls showed almost the same distribution of the four distinct populations in both cell lines at the two time points analyzed. Only the irradiated control, 48 hr after drug addition, had a minor increase in its contents of cell nuclei fragments. Furthermore, there were only minor differences between the irradiated and nonirradiated epothilone B-treated cells in both cell lines.

Influence of metabolic activity

To explore the effect of various epothilone B concentrations as well as irradiation on the metabolic activity of the cells, the XTT-test was used (Figure 7). Figures 7(a) and (b) present the results for an incubation time of 24 hr for both cell lines with and without additional irradiation. The data from the control cultures were set at 100%, and the values from the treated cells were normalized to the control. As shown in the figures, the metabolic activity decreased with increasing epothilone B concentrations.

However, cultures which were irradiated with 6 Gy showed comparable values. The nonirradiated FaDu cells, incubated with 5 nM epothilone B, revealed a metabolic activity of 60%, whereas the average metabolic activity of the irradiated cells treated with the same epothilone B concentration increased slightly to 65%. The A549 cells incubated with 5 nM epothilone B showed, in contrast to the FaDu cells, a higher metabolic activity of 80% for nonirradiated cultures and 84% for irradiated cells. The findings demonstrate that the toxic influence of epothilone B leads to significantly decreased metabolic activity, a factor more predominant than the damaging effect of the irradiation. In addition, the incubation with the vehicle DMSO revealed a reduced metabolic activity.

FaDu and A549 cells incubated for 1 hr with different epothilone B concentrations (data not shown) also showed a significant decreased metabolic activity. The results implicate that epothilone B molecules were able to accumulate in the cells within an hour, leading to reduced metabolic activity as a first sign of cytotoxicity.

Formation of multinucleated cells

To study the hyperdiploid cell population which was observed during the cell cycle analysis, the cell nuclei were stained with bisbenzimidazole. Figure 8 presents the FaDu cells after 24 hr of incubation with 1 nM epothilone B (Figure 8(b)) and the DMSO controls (Figure 8(a)). The control cells had normal nuclei. On the other hand, the epothilone B-treated cells showed a lot of diffuse smaller nuclei fragments, so that almost $68 \pm 8\%$ of the drug incubated FaDu cells could be titled as multinucleated. The findings were confirmed for the A549 cells as well; however, only $50 \pm 8\%$ of multinucleated cells were counted.

DISCUSSION

Tubulin molecules are important targets for anticancer therapy because of their central role in mitosis (4). The depression of microtubule dynamics by chemotherapeutic agents can lead to modified cell cycle distribution. This fact suggests that microtubule-interfering agents are potential radiosensitizers (20). Our previous *in vitro* study with the microtubule stabilizer epothilone B combined with ionizing radiation showed that the drug increases radiation response in FaDu and in A549 cells. The radiosensitizing effect observed may be supported by a decreased DNA double-strand break repair capacity caused by epothilone B (2).

In the present study, we analyzed the effects of epothilone B in combination with irradiation on the cell cycle perturbation and on cell destruction as well as the influence on the metabolic activity of the cells. For the flow cytometry experiments, the cells were exposed to 10 nM epothilone B, which is a drug concentration that correlates with the maximum tolerable dose measured in human plasma (31). Interestingly, we observed that concentrations between 0.5 nM and 2.5 nM epothilone B induced a strong sub-G1 peak and the content was reduced after a treatment with higher drug concentrations like 10 or 20 nM epothilone B (data not shown). This phenomenon could be typically shown in drugs that target the microtubule skeleton. Altmann *et al.* (21) and Chen and Horwitz (32) showed this effect for epothilone and Das *et al.* demonstrated this observation for paclitaxel in different lung cancer cell lines (33).

We demonstrated here that epothilone B is able to cause a concentration- and time-dependent G2/M arrest in FaDu and A549 cells, as analyzed by flow cytometry. Our findings are consistent with previous reports for a lot of different cell lines (1, 21, 32, 34–38), in which all publishers generally argue that this arrest is the main rationale for the epothilone B-induced radiosensitivity. The G2/M accumulation was followed by signs of apoptotic cell death and formation of hyperdiploid cell populations, whereby this phenomenon was observed in particular for the FaDu cells. Borgmann *et al.* published findings that G2-radiosensitivity is associated with aberrations of chromatid types as a sign of genomic instability and these aberrations are not necessarily correlated with the loss of proliferative capacity (39).

The detection of a hypodiploid cell population as evidence of apoptosis, observed during cell cycle analysis, was confirmed by the AnnexinV-FITC/7-AAD double staining

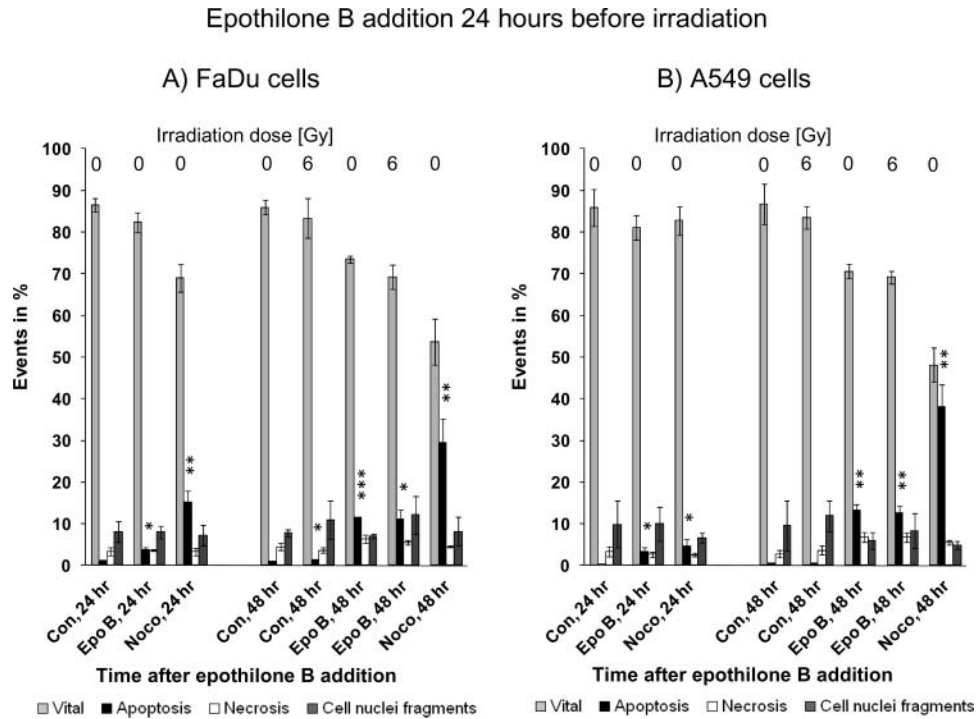


Figure 6. Quantitative analysis of (a) FaDu and (b) A549 cells of apoptotic, necrotic, and viable populations by flow cytometry. Ten nanomolar epothilone B was added 24 hr prior to irradiation (0 Gy or 6 Gy). The cells were stained and measured following treatment with epothilone B at 24 hr and 48 hr after drug addition. Nocodazole was used as a positive control. Asterisks illustrate significance: * $p < .05$, ** $p < .003$, and *** $p < .0001$. The calculated significances refer to the apoptotic fraction of the untreated control. Abbr. Con = control, Epo B = epothilone B, Noco = nocodazole.

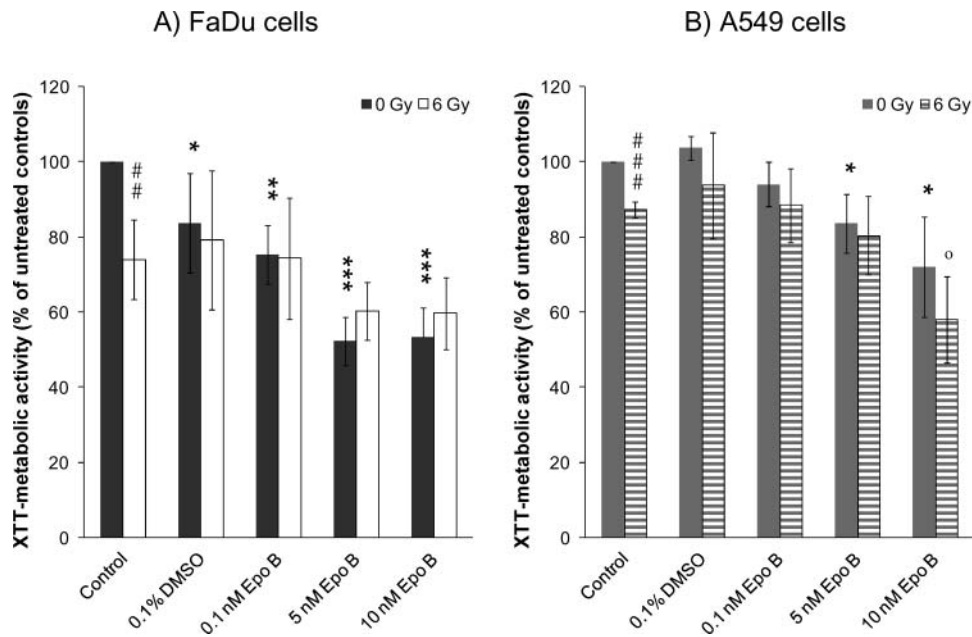


Figure 7. Metabolic activity of drug-treated cells. (a) FaDu and (b) A549 cells were incubated for 24 hr with epothilone B and then irradiated (0 Gy or 6 Gy). The addition of the XTT-test substance followed immediately. Values from the treated cells were normalized to the untreated controls (100%). Asterisks illustrate significance: */ $p < .05$, **/## $p < .003$, and ***/### $p < .0001$. The calculated significances (*) refer to the untreated control, the significances (#) refer to the corresponding unirradiated concentration, and the significance (o) to the irradiated control. Abbr. Epo B = epothilone B.

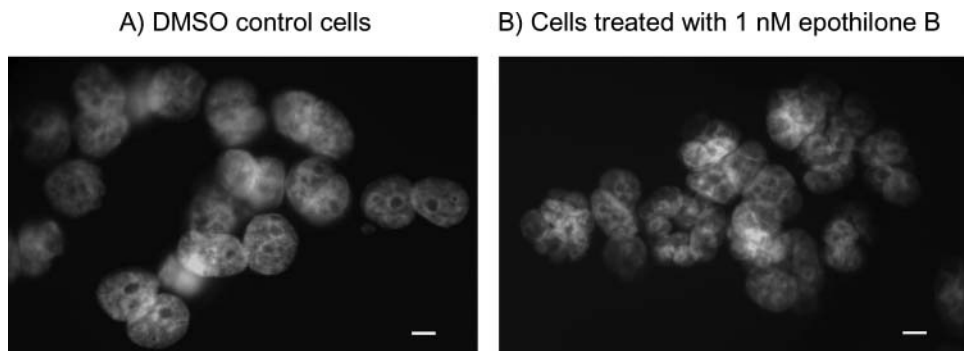


Figure 8. Nuclei staining of FaDu cells with bisbenzimidazole. (a) DMSO incubated control. (b) Cells treated with 1 nM epothilone B for 24 hr. Scale: 8 μm .

assay. The percentages of apoptotic cells increased with the incubation time with epothilone B for both cell lines equally. Interestingly, the percentages determined for the apoptotic sub-G1 peak in the cell cycle analysis were higher than the fractions for the apoptotic cells obtained via analysis of the AnnexinV/7-AAD assay. These observations were also described by Chen and Horwitz and they suggest that not all cells in the sub-G1 peak are apoptotic and a not negligible amount of hypodiploid cells exist which are already viable (32). This conclusion is in the line with our findings that the escape from the cell cycle stop leads to the formation of a living hyperdiploid cell population. The hyperdiploid cell fraction could be detected in our study by fluorescence microscopy of bisbenzimidazole stained cells and monitored as multinucleated cells. The destructive effect of epothilone B on the nuclear morphology has already been observed for NCI-H460 lung cancer cells (40). This event was also described for the clinically validated microtubule stabilizer paclitaxel (41). Cell cycle arrest and subsequent formation of aneuploid or polyploid cells are hallmarks of mitotic catastrophe (42), which is a cell death mechanism and can be induced by drugs (42) or even irradiation (43).

Cell rescue through mitotic slippage and unequal division, which results in production of hypodiploid cells and pseudo G1 cells with more than a diploid DNA content, was also observed by Chen and Horwitz and Chen *et al.* for the A549 cells after an 18-hr incubation with epothilone B (32, 35). We demonstrated that the G2/M block induced through 10 nM epothilone B had its greatest extent between 8 hr and 24 hr after drug addition for both cell types and was more pronounced in the A549 cell line, implicating a higher sensitivity to epothilone B. These time-relevant findings may implicate a beneficial period of time for the irradiation of patients in the daily routine. And the results underline our published findings that a 24-hr preincubation time in colony-forming assays is favorable for achieving significant synergistic radiosensitive effects on the FaDu and A549 cells (2).

In addition, the metabolic activity through the EZ4U proliferation assay was tested. One hour of drug incubation disclosed a concentration-dependent decrease of metabolic activity; this is a sign for the enhancement of epothilone B in the tumor cells. Lichtner *et al.* published findings stat-

ing that the kinetics of cellular drug uptake was cell type- and concentration-dependent and saturation of uptake for the tested cell lines was achieved in 2 hr (44). In contrast, a 24-hr epothilone B incubation following irradiation revealed no significant differences between irradiated and nonirradiated drug-treated cells, suggesting that the cytotoxic effect of epothilone B dominated over the damaging effect of irradiation.

In conclusion, the present study demonstrates that epothilone B treatment leads to an accumulation of cells in the radiosensitive G2/M phase. Escape from the G2/M block was accompanied by apoptotic cell death and formation of multinucleated cells. G2/M accumulation of the tumor cells is commonly regarded as the main rationale for drug-induced radiosensitivity. This finding gives crucial evidence that combined radiochemotherapy with epothilone B is worth being tested in additional preclinical and clinical trials for epithelial carcinomas.

DECLARATION OF INTEREST

The authors report no conflicts of interest. The authors alone are responsible for the content and writing of the paper.

REFERENCES

- Oehler C, von Bueren AO, Furmanova P, Broggin-Tenzer A, Orłowski K, Rutkowski S, Frei K, Grotzer MA, Pruschy M. The microtubule stabilizer patupilone (epothilone B) is a potent radiosensitizer in medulloblastoma cells. *Neuro Oncol* 2011;13:1000–1010.
- Baumgart T, Klautke G, Kriesen S, Kuznetsov SA, Weiss DG, Fietkau R, Hildebrandt G, Manda K. Radiosensitizing effect of epothilone B on human epithelial cancer cells. *Strahlenther Onkol* 2012;188:177–184.
- Downing KH, Nogales E. Tubulin and microtubule structure. *Curr Opin Cell Biol* 1998;10:16–22.
- Perez EA. Microtubule inhibitors: differentiating tubulin-inhibiting agents based on mechanisms of action, clinical activity, and resistance. *Mol Cancer Ther* 2009;8:2086–2095.
- Agrawal NR, Ganapathi R, Mekhail T. Tubulin interacting agents: novel taxanes and epothilones. *Curr Oncol Rep* 2003;5:89–98.
- Hei TK, Piao CQ, Geard CR, Hall EJ. Taxol and ionizing radiation: interaction and mechanisms. *Int J Radiat Oncol Biol Phys* 1994;29:267–271.

7. Liebmann J, Cook JA, Fisher J, Feague D, Mitchell JB. In vitro studies of taxol as a radiation sensitizer in human tumor cells. *J Natl Cancer Inst* 1994;86:441–446.
8. Choe KS, Salama JK, Stenson KM, Blair EA, Witt ME, Cohen EE, Haraf DJ, Vokes EE. Adjuvant chemotherapy prior to postoperative concurrent chemoradiotherapy for locoregionally advanced head and neck cancer. *Radiother Oncol* 2010;97:318–321.
9. Schiff PB, Horwitz SB. Taxol stabilizes microtubules in mouse fibroblast cells. *Proc Natl Acad Sci USA* 1980;77:1561–1565.
10. Yeung TK, Germond C, Chen X, Wang Z. The mode of action of taxol: apoptosis at low concentration and necrosis at high concentration. *Biochem Biophys Res Commun* 1999;263:398–404.
11. Rowinsky EK, Donehower RC. Paclitaxel (taxol). *N Engl J Med* 1995;332:1004–1014.
12. Piccart M. The role of taxanes in the adjuvant treatment of early stage breast cancer. *Breast Cancer Res Treat* 2003;79(Suppl. 1):S25–S34.
13. Donehower RC, Rowinsky EK. An overview of experience with Taxol (paclitaxel) in the U.S.A. *Cancer Treat Rev* 1993;19(Suppl. C):63–78.
14. Bollag DM, McQueney PA, Zhu J, Hensens O, Koupal L, Liesch J, Goetz M, Lazarides E, Woods CM. Epothilones, a new class of microtubule-stabilizing agents with a taxol-like mechanism of action. *Cancer Res* 1995;55:2325–2333.
15. Kowalski RJ, Giannakakou P, Hamel E. Activities of the microtubule-stabilizing agents epothilones A and B with purified tubulin and in cells resistant to paclitaxel (Taxol®). *J Biol Chem* 1997;272:2534–2541.
16. Gerth K, Bedorf N, Höfle G, Irschik H, Reichenbach H. Epothilones A and B: antifungal and cytotoxic compounds from *Sorangium cellulosum* (Myxobacteria). Production, physico-chemical and biological properties. *J Antibiot (Tokyo)* 1996;49:560–563.
17. Nettles JH, Li H, Cornett B, Krahn JM, Snyder JP, Downing KH. The binding mode of epothilone A on alpha, beta-tubulin by electron crystallography. *Science* 2004;305:866–869.
18. Hofstetter B, Vuong V, Broggin-Tenzer A, Bodis S, Ciernik IF, Fabbro D, Wartmann M, Folkers G, Pruschy M. Patupilone acts as radiosensitizing agent in multidrug-resistant cancer cells in vitro and in vivo. *Clin Cancer Res* 2005;11:1588–1596.
19. Kim JC, Kim JS, Saha D, Cao Q, Shyr Y, Choy H. Potential radiation-sensitizing effect of semisynthetic epothilone B in human lung cancer cells. *Radiother Oncol* 2003;68:305–313.
20. Bley CR, Jochum W, Orlowski K, Furmanova P, Vuong V, McSheehy PM, Pruschy M. Role of the microenvironment for radiosensitization by patupilone. *Clin Cancer Res* 2009;15:1335–1342.
21. Altman KH, Wartmann M, O'Reilly T. Epothilones and related structures - a new class of microtubule inhibitors with potent in vivo antitumor activity. *Biochim Biophys Acta* 2000;1470:M79–M91.
22. Fogh S, Machtay M, Werner-Wasik M, Curran WJ Jr, Bonanni R, Axelrod R, Andrews D, Dicker AP. Phase I trial using patupilone (epothilone B) and concurrent radiotherapy for central nervous system malignancies. *Int J Radiat Oncol Biol Phys* 2010;77:1009–1016.
23. Argyriou AA, Marmiroli P, Cavaletti G, Kalofonos HP. Epothilone-induced peripheral neuropathy: a review of current knowledge. *J Pain Symptom Manage* 2011;42:931–940.
24. Rothermel J, Wartmann M, Chen T, Hohneker J. EPO906 (epothilone B): a promising novel microtubule stabilizer. *Semin Oncol* 2003;30(Suppl. 6):51–55.
25. Larkin JMG. Patupilone. Antimitotic drug, microtubule-stabilizing agent, oncolytic. *Drugs Future* 2007;32:323–336.
26. Bystricky B, Chau I. Patupilone in cancer treatment. *Expert Opin Investig Drugs* 2011;20:107–117.
27. Pentenero M, Donadini A, Di Nallo E, Maffei M, Marino R, Familiari U, Broccoletti R, Castagnola P, Gandolfo S, Giaretti W. Distinctive chromosomal instability patterns in oral verrucous and squamous cell carcinomas detected by high-resolution DNA flow cytometry. *Cancer* 2011;117(22):5052–5057.
28. Swanton C, Nicke B, Schuett M, Eklund AC, Ng C, Li Q, Hardcastle T, Lee A, Roy R, East P, Kschischo M, Endesfelder D, Wylie P, Kim SN, Chen JG, Howell M, Ried T, Habermann JK, Auer G, Brenton JD, Szallasi Z, Downward J. Chromosomal instability determines taxane response. *Proc Natl Acad Sci USA* 2009;106(21):8671–8676.
29. Kallas A, Pook M, Maimets M, Zimmermann K, Maimets T. Nocodazole treatment decreases expression of pluripotency markers Nanog and Oct4 in human embryonic stem cells. *PLoS One* 2011;6:e19114.
30. Beswick RW, Ambrose HE, Wagner SD. Nocodazole, a microtubule de-polymerising agent, induces apoptosis of chronic lymphocytic leukaemia cells associated with changes in Bcl-2 phosphorylation and expression. *Leuk Res* 2006;30:427–436.
31. Stalder MW, Anthony CT, Woltering EA. Metronomic dosing enhances the anti-angiogenic effect of epothilone B. *J Surg Res* 2011;169:247–256.
32. Chen JG, Horwitz SB. Differential mitotic responses to microtubule-stabilizing and -destabilizing drugs. *Cancer Res* 2002;62:1935–1938.
33. Das GC, Holiday D, Gallardo R, Haas C. Taxol-induced cell cycle arrest and apoptosis: dose-response relationship in lung cancer cells of different wild-type p53 status and under isogenic condition. *Cancer Letters* 2001;165:147–153.
34. Sepp-Lorenzino L, Balog A, Su DS, Meng D, Timaul N, Scher HI, Danishefsky SJ, Rosen N. The microtubule-stabilizing agents epothilones A and B and their desoxy-derivatives induce mitotic arrest and apoptosis in human prostate cancer cells. *Prostate Cancer Prostatic Dis* 1999;2:41–52.
35. Chen JG, Yang CP, Cammer M, Horwitz SB. Gene expression and mitotic exit induced by microtubule-stabilizing drugs. *Cancer Res* 2003;63:7891–7899.
36. Khabele D, Lopez-Jones M, Yang W, Arango D, Gross SJ, Augenlicht LH, Goldberg GL. Tumor necrosis factor-alpha related gene response to epothilone B in ovarian cancer. *Gynecol Oncol* 2004;93:19–26.
37. Lin B, Catley L, LeBlanc R, Mitsiades C, Burger R, Tai YT, Podar K, Wartmann M, Chauhan D, Griffin JD, Anderson KC. Patupilone (epothilone B) inhibits growth and survival of multiple myeloma cells in vitro and in vivo. *Blood* 2005;105:350–357.
38. Kong Z, Raghavan P, Xie D, Boike T, Burma S, Chen D, Chakraborty A, Hsieh JT, Saha D. Epothilone B confers radiation dose enhancement in DAB2IP gene knock-down radioresistant prostate cancer cells. *Int J Radiat Oncol Biol Phys* 2010;78:1210–1218.
39. Borgmann K, Raabe A, Reuther S, Szymczak S, Schlomm T, Isbarn H, Gomolka M, Busjahn A, Bonin M, Ziegler A, Dikomey E. The potential role of G2- but not of G0-radiosensitivity for predisposition of prostate cancer. *Radiother Oncol* 2010;96:19–24.
40. Bröker LE, Huisman C, Ferreira CG, Rodriguez JA, Kruyt FA, Giaccone G. Late activation of apoptotic pathways plays a negligible role in mediating the cytotoxic effects of discodermolide and epothilone B in non-small cell lung cancer cells. *Cancer Res* 2002;62:4081–4088.
41. Blagosklonny MV, Darzynkiewicz Z, Halicka HD, Pozarowski P, Demidenko ZN, Barry JJ, Kamath KR, Herrmann RA. Paclitaxel induces primary and postmitotic G1 arrest in human arterial smooth muscle cells. *Cell Cycle* 2004;3:1050–1056.
42. Rello-Varona S, Stockert JC, Canete M, Acedo P, Villanueva A. Mitotic catastrophe induced in HeLa cells by photodynamic treatment with Zn(II)-phthalocyanine. *Int J Oncol* 2008;32:1189–1196.
43. Ianzini F, Kosmacek EA, Nelson ES, Napoli E, Erenpreisa J, Kalejs M, Mackey MA. Activation of meiosis-specific genes is associated with depolyploidization of human tumor cells following radiation-induced mitotic catastrophe. *Cancer Res* 2009;69:2296–2304.
44. Lichtner RB, Rotgeri A, Bunte T, Buchmann B, Hoffmann J, Schwede W, Skuballa W, Klar U. Subcellular distribution of epothilones in human tumor cells. *Proc Natl Acad Sci USA* 2001;98:11743–11748.

3.3 Publikation 3: Investigation of epothilone B-induced cell death mechanisms in human epithelial cancer cells - in consideration of combined treatment with ionizing radiation

T. Baumgart, S. Kriesen, O. Neels, G. Hildebrandt, K. Manda

Cancer Invest. 2015 Jul;33(6):213-224.

Kurze Zusammenfassung:

In dieser dritten Studie wurde erforscht, wie ausgewählte Zelltod-Mechanismen durch Epothilon B-Gabe in den beiden untersuchten epithelialen Tumorzelllinien (FaDu und A549) ausgelöst werden. Western Blot Analysen dienten der Untersuchung spezieller Apoptosemarker (p53 und PARP). Daneben zeigten Immunhistochemische Färbungen mit anschließender Messung im Durchflusszytometer, dass der Epothilon B-induzierte Zelltod auch durch die mitotische Katastrophe eingeleitet wird. Dabei war das Herbeiführen des Zelltodes durch eine Zelltyp-spezifische Proteinausprägung gekennzeichnet. Desweiteren konnte durch die Untersuchung der Mikrokernrate die verminderte DNA-Reparaturkapazität der bestrahlten Zellen nach Epothilon B-Gabe bestätigt werden.

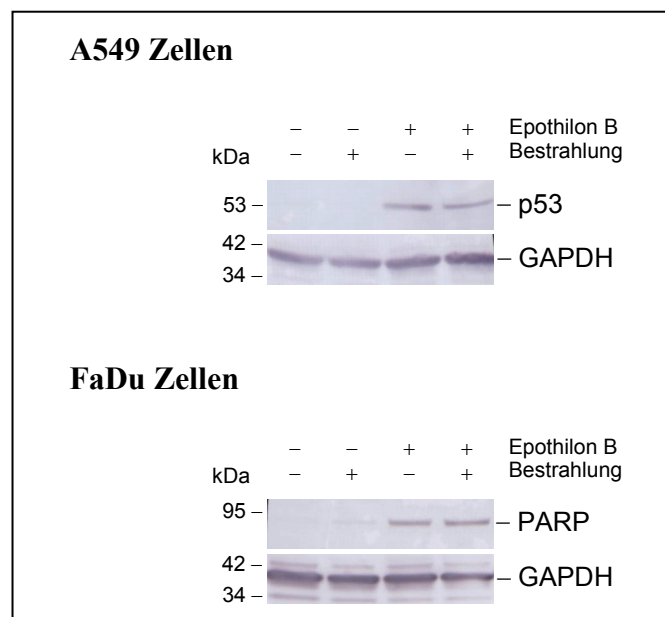


Abb. 4: Proteinexpressionen ausgewählter Apoptosemarker in den A549- und FaDu-Zellen nach einer 48-stündigen Inkubation mit 10 nM Epothilon B [Baumgart et al., 2015].

ORIGINAL ARTICLE

Investigation of Epothilone B-Induced Cell Death Mechanisms in Human Epithelial Cancer Cells – in Consideration of Combined Treatment With Ionizing Radiation

Tonja Baumgart,¹ Stephan Kriesen,¹ Oliver Neels,² Guido Hildebrandt,¹ and Katrin Manda¹

¹Department of Radiotherapy and Radiation Oncology, University Medical Centre Rostock, Rostock, Germany,

²Department of Nuclear Medicine, University Medical Centre Rostock, Rostock, Germany

Epothilone B was shown to have promising chemo- and radiosensitizing effects on cells, but the mechanisms underlying cell death remain ambiguous. The aim of the study was to examine selected cell death pathways on the basis of FaDu and A549 cells. Western blot analyses were used for investigation of specific apoptotic markers.

Immunofluorescence imaging and flow cytometry were utilized for examination of cell death mechanisms.

DNA-staining was used for studying influence of epothilone B on micronucleus rate. We showed that epothilone B can initiate cell death via apoptosis and mitotic catastrophe, but induction of cell death was cell type specific.

Keywords: Epothilone B, Irradiation, Apoptosis, Mitotic catastrophe, Micronucleus

INTRODUCTION

For the treatment of cancer, clinical indications for simultaneous radiochemotherapy are continuously expanding and research on combined modality therapy is being extensively investigated (1). In 1979, Peckham and Steel published the classical framework for discussing exploitable mechanisms for the combined usage of drugs and radiation (2) mainly focused on *in vitro* cytotoxicity. Bentzen et al. adapted this framework in 2007 and proposed five distinct mechanisms which are relevant for effective drug–radiation interactions; spatial cooperation, cytotoxic enhancement, biological cooperation, temporal modulation, and normal tissue protection (1). Presently, numerous chemotherapy agents, drug combinations, and dosing schedules for combined modality strategies are used either as a standard treatment or for investigational testing (3, 4), with the aim of improving the overall survival of cancer patients.

The epothilones are a family of microtubule-stabilizing agents like the clinically validated taxanes. Radiation with concomitant taxane therapy plays an important role in

cancer treatment (5, 6). However, taxane application is often impeded by development of chemoresistance or toxic side effects based on the poor water solubility of the taxanes (7, 8). Here, we evaluated the effect of the nontaxoid antitumor agent epothilone B alone and also combined with ionizing radiation, in two human epithelial cancer cell lines. The substance stabilizes microtubules with a taxane-like mechanism of action (9, 10).

Epothilone B (Patupilone, EPO906) is a bioactive secondary metabolite of bacterial origin and was developed by Novartis pharma GmbH (11). It is, along with Ixabepilone a semisynthetic epothilone derivative, the most widely investigated compound within this remarkable microtubule-stabilizing nontaxoid class (12) and has been tested in multiple clinical trials, including taxane-resistant tumors (13, 14). Application of epothilone B combined with ionizing radiation appears to be a promising cancer therapy for diverse tumor models like lung and colon adenocarcinomas (15–19) as well as for cancer of the central nervous system (20, 21).

The radiosensitizing effect of epothilone B was demonstrated in our previous studies using colony forming assays and the γ H2AX-foci method (17). Subsequently, we examined the mode of action of the drug in combination with ionizing radiation by analyzing endpoints including cell cycle distribution and induction of apoptosis (18). It could be demonstrated that epothilone B treatment leads to a significant accumulation of cells in the radiosensitive G2/M cell cycle phase followed by apoptotic cell death and formation of multinucleated cells. The experiments were performed with the FaDu squamous tumor cell line and the A549 lung cancer cell line.

The aim of our follow-up study was to examine selected molecular mechanisms, underlying epothilone B-induced antiproliferative and radiosensitive effects leading to cell death using the same cell lines. The two epithelial cancer cell lines were chosen, because chromosomal instability is widespread in squamous carcinomas (22) and also in the

Correspondence to: Katrin Manda, Department of Radiotherapy and Radiation Oncology, University Medical Centre Rostock, Südring 75, Rostock 18059 Germany. E-mail: katrin.manda@uni-rostock.de

Received 03 November 2014; revised 07 February 2015; accepted 12 February 2015.

A549 lung cancer cells (23); furthermore chromosomal instability is often associated with taxane resistance. In previous studies, we could demonstrate by flow cytometric analysis of AnnexinV-FITC and 7-AAD labelled epithelial tumor cells, that apoptotic cell death was triggered by epothilone B (18). Moreover, another cell death-related event called mitotic catastrophe could be observed. Although apoptosis is commonly seen as the principal mechanism of programmed cell death, it was reported that some antitumor drugs can additionally induce other forms of cell death, such as mitotic catastrophe (24).

For the flow cytometry experiments, the cells were exposed to 10 nM epothilone B which is a concentration that correlates with the maximum tolerable dose measured in human plasma (25). The effect of this epothilone B concentration was analyzed in combination with an irradiation dose of 6 Gy. This radiation dose was chosen due to the significant radiosensitive effect discovered by previously performed colony-forming assays (17). In this study we show that epothilone B, alone or combined with irradiation, can initiate different types of cell death, whereas apoptosis is not the main mechanism. Stability testing revealed that the epothilone B molecules are stable over the observed time period. In addition, we could demonstrate that the drug can significantly reduce the DNA repair capacity.

METHODS AND MATERIALS

Materials

Dulbecco's modified Eagle's medium (DMEM), foetal bovine serum (FBS), penicillin/streptomycin (P/S), HEPES buffer solution, phosphate buffered saline (PBS), and trypsin/EDTA (0.05%) were obtained from GE Healthcare Europe GmbH (Freiburg, Germany). Sodium pyruvate and nonessential amino acids (NEA) were purchased from Merck Millipore (Berlin, Germany). Epothilone B, nocodazole, cytochalasin B, RNase (Ribonuclease A, from bovine pancreas), bisbenzimidazole (Hoechst 33258) and Triton X-100 were ordered from Sigma-Aldrich Fine Chemicals (Taufkirchen, Germany). Dimethyl sulfoxide (DMSO), methanol and 37% paraformaldehyde were provided from Merck KGaA (Darmstadt, Germany). For the western blot experiments the equipment included the mini trans-blot module with the mini-PROTEAN tetra cell 2-gel system and a blotting tank, and all chemicals used, the mini-PROTEAN TGX precast gels, 10x Tris/Glycine/SDS buffer, 10x Tris/Glycine buffer, Laemmli sample buffer, the immunoblot assay kit, goat anti-mouse IgG and the opti-4CN substrate kit, were purchased from Bio-Rad Laboratories GmbH (Munich, Germany).

Drug preparation

Drugs were both dissolved in DMSO to generate stock solutions (epothilone B: 10 μ M; nocodazole: 1 mM). The stock solutions were diluted with DMEM for the experiments. The final concentration of DMSO in the experiments was 0.1% or less.

Cell culture conditions

FaDu cells were cultured in DMEM supplemented with 10% FBS, 2% HEPES buffer solution, 1% sodium pyruvate, 1% NEA, and 1% P/S at 37°C under a 5% CO₂ humidified atmosphere. The A549 cells were grown in DMEM containing 10% FBS and 1% P/S at 37°C and 5% CO₂.

Western blot analysis

Protein lysates from drug-treated, DMSO-treated (solvent control) and untreated control cells were prepared using lysis buffer containing 150 mM sodium chloride, 1 mM ethylene diamine tetraacetic acid, 1 mM ethylene glycol tetraacetic acid, 1 mM sodium orthovanadate, 1 mM sodium fluoride, 1% Triton X-100, 1 mM phenylmethylsulfonyl fluoride, 1 μ g/mL pepstatin A, 1 μ g/mL aprotinin, and 1 μ g/mL leupeptin in 50 mM Tris-HCl, pH 7.5. Bio-Rad Quick Start Bradford Protein Assay Kit was used to perform protein quantification. The protein lysates were mixed with 5x Laemmli sample buffer and stored at -20°C. An equal amount of total protein (100 μ g) was subjected to Sodium Dodecyl Sulfate Polyacrylamide Gel Electrophoresis (SDS-PAGE) with Bio-Rad Mini-Protean TGX Precast gels (4–20%) and transferred to nitrocellulose membrane. The gel electrophoresis and tank blotting were done according to the manufacturer's instructions (Bio-Rad Laboratories). The membrane was probed with primary antibodies, using apoptosis sample kit I and II (BD Bioscience, Heidelberg, Germany) for preliminary tests, and purified mouse anti-p53 antibody (1:500, BD Bioscience) and cleaved poly-(adenosine diphosphate)-ribose-polymerase 1 (PARP1; Asp 214) mouse monoclonal antibody (1:1000, New England Biolabs GmbH, Frankfurt, Germany) for the main experiments. The blot was incubated with the corresponding goat anti-mouse IgG (1:1600, Bio-Rad) or goat anti-rabbit IgG (1:1600, Santa Cruz Biotechnology, Heidelberg, Germany) conjugated with horseradish peroxidase. The opti-4CN substrate kit from Bio-Rad Laboratories was used for the colorimetric detection of the immunoprecipitation. Housekeeping proteins were monoclonal anti- β -Actin antibody produced in mouse (1:3000, Sigma-Aldrich) and rabbit polyclonal GAPDH antibody (1:500, Santa Cruz Biotechnology). Densitometric analyses of the results of at least three independent experiments were performed using ImageJ analysis software (National Institutes of Health, USA) and the bands of the cell death-related proteins were compared and related to the control bands of the housekeeping proteins.

Flow cytometry experiments

1. Experimental design for flow cytometry studies

About 10 nM epothilone B was added to the cells 24 hr prior to irradiation. Control cells were incubated free of drugs (native cells) or with the solvent DMSO. Irradiation was carried out 48 hr after cell seeding. Two different time points; 24 and 48 hr after irradiation, were investigated depending on the analyzed proteins.

2. Investigation of mitotic catastrophe by cyclin B1 and checkpoint kinase 1 detection via flow cytometry

Approximately 48 hr after drug treatment, the cells were fixed in 2% paraformaldehyde, washed in PBS and permeabilized with 1% Triton X-100 in PBS on ice. Following a wash step with 0.1% Triton X-100 in PBS, unspecific antibody binding sites were blocked with 5% goat serum in PBS. For the antibody incubation, the FITC-conjugated cyclin B1 antibody reagent set and the phycoerythrin (PE)-conjugated Chk 1 antibody were used alongside corresponding isotype controls, FITC- and PE-conjugated normal mouse IgG antibodies. Two washing steps with staining buffer followed, before measurement of the samples.

The flow cytometer Cytomics FC500 (Beckman Coulter GmbH, Krefeld, Germany) with an argon laser and an excitation wavelength of 488 nm was used for the measurements. Data acquisition and analysis of histograms and dot plots, by interpreting the mean fluorescence intensity, were performed by the Beckman Coulter CXP Analysis software. For this experiment, the FITC-conjugated cells were measured with a wavelength of 525 nm and the PE-conjugated cells with a wavelength of 575 nm.

3. Analysis of MitoTracker Green FM stained cells and anti-cytochrome C labelled cells via flow cytometry by measurement of the mean fluorescence intensity

Cells were collected, fixed and stained as described above. Experiments were initiated 24 hr after epothilone B incubation for the investigation of the early apoptosis marker cytochrome C and 48 hr after drug exposure for the detection of mitochondrial activity. Cells were labelled with purified mouse anti-cytochrome C antibody (1:200, BD Biosciences), followed by incubation with Alexa Fluor 488 goat anti-mouse IgG (1:300, Life Technologies GmbH, Darmstadt, Germany) and MitoTracker Green FM (Life Technologies GmbH) was applied at a concentration of 200 nM. To ensure that the cancer cells were able to undergo apoptosis, a positive control was generated using 1 μ M nocodazole (26, 27).

A Cytomics FC500 was used for the flow cytometry experiments. Data acquisition and analysis of the histograms by interpreting the mean fluorescence intensity were performed by the Beckman Coulter CXP Analysis software. Both dyes were measured at a wavelength of 525 nm.

Immunofluorescence analysis of different cell markers

1. Immunofluorescence staining of mitochondria and cytochrome C

Cells were grown on glass coverslips. After cells were left to attach for 24 hr, 10 μ M epothilone B was added. The samples were incubated with the drug for 24 hr for cytochrome C staining, and 48 hr for the vital staining of the mitochondria with 1 μ M MitoTracker Green FM. Cell fixation was done with 4% paraformaldehyde in PBS for 15 min and blocking of unspecific antibody binding sites with 1% gelatine in PBS. Cells were labelled for antibody staining with mouse monoclonal anti-cytochrome C antibody (1:150, BD Biosciences), followed by incubation with Alexa Fluor 488 goat anti-mouse IgG (1:300, Molecular Probes, Karlsruhe, Germany). Finally, the DNA was stained with 1 μ g/mL Hoechst 33258. For

fluorescence imaging of the mitochondria, the vital cells were incubated with MitoTracker Green FM (Life Technologies) and after fixation with 4% paraformaldehyde, the DNA was stained with 1 μ g/mL Hoechst 33258. Images of the cells were acquired at a magnification of 1000x using an Eclipse TE300 inverted microscope (Nikon, Tokyo, Japan). These preliminary tests were carried out without irradiation.

2. Immunofluorescence staining of micronuclei

Cells were seeded onto glass slides in 24-well plates. 24 hr later, 0.05 nM epothilone B was added and the samples were incubated with the drug for 4 days. The negative controls were drug-free and DMSO-incubated. 24 hr before cells were fixed with -20°C methanol, 1 μ g/mL cytochalasin B was added to inhibit cytoplasmic division. DNA was stained with Hoechst 33258. Images of the cells were acquired at a magnification of 1000x with an Eclipse TE300 inverted microscope. Five hundred cells were scored per glass slide and each dose was carried out in duplicate.

Irradiation

The irradiation of cells was performed at room temperature using a Siemens Oncor linear accelerator (Siemens, Erlangen, Germany) at a dose rate of 3.7 Gy/min (photons 6 MV). The irradiation doses used were 6 and 0 Gy as a control. The 6 Gy radiation dose was chosen due to the significant radiosensitive effect discovered by previously performed colony-forming assays (17).

Statistical analysis

All error bars indicate the standard deviation of the mean for at least three independent experiments in the figures. The significance of treatments with the drugs was determined with Student's *t*-tests. *p*-values originate from two-sided tests; significant differences were presumed when $p \leq 0.05$.

High performance liquid chromatography (HPLC) to investigate drug stability

To investigate the stability of the molecules in the media alongside the stock solution, different supernatants with 10 nM epothilone B, with or without cells, were measured by HPLC. Cells were grown in T25 flasks and incubated with 10 nM epothilone B after being left to attach for 24 hr. The supernatant was collected and filtered to eliminate interference from particles after specified time points, listed as; 0.5, 24, 48, and 72 hr following drug treatment. The epothilone B solutions were analyzed by a Shimadzu HPLC system with a LC 10 AD pump and an UV/VIS detector SPD-20AV (Shimadzu Europa GmbH, Duisburg, Germany) on a 5- μ m MultoHigh[®] 100 250-4 RP18 column (Chromatographie Service GmbH, Langerwehe, Germany) at a flow rate of 1.0 mL/min. The solvent was 20% methanol in distilled water. Epothilone B was detected by absorption at 254 nm with a retention time of 2 min in the DMSO stock solution and 2.5 min in the media.

Our findings revealed that epothilone B is highly stable in media for approximately 72 hr. An exemplarily HPLC-spectrum is illustrated in Supplemental file 1A, which showed a retention time of epothilone B at 2.01 min. As

seen in Supplemental file 1B, the supernatants containing epothilone B, collected at different time points, demonstrated a stable drug concentration. The peak areas of the substance differed only marginally between 85 and 106%. Therefore the stability of epothilone B in the media during the incubation time could be verified.

RESULTS

Epothilone B alone and in combination with radiation induces the expression of proapoptotic proteins: p53 in A549 cells and cleavage of poly-(ADP)-ribose-polymerase 1 in FaDu cells

Western blot experiments were undertaken to analyze apoptotic pathways by focusing on two important proapoptotic molecules, p53 for the A549 cells and poly-(ADP)-ribose-polymerase 1 (PARP1) for the FaDu cells. While the A549 cell line originates from an epithelial cancer which expresses the p53 wild-type protein, the FaDu cell line is mutated and could only express a reduced level of p53 transcripts with a point mutation in codon 248 (28). As a result of pretests, PARP1 was chosen for the FaDu cells because it is a main target of caspase 3 and therefore cleavage of PARP1 serves as a marker of apoptosis (29).

Western blot analysis was performed following 48 hr of epothilone B treatment. In A549 cells an investigation into the effect of epothilone B alone and combined with radiation on the proapoptotic protein p53 showed a prominent discrepancy in the protein expression between the control samples and the epothilone B-incubated cells [Figure 1(A)]. After 48 hr of epothilone B treatment a clear-cut expression band could be observed in the nonirradiated drug-incubated samples and also in the 6 Gy irradiated epothilone B-treated samples. We then examined the cleavage of PARP1 in both cell lines. Using the PARP1 antibody, the 89 kDa band of the large cleavage PARP1-fragment is detectable. Surprisingly, PARP1 expression for the nonirradiated and the irradiated epothilone B-treated samples of the FaDu cells were observed in the same intensity [Figure 1(B)], but no protein expression was visible for the A549 cells (blots not shown).

Semi-quantitative analyses of the results of three independent experiments were performed and the bands of the proapoptotic proteins were compared and related to the control bands of GAPDH using Image J software. Obviously, the densitometric analysis revealed no significant differences in the protein expression scatter of both p53 for the A549 cells and PARP1 for the FaDu cells between the nonirradiated drug-incubated and the irradiated epothilone B-treated cells.

In addition, western blot pretests without radiation treatment of further pro- and antiapoptotic cell death regulatory proteins; such as Apaf-1, Bax, Bad, caspase 2, and caspase 3, were performed. A complete list of all tested antibodies and the densitometric analysis of the protein levels in the cell lysates after 48 hr of drug exposure are shown in Supplemental file 2. Based on the preliminary tests, it was decided to choose p53 for the A549 cells and PARP1 for the FaDu cells to go forth for specific analyses, including combined treatment with irradiation, because they were the only proteins with distinct differences in the expression between the con-

rol samples and the epothilone B-incubated cells. In addition, more data from the pretests revealed a slightly increased expression of proapoptotic proteins like FADD and NIP1 in both cell lines and a down-regulation of the antiapoptotic factor XIAP in FaDu cells, while XIAP seems to be upregulated in the A549 cells. These data are highly interesting and further studies are required for detailed analysis in future.

Our results yield the prospect that both cell lines are undergoing apoptotic processes, but presumably in different cell signalling pathways. The evidence of proapoptotic proteins in the cell lysates after epothilone B treatment alone and combined with ionizing radiation supports our earlier results. We previously reported (18), that the detection of externalized phosphatidyl serine as an early event during apoptotic processes could be proved as well as a sub G1 peak. This peak was observed during cell cycle analysis, which is developed through decreased DNA content as a sign of apoptosis.

Epothilone B does not stimulate notable cytochrome C release as well as mitochondrial integrity loss

To study the release of cytochrome C as an early apoptosis marker and the accompanying degradation of mitochondrial membrane integrity, immunostaining of cytochrome C with an antibody and a vital dye staining of mitochondria with MitoTracker Green FM were performed (Figure 2). MitoTracker Green FM is a mitochondrial indicator dye and needs an intact mitochondrial membrane potential to accumulate for retention (30).

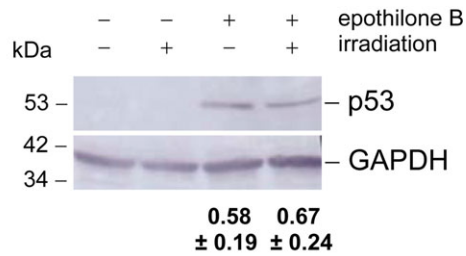
In comparison to the control, the epothilone B-treated cells did not result in a visually stronger staining of cytochrome C areas and therefore an epothilone B-induced cytochrome C release via immunofluorescence microscopy could not be detected 48 hr after addition of epothilone B (Supplemental file 3A). Intracellular staining of cytochrome C following measurement by flow cytometry resulted in an increased intensity of the cytochrome C fluorescence signal in both cell lines 24 hr following drug treatment. However, this only manifested in the nocodazole-treated, positive control cells (Figure 3). In addition, 48 hr after epothilone B treatment flow cytometric measurement of cytochrome C stained cells revealed no differences in the fluorescence intensities of the samples (data not shown). Treatment of cells with epothilone B showed no clear difference in intensity of cytochrome C fluorescence signal in comparison with the untreated control. Also drug therapy in combination with irradiation or with an X-ray irradiation alone showed no significant variances in the mean fluorescence signal of the samples.

Furthermore, fluorescence microscopy experiments revealed that epothilone B-incubated cells showed no diminished MitoTracker Green FM fluorescence signals 48 hr after drug treatment (Supplemental file 3B), compared to control cells. A weaker fluorescence signal as a sign of lower MitoTracker Green FM storage would indicate a loss of the mitochondrial membrane potential. Even a mitochondrial perinuclear aggregation, as an event during apoptosis (31), could not be observed.

Additionally, cell counting for the flow cytometry experiments revealed that one-third of the epothilone B-exposed

48 hours epothilone B treatment:

A) A549 cells



B) FaDu cells

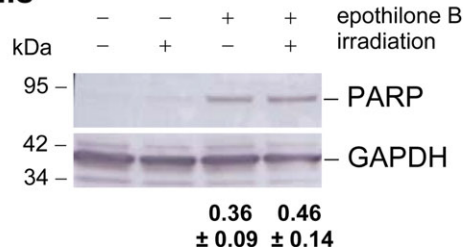


Figure 1. Protein expression after irradiation and drug treatment with 10 nM epothilone B by western blot analysis. At least three independent experiments were performed. Representative blots are shown: (A) time-dependent expression of the proapoptotic protein p53 (53 kDa) in A549 cells and (B) cleavage of PARP1-fragment (89 kDa) 48 hr following drug treatment in FaDu cells. Epothilone B was added 24 hr prior to irradiation (0 or 6 Gy). GAPDH (36 kDa) was used as a housekeeping protein. Densitometric analyses of the p53-levels or the PARP1-levels, respectively, normalized to the control bands of GAPDH, were performed.

cells were dead compared to the control cells after 48 hr of drug treatment.

These results imply a cell death mechanism occurring in a mitochondria-independent fashion without cytochrome C release and no obvious change in the mitochondrial membrane potential.

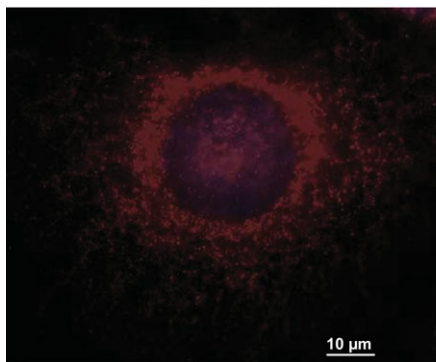
Epothilone B alone and combined with irradiation causes an increase in mitochondrial expression

To investigate the mitochondrial accumulation, which is increased for mitotic division during the cell cycle (32), flow cytometry measurements by analysis of the mean fluores-

cence intensity of MitoTracker Green FM stained cells were used. Initially flow cytometry experiments revealed an enlargement of the size and granularity of the drug-stimulated cells [(Figure 4(A)]. Histograms of an exemplarily experiment with the FaDu cells are shown in Figure 4(B) and the mean fluorescence intensities of both cell lines are illustrated in Figure 4(C).

In general, epothilone B incubation in FaDu cells resulted in an increase of the mean fluorescence signal thus indicating a higher amount of mitochondria even in the nonirradiated drug-incubated cells and the irradiated drug-treated samples compared to the corresponding control cells. The

A) Cytochrome C staining



B) MitoTracker Green FM staining

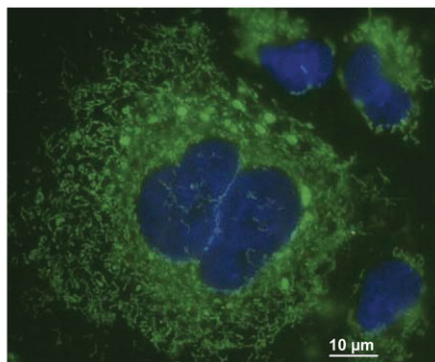


Figure 2. Immunofluorescence imaging of: (A) Cytochrome C-stained cell after incubation with 10 nM epothilone B for 27 hr. Cytochrome C is located around the cell nuclei of a giant FaDu cell. (B) MitoTracker Green FM-stained cell after incubation of 48 hr with 10-nM epothilone B. Mitochondria are located around the cell nuclei of a giant A549 cell.

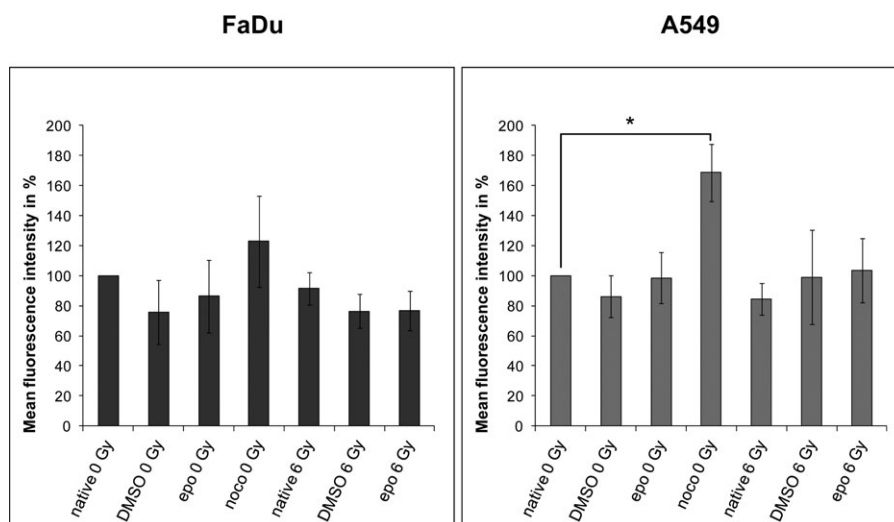


Figure 3. Investigation of the early apoptosis marker cytochrome C, 27 hr following treatment with 10 nM epothilone B. Investigation started 3 hr after time of irradiation. Flow cytometric analysis of the fluorescence intensity of cytochrome C. Error bars indicate the standard deviation for three independent experiments. Asterisks illustrate significance: $*p < 0.05$. nat: native (without epothilone B and irradiation); epo: epothilone B; nocco: nocodazole.

nonirradiated epothilone B-treated samples revealed a result of 202.1%, a significantly higher fluorescence intensity ($p < 0.05$) compared to the native control, set as 100%. Also the 6 Gy irradiated epothilone B-treated FaDu cells showed a significantly higher mitochondrial expression ($p < 0.003$) with a fluorescence intensity of 241.7% in contrast to 126.7% of the irradiated control cells.

In the A549 cells, a higher fluorescence intensity of the drug-treated samples could be observed compared to the corresponding controls. This effect was more pronounced in the nonirradiated epothilone B-treated cells, which showed a clear significance to the nonirradiated control cells ($p < 0.05$). Thus, our results demonstrate that epothilone B can cause an enhancement of mitochondrial levels as a sign of prometaphase arrest. This cell cycle arrest is accompanied by the increased expression of mitochondria during mitochondrial biogenesis (33).

Epothilone B-induced mitotic catastrophe is characterized by a cell type specific increase in the expression of G2-checkpoint proteins

To investigate our observations of the epothilone B-induced formation of multinuclear cells as a sign of a special cell death mechanism called mitotic catastrophe, two protein markers were analyzed using flow cytometry. The proteins cyclin B1 and checkpoint kinase 1 (Chk1) were examined because they are important cell cycle mediators of the G2-checkpoint arrest (34, 35).

Analysis of the fluorescence intensity of stained cyclin B1 and Chk1 after 48 hr of epothilone B incubation displayed a surprising difference in the development of the protein expression in the FaDu and A549 tumor cell lines (Figure 5). Whereas the epothilone B treatment induced an increase in cyclin B1 expression in FaDu cells and in A549 cells a decreased expression was caused. For example, in the irradiated epothilone B-incubated FaDu cells the protein expres-

sion was with 206.9% significantly higher ($p < 0.05$) than in the 6 Gy control (without epothilone B treatment) with 143.9%. Protein expression of the A549 cells revealed a significant decrease ($p \leq 0.05$) of the cyclin B1 expression in the drug-incubated nonirradiated and irradiated cells. For example, the irradiated epothilone B-treated tumor cells presented with 57.5% a lower fluorescence signal versus 84.4% in the 6 Gy irradiated control cells.

Analyses of Chk1 expression resulted in differences between both cell lines. In A549 cells the mean fluorescence intensities of the nonirradiated and the irradiated drug-induced samples were visibly higher than the fluorescence intensities of the corresponding control cells. The increase of the Chk1 expression in the A549 cells was significant higher for the irradiated epothilone B-treated samples with 192.3% compared to 120.2% of the irradiated controls. In contrast, no differences in the protein expression of Chk1 were observed for the FaDu cells.

The observations imply that epothilone B alone and combined with ionizing radiation can cause mitotic catastrophe in both cell lines. However the profound machinery beneath this cell death mechanism varied between both cell lines.

Epothilone B combined with ionizing radiation induces the formation of micronuclei

To prove our findings of the epothilone B-induced reduced DNA repair capacity, as seen in the γ H2AX-foci-assays published previously (17), the micronucleus rate via staining with bisbenzimidazole (Hoechst 33258) was analyzed [Figure 6(A)]. As expected and frequently published (e.g., 36), the radiation-induced micronucleus rate increased noticeably, both in the irradiated native cells and in the irradiated drug-treated samples, compared to the nonirradiated control cell cultures. For example, in FaDu cells the amount of binucleated cells with micronuclei increased for the nonirradiated

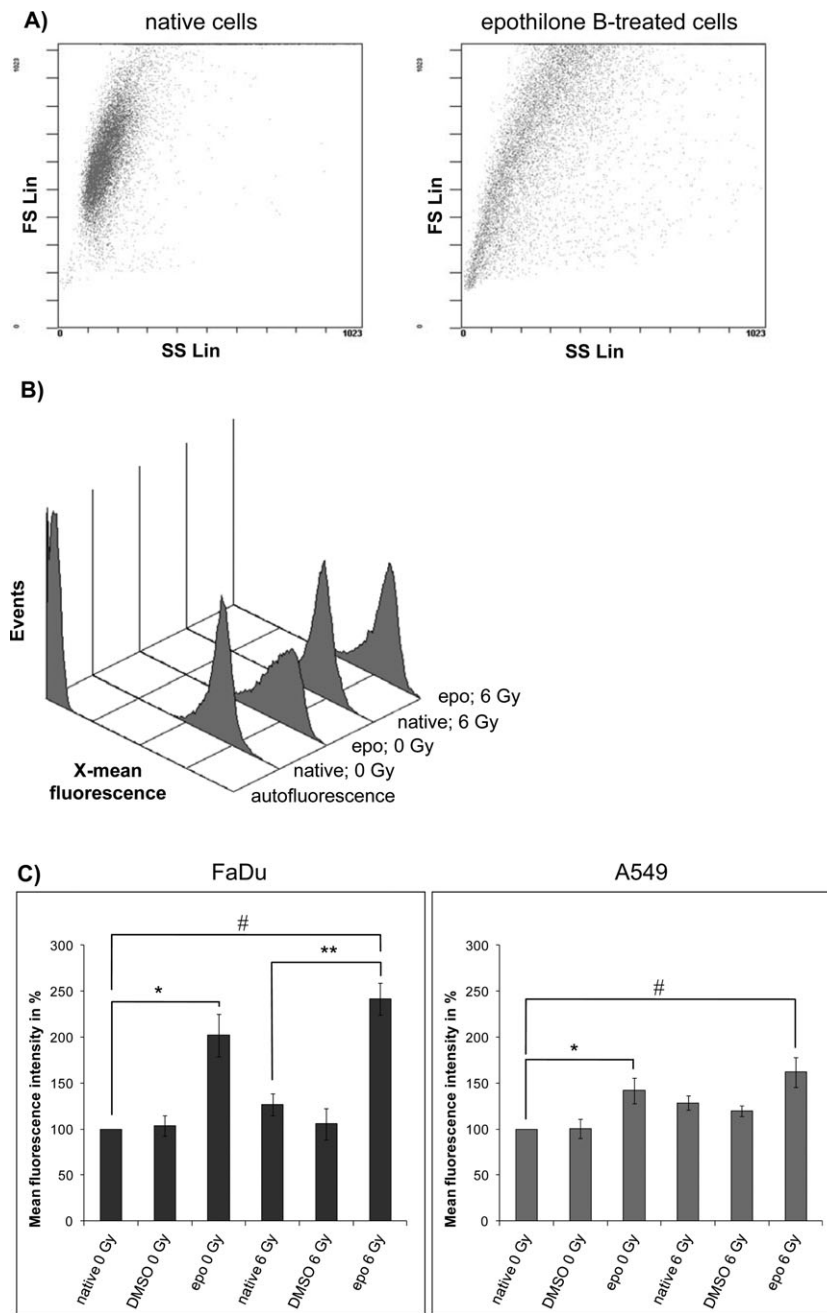


Figure 4. Examination of MitoTracker Green FM-stained mitochondria after incubation for 48 hr with 10 nM epothilone B. Investigation started 24 hr after time of irradiation. (A) Two representative dot plots of the forward and side scatter of native and epothilone B-treated FaDu cells. (B) Histograms of an exemplary experiment with FaDu cells. (C) Flow cytometric analysis of the fluorescence intensity of stained mitochondria. Error bars indicate the standard deviation for three independent experiments. Asterisks illustrate significance: $*/\#p < 0.05$, $**p < 0.003$. FS: forward scatter; SS: side scatter; Lin: linear; epo: epothilone B.

native cells from 1 to 3.3 for the 6 Gy irradiated native tumor cells ($p < 0.004$).

Evaluation of micronuclei in binucleated cells following 4 day incubation after 0.05 nM epothilone B treatment showed a significant increase in quantity when combined with a dose of 6 Gy for both cell lines ($p < 0.05$), in comparison with irradiated non-epothilone B-treated cells [Figure 6(B)]. For the FaDu cells, the micronucleus rate was 4.3 in the drug-treated irradiated samples and 3.3 in the with 6 Gy-treated control cells. Conversely, in A549 cells the micronucleus rate

was 9.9 (irradiated, epothilone B-incubated) versus 6.2 (6 Gy control).

DISCUSSION

Chemotherapeutic agents that target mitotic spindle assembly are often used to treat a variety of cancer diseases (37). The depression of microtubule dynamics can lead to cell cycle arrest in the radiosensitive G2/M phase advising that these drugs are potential radiosensitizers (16).

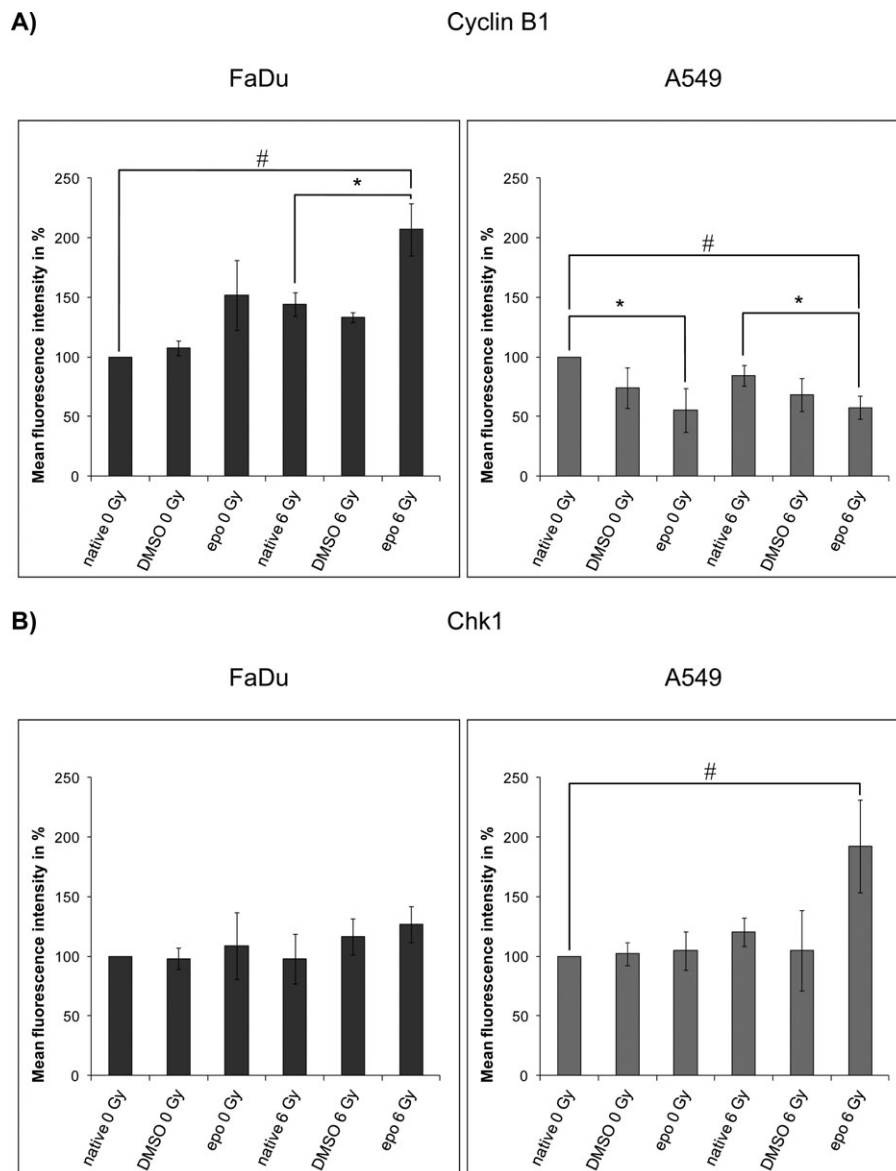


Figure 5. Flow cytometric analysis of the fluorescence intensity of (A) cyclin B1 and (B) Chk1 after incubation of 48 hr with 10 nM epothilone B. Investigation started 24 hr after time of irradiation. Error bars indicate the standard deviation for three independent experiments. Asterisks illustrate significance: $*/#p \leq 0.05$. epo: epothilone B.

We previously published studies with the microtubule-stabilizing agent epothilone B combined with ionizing radiation, which showed that the drug increases radiation response in two epithelial cancer cell lines (17). The radiosensitizing effect observed was supported by epothilone B-induced G2/M accumulation as the main rationale for drug-induced radiosensitivity and additionally by a decreased epothilone B-induced DNA double-strand break repair capacity. The cytotoxic activity of epothilone B resulted in apoptotic cell death, decreased metabolic activity, and the formation of multinucleated cells (18).

In the present study, the effect of epothilone B alone and in combination with irradiation was analyzed to investigate different mechanisms of cell death pathways considering concurrent p53 prominence in the cell lines. The stability of epothilone B molecules in the media was also examined in

a time-dependent manner. Furthermore, experiments were performed to investigate radiation-induced micronuclei formation.

The initial priority was to investigate the way epothilone B stimulates cells to undergo apoptosis in order to confirm our results that were previously published (18), where drug-induced apoptosis with and without 6 Gy irradiation by AnnexinV-FITC staining was demonstrated. Since cell death pathways depend on the p53 protein alterations (38) and p53 polymorphism suggests clinical significance in anticancer therapy (39), we wanted to elucidate how epothilone B alone and combined with ionizing radiation can induce different modes of cell death with respect to the p53 protein. The p53 protein is an important tumor suppressor (see review: 40) and almost 50% of all human tumors are characterised by a mutated form of p53 (41). While the

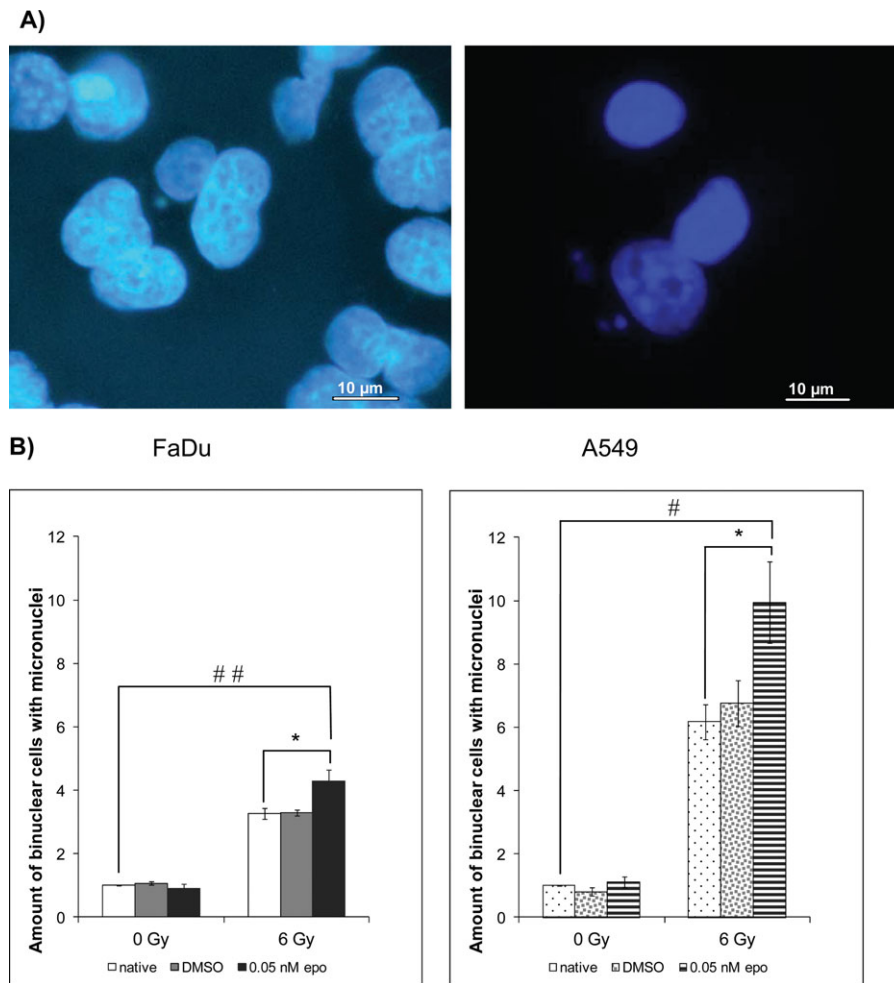


Figure 6. Analysis of the micronucleus rate via staining with bisbenzimidazole (Hoechst 33258). (A) Representative images of binucleated A549 cells with micronuclei after drug treatment (right) and control cells (left). (B) Micronucleus formation after incubation for 4 days with 0.05 nM epothilone B. Investigation started 3 days after time of irradiation. Error bars indicate the standard deviation for three independent experiments. Asterisks illustrate significance: */#*p* < 0.05, ##*p* < 0.004. epo: epothilone B.

A549 cell line represents the p53 wild type, the FaDu cells are mutated and cannot express the wild-type form of the p53 protein (29,42). Western blot experiments revealed that epothilone B alone and combined with ionizing radiation induces the expression of two proapoptotic proteins; p53 in A549 cells and a drug-induced cleavage of PARP1 in FaDu cells.

However, typical signs of apoptosis examined by immunostaining; both the release of cytochrome C from the mitochondria as a nuclear translocation of the protein (43) and mitochondria perinuclear aggregation (31) could not be observed in our study. These results are in contrast to Khawaja et al., who demonstrated an epothilone B-produced release of cytochrome C in two neuroblastoma cell lines after a 24 hr incubation time following treatment with the drug (44). Moreover, we could also not show a reduced fluorescence intensity of stained mitochondria, which would indicate a loss of membrane integrity (30), in both cell lines.

The tumor suppressor protein p53 is an important initiator of the intrinsic apoptotic pathway by activating different downstream proteins and thus permitting release of

apoptogenic factors; like cytochrome C (45). The p53 protein can itself be stimulated not only by DNA damage but also by spindle damage (46). PARP1 cleavage through proteolytic activated caspase 3, results in DNA fragmentation by irreversible binding of the small PARP1 fragment to DNA strand breaks by inhibition of DNA repair enzymes (47). In A549 cells, which possess the wild type p53 gene, we could detect the epothilone B-induced expression of the tumor suppressor p53 at 48 hr after epothilone B addition, but a PARP1 cleavage could not be found. In contrast, in p53 deficient FaDu cells we identified an epothilone B-induced PARP1 cleavage 48 hr after drug treatment. Our findings of epothilone B-induced expression of different proapoptotic markers are consistent with several observations in different cell lines. For example, our observations of p53 in A549 cells verify those of Chen et al. who demonstrated that epothilone B produced a concentration-dependent increase in the p53 expression 18 hr after epothilone B treatment (48). Lee et al. published findings with the SW620 human colon cancer cell line, that epothilone B can trigger the expression of different proapoptotic proteins like p53, caspase 3, and Bax and diminish the

expression of the antiapoptotic protein Bcl2 (49). Lin et al. examined the protein levels of PARP1, caspase 3, Bax, and Bcl2 for two multiple myeloma cell lines under the influence of 10 nM epothilone B, with cleavage of PARP1 observed ranging from 24 to 72 hr following drug treatment (50).

We imply that apoptotic pathways are activated by epothilone B, but they are cell type specific. Since the role of tumor suppressor p53 is clearly defined as an initiator of the intrinsic apoptotic pathway, PARP1 cleavage through proteolytic-activated caspase 3 can be a result of both apoptotic pathways. Caspase 3 can itself be activated by caspase 9 in the intrinsic pathway or even through caspase 8 activation as a result of the extrinsic apoptotic pathway (24). Furthermore, it should be mentioned that PARP1 plays a role in diverse DNA repair pathways, like the alternative pathway of nonhomologous end joining for double-strand break repair (51). In light of this, further investigations are needed to analyze the molecular mechanisms of apoptotic cell death induced by epothilone B combined with radiation in more detail.

In addition, the relatively weak development of protein expression in the western blot experiments did not explain the enormous cell loss after 48 hr of exposure to the drug. We agree with Bröker et al. who explained for different non-small cell lung carcinomas that although several apoptotic characteristics could be detected for relatively late time points after epothilone B addition, the apoptotic machinery is not the dominant mode of cell death and that alternative routes are responsible for the cytotoxic effect of this drug (52). Oehler et al. reported for three human medulloblastoma cell lines that epothilone B combined with radiation leads to different modes of cell death in a cell line-dependent way and drug-induced cell viability was not reduced through pretreatment with a broad-range caspase inhibitor, suggesting apoptosis could be a secondary endpoint (21). Rogalska et al. published data suggesting that epothilone B-triggered apoptosis is induced by the TRAIL (TNF-related apoptosis-inducing ligand)-mediated extrinsic pathway in human SKOV-3 ovarian cancer cells (53).

In light of this, we focused on investigating whether the previously observed mitotic catastrophe could be detected and identified by the morphological characteristic of multi-nucleated cells using flow cytometry. Our experiments yielded a result of an epothilone B- and irradiation-induced increase of mitochondria expression. A higher amount of mitochondria could be interpreted as a sign of prometaphase arrest and a long-standing cell cycle arrest is typical for a mitotic catastrophe (54). The observed prometaphase arrest supports our earlier findings of the epothilone B-induced G2/M cell cycle block followed by the production of a hyperdiploid cell population, which was shown by fluorescence microscopy as multinucleated cells, an indication for a mitotic catastrophe (18).

In addition, the enlargement of the size and granularity of the drug-stimulated cells could be shown in all flow cytometry experiments. These findings, especially the increased cellular granularity indicate a mitotic arrest which is accompa-

nied by an increase in the intracellular organelles and a higher total amount of DNA (32).

Furthermore, flow cytometry analysis was used in the investigation of two markers indicating mitotic catastrophe, cyclin B1, and checkpoint kinase 1, which are important cell cycle mediators of the G2-checkpoint arrest. We could demonstrate a cell-type specific enhancement of the protein expressions in epothilone B-incubated nonirradiated and 6 Gy irradiated samples. While the cyclin B1 expression in the drug-exposed samples, particularly the irradiated cells, was significantly increased for the FaDu cells, the A549 cells demonstrated a decrease in cyclin B1 expression for the epothilone B-treated samples. Interestingly, it could be shown that the checkpoint kinase 1 expression for the irradiated and epothilone B-treated A549 cells was enhanced compared to the controls, but no change in the protein level of the FaDu cells could be observed.

To our knowledge, this is the first study which investigated the expression status of these particular two proteins by immunostaining following flow cytometry measurement, but analysis by western blotting is comparable to our studies. Winsel et al. published findings using Sagopilone; a synthetic epothilone, in which a drug-induced upregulation of cyclin B1 expression was found in the A549 cells, this was demonstrated by western blot analysis (55). Bekier et al. examined aurora kinases, also sensors in the checkpoint pathway, by inhibiting the kinases in an epothilone B-treated HeLa-subline using time-lapse microscopy and expressed that the death induced by microtubule-stabilizing drugs is correlated with a sustained mitotic block (56).

HPLC-measurements verified a stable epothilone B concentration in the media during the analyzed time points. This finding is interesting because it is routine for companies to carry out stability tests internally. Customarily, suppliers advise to keep the drugs refrigerated and stored away from light, its use in cell culture in turn remains difficult. Most of the published data for stability measurements of drugs like the epothilones refer to HPLC-tests in human plasma for pharmacokinetic studies (for example: 57).

The last key aspect was the investigation of the influence of radiation-induced micronuclei development and the effect of epothilone B on DNA repair capacity. The micronucleus technique is one of the preferred assays to evaluate chromosome damage and it allows for dependable measuring of chromosome loss and chromosome breakage (58). Our experiments could demonstrate that epothilone B combined with radiation treatment is able to increase the micronucleus rate significantly in both cell lines compared with the irradiated control samples. The micronucleus tests were completed to underline our observations from the γ H2AX-foci-assays in our previous publication; where we could demonstrate that epothilone B combined with ionizing radiation resulted in a concentration-dependent increase of the number of residual double-strand breaks indicating a reduction in DNA repair capacity. Reasons for the drug-induced influence of the DNA repair capacity were already mentioned in our previous publication (17) and could be founded in the

strong accumulation of epothilone B molecules in the cell nucleus, notably in the fraction of nuclear proteins (59) and possibly resulting in the repression of genes which play a role in DNA repair (e.g., BRCA1, H2AFX) (60).

We previously published findings (18) which demonstrated that epothilone B treatment leads to an accumulation of tumor cells in the radiosensitive G2/M-phase of the cell cycle. The G2/M accumulation was followed by apoptotic cell death and the formation of multinucleated cells. The cell cycle arrest may originate in the drug-induced microtubule stabilization followed by deficient chromosome segregation. For a better understanding of this phenomenon, continuous studies are necessary possibly employing the multigene fluorescence in situ hybridization (mFISH) method.

In conclusion, the results of the current manuscript verify and expand on the findings of our former investigations where we could demonstrate that epothilone B showed promising chemo- and radiosensitizing effects on the epithelial cancer cells tested. Considering that this cell death machinery currently remains ambiguous, we performed follow-up studies to make a contribution to gain a better understanding of the molecular mechanisms responsible for the epothilone B-induced effects on cancer cells. By analyzing selected apoptotic mediators, like p53, PARP1, and cytochrome C and markers for mitotic catastrophe (e.g., cyclin B1) we emphasize that both aspects of cell death, apoptosis and mitotic catastrophe, could be optimal clinical end points for assessing therapeutic benefit in cancer treatment. Moreover, the radiosensitive effect of epothilone B is cofounded in the reduced DNA repair capacity of drug-treated cells. The results give crucial evidence that concurrent radiochemotherapy with epothilone B is worth being tested in further pre-clinical and clinical trials for epithelial carcinomas.

DECLARATION OF INTEREST

The authors report no conflicts of interest. The authors alone are responsible for the content and writing of the paper.

REFERENCES

1. Bentzen SM, Harari PM, Bernier J. Exploitable mechanisms for combining drugs with radiation: concepts, achievements and future directions. *Nat Clin Pract Oncol* 2007;4(3):172–180.
2. Steel GG, Peckham MJ. Exploitable mechanisms in combined radiotherapy-chemotherapy: The concept of additivity. *Int J Radiat Oncol Biol Phys* 1979;5(1):85–91.
3. Seiwert TY, Salama JK, Vokes EE. The concurrent chemoradiation paradigm – general principles. *Nat Clin Pract Oncol* 2007;4(2):86–100.
4. Higgins GS, O’Cathail SM, Muschel RJ, et al. Drug radiotherapy combinations: Review of previous failures and reasons for future optimism. *Cancer Treat Rev* 2015;pii: S0305-7372(14)00217-5.
5. Liebmann J, Cook JA, Fisher J, et al. In vitro studies of taxol as a radiation sensitizer in human tumor cells. *J Natl Cancer Inst* 1994;86:441–446.
6. Choe KS, Salama JK, Stenson KM, et al. Adjuvant chemotherapy prior to postoperative concurrent chemoradiotherapy for locoregionally advanced head and neck cancer. *Radiother Oncol* 2010;97:318–321.

7. Piccart M. The role of taxanes in the adjuvant treatment of early stage breast cancer. *Breast Cancer Res Treat* 2003;79(Suppl 1):S25–S34.
8. Donehower RC, Rowinsky EK. An overview of experience with Taxol (paclitaxel) in the U.S.A. *Cancer Treat Rev* 1993;19(Suppl C):63–78.
9. Bollag DM, McQueney PA, Zhu J, et al. Epothilones, a new class of microtubule-stabilizing agents with a taxol-like mechanism of action. *Cancer Res* 1995;55:2325–2333.
10. Kowalski RJ, Giannakakou P, Hamel E. Activities of the microtubule-stabilizing agents epothilones A and B with purified tubulin and in cells resistant to paclitaxel (Taxol®). *J Biol Chem* 1997;272:2534–2541.
11. Agrawal NR, Ganapathi R, Mekhail T. Tubulin interacting agents: novel taxanes and epothilones. *Curr Oncol Rep* 2003;5: 89–98.
12. Argyriou AA, Marmiroli P, Cavaletti G, et al. Epothilone-induced peripheral neuropathy: a review of current knowledge. *J Pain Symptom Manage* 2011;42:931–940.
13. Rothermel J, Wartmann M, Chen T, et al. EPO906 (epothilone B): a promising novel microtubule stabilizer. *Semin Oncol* 2003;30(Suppl 6):51–55.
14. Larkin JMG. Patupilone. Antimitotic drug, microtubule-stabilizing agent, oncolytic. *Drugs Future* 2007;32:323–336.
15. Hofstetter B, Voung V, Broggin-Tenzer A, et al. Patupilone acts as radiosensitizing agent in multidrug-resistant cancer cells in vitro and in vivo. *Clin Cancer Res* 2005;11:1588–1596.
16. Bley CR, Jochum W, Orłowski K, et al. Role of the microenvironment for radiosensitization by patupilone. *Clin Cancer Res* 2009;15:1335–1342.
17. Baumgart T, Klautke G, Kriesen S, et al. Radiosensitizing effect of epothilone B on human epithelial cancer cells. *Strahlenther Onkol* 2012;188:177–184.
18. Baumgart T, Kriesen S, Hildebrandt G, et al. Effect of epothilone B on cell cycle, metabolic activity, and apoptosis induction on human epithelial cancer cells - under special attention of combined treatment with ionizing radiation. *Cancer Invest* 2012;30(8):593–603.
19. Furmanova-Hollenstein P, Broggin-Tenzer A, Eggel M, et al. The microtubule stabilizer patupilone counteracts ionizing radiation-induced matrix metalloproteinase activity and tumor cell invasion. *Radiat Oncol* 2013;8:105.
20. Fogh S, Machtay M, Werner-Wasik M, et al. Phase I trial using patupilone (epothilone B) and concurrent radiotherapy for central nervous system malignancies. *Int J Radiat Oncol Biol Phys* 2010;77:1009–1016.
21. Oehler C, von Bueren AO, Furmanova P, et al. The microtubule stabilizer patupilone (epothilone B) is a potent radiosensitizer in medulloblastoma cells. *Neuro Oncol* 2011;13:1000–1010.
22. Pentenero M, Donadini A, Di Nallo E, et al. Distinctive chromosomal instability patterns in oral verrucous and squamous cell carcinomas detected by high-resolution DNA flow cytometry. *Cancer* 2011;117(22):5052–5057.
23. Swanton C, Nicke B, Schuett M, et al. Chromosomal instability determines taxane response. *Proc Natl Acad Sci USA* 2009;106(21):8671–8676.
24. Mansilla S, Llovera L, Portugal J. Chemotherapeutic targeting of cell death pathways. *Anticancer Agents Med Chem* 2012;12(3):226–238.
25. Stalder MW, Anthony CT, Woltering EA. Metronomic dosing enhances the anti-angiogenic effect of epothilone B. *J Surg Res* 2011;169:247–256.
26. Beswick RW, Ambrose HE, Wagner SD. Nocodazole, a microtubule de-polymerising agent, induces apoptosis of chronic lymphocytic leukaemia cells associated with changes in Bcl-2 phosphorylation and expression. *Leuk Res* 2006;30:427–436.
27. Kallas A, Pook M, Maimets M, et al. Nocodazole treatment decreases expression of pluripotency markers Nanog and Oct4 in human embryonic stem cells. *PLoS One* 2011;6:e19114.

28. Reiss M, Brash DE, Munoz-Antonia T, et al. Status of the p53 tumor suppressor gene in human squamous carcinoma cell lines. *Oncology Res* 1992;4:349–357.
29. Oliver FJ, de la Rubia G, Rolli V, et al. Importance of poly(ADP-ribose) polymerase and its cleavage in apoptosis. Lesson from an uncleavable mutant. *J Biol Chem* 1998;273:33533–33539.
30. Pendergrass W, Wolf N, Poot M. Efficacy of MitoTracker Green and CMXRosamine to measure changes in mitochondrial membrane potentials in living cells and tissues. *Cytometry A* 2004;61(2):162–169.
31. Haga N, Fujita N, Tsuruo T. Mitochondrial aggregation precedes cytochrome c release from mitochondria during apoptosis. *Oncogene* 2003;22(36):5579–5585.
32. Zanet J, Freije A, Ruiz M, et al. A mitosis block links active cell cycle with human epidermal differentiation and results in endoreplication. *PLoS One* 2010;5(12):e15701.
33. Chiu WH, Luo SJ, Chen CL, et al. Vinca alkaloids cause aberrant ROS-mediated JNK activation, Mcl-1 downregulation, DNA damage, mitochondrial dysfunction, and apoptosis in lung adenocarcinoma cells. *Biochem Pharmacol* 2012;83(9):1159–1171.
34. Wolanin K, Magalska A, Mosieniak G, et al. Curcumin affects components of the chromosomal passenger complex and induces mitotic catastrophe in apoptosis-resistant Bcr-Abl-Expressing cells. *Mol Cancer Res* 2006;4(7):457–469.
35. Xiao Z, Xue J, Semizarov D, et al. Novel indication for cancer therapy: Chk1 inhibition sensitizes tumor cells to antimetabolites. *Int J Cancer* 2005;115(4):528–538.
36. Countryman PI, Heddle JA. The production of micronuclei from chromosome aberrations in irradiated cultures of human lymphocytes. *Mutat Res* 1976;41(2–3):321–332.
37. Weaver BA, Cleveland DW. Decoding the links between mitosis, cancer, and chemotherapy: The mitotic checkpoint, adaptation, and cell death. *Cancer Cell* 2005;8(1):7–12.
38. Portugal J, Bataller M, Mansilla S. Cell death pathways in response to antitumor therapy. *Tumori* 2009;95:409–421.
39. Pellicciotta I, Yang CP, Venditti CA, et al. Response to microtubule-interacting agents in primary epithelial ovarian cancer cells. *Cancer Cell Int* 2013;10:13(1):33.
40. May P, May E. Twenty years of p53 research: structural and functional aspects of the p53 protein. *Oncogene* 1999;18(53):7621–7636.
41. Weller M. Predicting response to cancer chemotherapy: the role of p53. *Cell Tissue Res* 1998;292(3):435–445.
42. Tokalov SV, Abolmaali N. Radiosensitization of p53-deficient lung cancer cells by pre-treatment with cytostatic compounds. *Anti-cancer Res* 2012;32:1239–1244.
43. Nur-E-Kamal A, Gross SR, Pan Z, et al. Nuclear translocation of cytochrome c during apoptosis. *J Biol Chem* 2004;279(24):24911–24914.
44. Khawaja NR, Carré M, Kovacic H, et al. Patupilone-induced apoptosis is mediated by mitochondrial reactive oxygen species through Bim relocation to mitochondria. *Mol Pharmacol* 2008;74(4):1072–1083.
45. Ricci MS, Zong WX. Chemotherapeutic approaches for targeting cell death pathways. *Oncologist* 2006;11(4):342–357.
46. Ha GH, Baek KH, Kim HS, et al. P53 activation in response to mitotic spindle damage requires signaling via BubR1-mediated phosphorylation. *Cancer Res* 2007;67(15):7155–7164.
47. D'Amours D, Sallmann FR, Dixit VM, et al. Gain-of-function of poly(ADP-ribose) polymerase-1 upon cleavage by apoptotic proteases: implications for apoptosis. *J Cell Sci* 2001;114(Pt 20):3771–3778.
48. Chen JG, Yang CP, Cammer M, et al. Gene expression and mitotic exit induced by microtubule-stabilizing drugs. *Cancer Res* 2003;63:7891–7899.
49. Lee SH, Son SM, Son DJ, et al. Epothilones induce human colon cancer SW620 cell apoptosis via the tubulin polymerization-independent activation of the nuclear factor- κ B/I κ B kinase signal pathway. *Mol Cancer Ther* 2007;6(10):2786–2797.
50. Lin B, Catley L, LeBlanc R, et al. Patupilone (epothilone B) inhibits growth and survival of multiple myeloma cells in vitro and in vivo. *Blood* 2005;105:350–357.
51. Wang M, Wu W, Wu W, et al. PARP-1 and Ku compete for repair of DNA double strand breaks by distinct NHEJ pathways. *Nucleic Acids Res* 2006;34(21):6170–6182.
52. Bröker LE, Huisman C, Ferreira CG, et al. Late activation of apoptotic pathways plays a negligible role in mediating the cytotoxic effects of discodermolide and epothilone B in non-small cell lung cancer cells. *Cancer Res* 2002;62:4081–4088.
53. Rogalska A, Gajek A, Marczak A. Epothilone B induces extrinsic pathway of apoptosis in human SKOV-3 ovarian cancer cells. *Toxicol In Vitro* 2014;28(4):675–683.
54. Galluzzi L, Vitale I, Abrams JM, et al. Molecular definitions of cell death subroutines: recommendations of the Nomenclature Committee on Cell Death 2012. *Cell Death Differ* 2012;19(1):107–120.
55. Winsel S, Sommer A, Eschenbrenner J, et al. Molecular mode of action and role of TP53 in the sensitivity to the novel epothilone sagopilone (ZK-EPO) in A549 non-small cell lung cancer cells. *PLoS One* 2011;6(4):e19273.
56. Bekier ME, Fischbach R, Lee J, et al. Length of mitotic arrest induced by microtubule-stabilizing drugs determines cell death after mitotic exit. *Mol Cancer Ther* 2009;8(6):1646–1654.
57. Zhang C, Zhao L, Qi W, et al. Simultaneous determination of epothilone D and its hydrolytic metabolite in human plasma by high performance liquid chromatography-tandem mass spectrometry for pharmacokinetic studies. *J Chromatogr B Analyt Technol Biomed Life Sci* 2009;877(29):3748–3752.
58. Fenech M. The in vitro micronucleus technique. *Mutat Res* 2000;455(1–2):81–95.
59. Lichtner RB, Rotgeri A, Bunte T, et al. Subcellular distribution of epothilones in human tumor cells. *Proc Natl Acad Sci USA* 2001;98(20):11743–11748.
60. Swanton C, Nicke B, Schuett M, et al. Chromosomal instability determines taxane response. *Proc Natl Acad Sci USA* 2009;106(21):8671–8676.

Supplemental Material Available Online

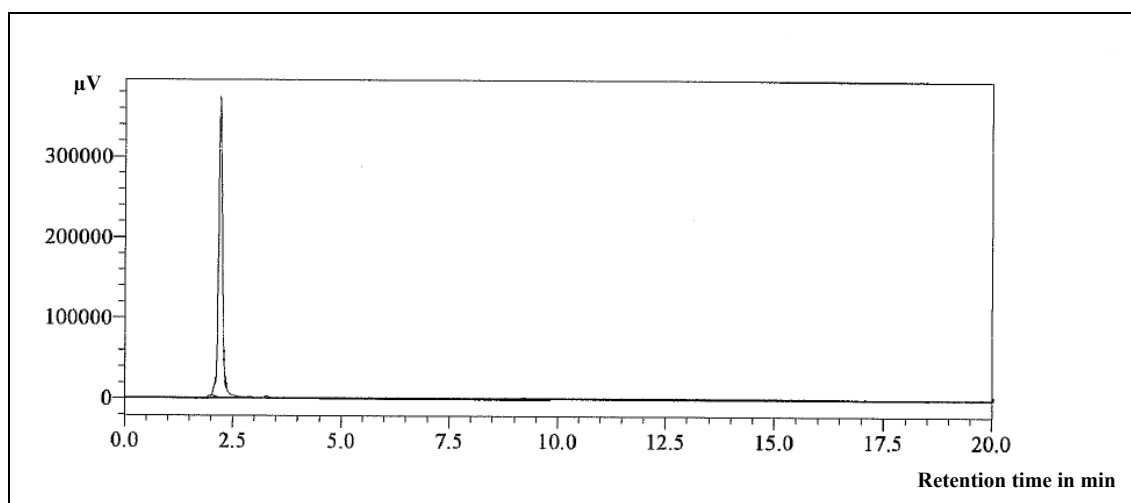
Supplemental file 1: HPLC measurement to study the stability of epothilone B molecules in the medium. (A) Representative HPLC-spectrum of 10 nM epothilone B in the media. (B) Examination of the peak area of the measured HPLC-spectra of different samples. (n = 1).

Supplemental file 2: Protein expression after 10 nM epothilone B treatment by western blot analysis. A variety of tested cell death-related antibodies and the densitometric analysis of the protein-levels in the cell lysates after 48 hours of drug exposure are presented. A densitometric analysis of the protein-levels, normalized to the control bands of beta-actin, was performed. (n = 1) Horizontal lines in the table mean “no protein detectable.”

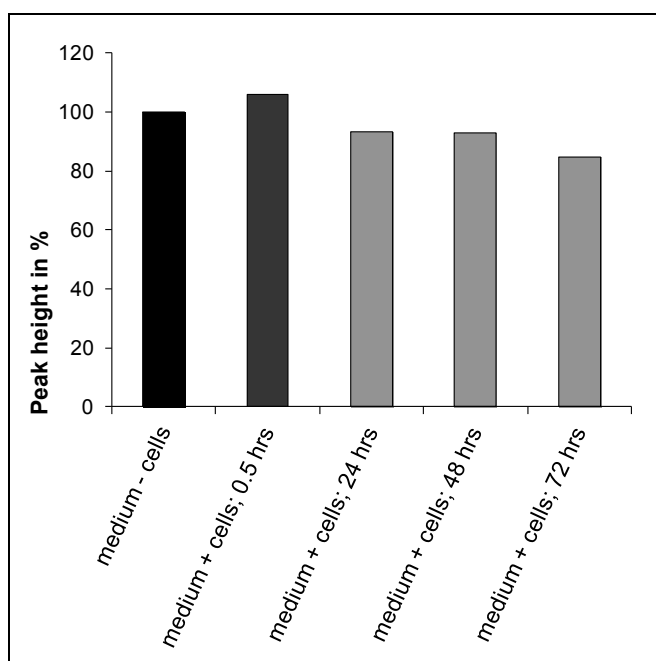
Supplemental file 3: Immunofluorescence imaging of: (A) Cytochrome C stained cells after incubation with 10 nM epothilone B for 27 hours. DMSO-treated control cells (above) and epothilone B-incubated cells (below) stained with cytochrome C antibody. (B) MitoTracker Green FM stained cells after incubation of 48 hours with 10 nM epothilone B. DMSO-treated control cells (above) and epothilone B-incubated cells (below) stained with MitoTracker Green FM.

Supplemental file 1

A)



B)



Supplemental file 2

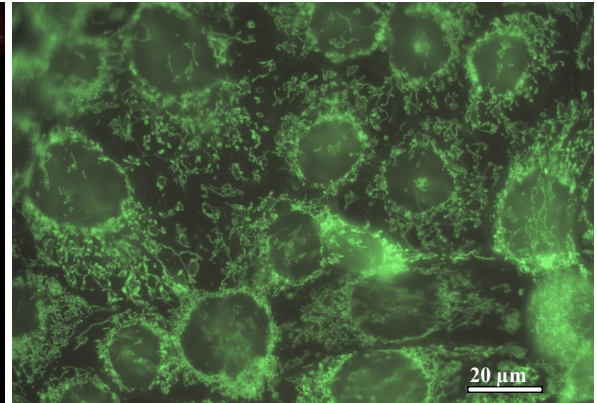
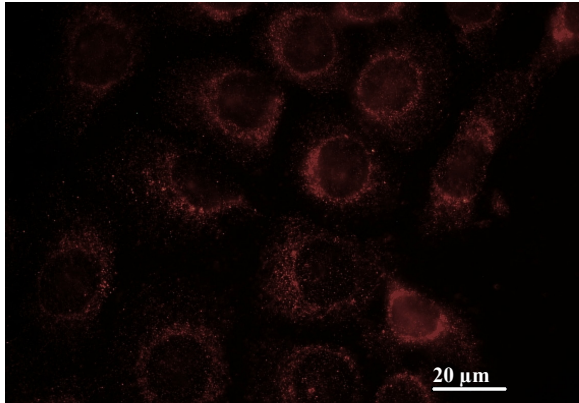
Proteins	Molecular Weight [kDa]	FaDu cells		A549 cells	
		DMSO control	10 nM epothilone B	DMSO control	10 nM epothilone B
Apaf-1	130	-	-	-	-
Bad	23	-	-	-	-
Bax	21	0.85	1.88	0.93	0.84
Caspase 3/ CPP32 (IgG1)	32	-	-	-	-
Caspase 7/ MCH-3	35	0.96	0.65	0.53	0.77
FADD	24	0.89	1.23	0.76	0.79
Fas/ CD95/ Apo-1	45	-	-	-	-
TRADD	34	-	-	0.45	0.51
Bcl-2	26	-	-	-	-
hILP/ XIAP	57	1.02	0.20	0.23	0.86
Nip 1	26	0.89	1.14	0.72	0.87

Supplemental file 3

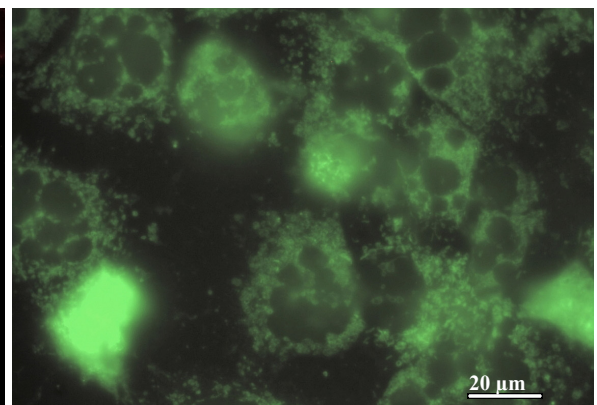
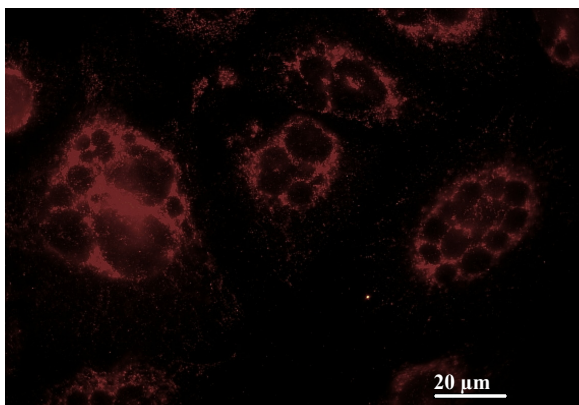
A) Cytochrome C staining

B) MitoTracker Green FM staining

DMSO treated cells



Epothilone B-incubated cells



4 Diskussion

In der vorliegenden Arbeit ist der Naturstoff Epothilon B auf seine potentielle Eignung als Chemotherapeutikum kombiniert mit ionisierender Strahlung in der Behandlung von epithelialen Tumorzellen geprüft worden. Dabei wurden die zytotoxischen und strahlensensibilisierenden Eigenschaften von Epothilon B sowie ausgewählte Zelltod-Signalwege anhand der beiden Tumorzelllinien FaDu und A549 untersucht.

4.1 Zytotoxischer Effekt von Epothilon B

4.1.1 Hemmung der Zellproliferation

Der potentielle Einsatz von Epothilonen in der Behandlung von Tumoren wurde durch die Entdeckung ihrer proliferationshemmenden Wirkung auf tierische Zellen ermöglicht [BOLLAG et al., 1995]. Seitdem wurden eine Vielzahl von Studien veröffentlicht, die den wachstumshemmenden Effekt von Epothilon B auf verschiedene humane Tumorzelllinien belegen [KOWALSKI et al., 1997; ALTMANN et al., 2000; BOCCI et al., 2002; ROHRER BLEY et al., 2009; OEHLER et al., 2011; ROGALSKA et al., 2013, u.a.].

Unsere Experimente zeigten, dass Epothilon B eine konzentrationsabhängige proliferationshemmende Wirkung auf die beiden getesteten epithelialen Tumorzelllinien ausübte, wobei die IC_{50} -Werte im niedrigen nanomolaren Bereich lagen. Die A549-Zellen reagierten dabei geringfügig sensitiver auf die Wirkstoffgabe als die FaDu-Zellen. Außerdem konnte nachgewiesen werden, dass die Hemmung der Zellproliferation von diversen Faktoren, wie der ausplattierten Zellzahl sowie der Anwendung unterschiedlicher Versuchsansätze, beispielweise einmalige versus tägliche Wirkstoffgabe, abhängig war [BAUMGART et al., 2012 (**Publikation 1**)].

4.1.2 Beeinflussung der metabolischen Aktivität

Die metabolische Aktivität der mit Etoposin B behandelten und bestrahlten FaDu- und A549-Tumorzellen wurde mittels EZ4U-Proliferationstests untersucht. Nach einer einstündigen Wirkstoffinkubation trat dabei eine konzentrationsabhängige Abnahme der metabolischen Aktivität auf [BAUMGART et al., 2012 (**Publikation 2**)], was als ein Zeichen für die Anreicherung der Etoposin B-Moleküle in den Tumorzellen gedeutet werden kann. Dieser Effekt wurde durch Lichtner und Mitarbeiter beschrieben [LICHTNER et al., 2001]. Sie wiesen nach, dass die Aufnahme von Etoposin B in die Zellen konzentrations- sowie zelltypabhängig war und eine Sättigung der Wirkstoffaufnahme in die Zellen nach zwei Stunden erreicht wurde. Desweiteren zeigten unsere Experimente, dass eine 24-stündige Etoposin B Inkubation mit anschließender Bestrahlung keine deutlichen Unterschiede in der Beeinflussung der metabolischen Aktivität zwischen den bestrahlten Etoposin B-behandelten und nichtbestrahlten wirkstoffinkubierten Proben hervorriefen. Somit ist anzunehmen, dass der toxische Effekt von Etoposin B dominanter ausgeprägt war als der schädigende Effekt der Bestrahlung [BAUMGART et al., 2012 (**Publikation 2**)].

4.1.3 Mikrotubuli-stabilisierende Wirkung

Übereinstimmend mit anderen Veröffentlichungen [beispielsweise BOLLAG et al., 1995; KOWALSKI et al., 1997; SEPP-LORENZINO et al., 1999; LEE et al., 2001; CHEN et al., 2003] konnte durch unsere Experimente die Mikrotubuli-stabilisierende Wirkungsweise von Etoposin B in den epithelialen Tumorzellen nachgewiesen werden.

Durch eine Antikörpermarkierung der Tubulin-Moleküle konnte mittels Fluoreszenzmikroskopie beobachtet werden, dass Etoposin B die Bildung von kompakten Mikrotubuli-Bündeln verursachte. Dabei bildeten sich charakteristische Mikrotubuli-Formationen in den epithelialen Tumorzellen, so dass das Mikrotubuli-Bildungszentrum (Zentrosom) durch das dichte Mikrotubuli-Netzwerk maskiert wurde [BAUMGART et al., 2012 (**Publikation 1**)].

Zusätzlich wurde ein Tubulin-Polymerisationsassay mit anschließender SDS-Gelelektrophorese zur Untersuchung der Interaktion von Etoposid B mit gereinigtem α - und β -Tubulin unter Anwesenheit von GTP und BRB80-Puffer durchgeführt. Dabei zeigte sich, dass die Fähigkeit von Etoposid B, Mikrotubuli-Filamente aus den Tubulin-Untereinheiten aufzubauen, um den Faktor 1,49 stärker ausgeprägt war als die des klinisch eingesetzten Chemotherapeutikums Paclitaxel [BAUMGART et al., 2012 (**Publikation 1**)]. Weiterführende Experimente anderer Forschergruppen offenbarten, dass Etoposid B sogar den Aufbau von Tubulin-Filamenten unter Abwesenheit von GTP und/oder Mikrotubuli-assoziierten Proteinen bewirkt [KOWALSKI et al., 1997] sowie, dass die entstandenen Mikrotubuli-Filamente nur aus acht bis neun anstatt der normalerweise nötigen 13 Protofilamenten bestanden [BOLLAG et al., 1995]. Durch Yu et al. konnte gezeigt werden, dass die durch Etoposid B gebildeten Mikrotubuli-Filamente weniger starr waren als die Paclitaxel-stabilisierten Mikrotubuli-Bündel [YU et al., 2013]. Sie vermuteten, dass die Mikrotubuli-Stabilisatoren nicht einfach „native“ Mikrotubuli nachbilden, sondern die Mikrotubuli in Struktur, Funktion und Mechanismus umgestalten.

4.2 Einfluss von Etoposid B auf die Strahlenempfindlichkeit der Tumorzellen

4.2.1 Strahlensensibilisierender Effekt

Durch unsere Experimente zur Koloniebildungsfähigkeit der bestrahlten epithelialen Tumorzellen konnte nachgewiesen werden, dass Etoposid B die Strahlenempfindlichkeit der getesteten Tumorzellen signifikant erhöht. Die kombinierte Anwendung von Etoposid B und ionisierender Strahlung resultierte in einem supraadditiven (synergistischen) strahlensensibilisierenden Effekt, deren Ausprägung von der Inkubationszeit mit Etoposid B vor der Bestrahlung sowie der angewendeten Wirkstoffkonzentration abhängig war [BAUMGART et al., 2012 (**Publikation 1**)]. Eine Abhängigkeit vom Zeitraum der Wirkstoffapplikation vor der Bestrahlung wurde ebenfalls für verschiedene andere Substanzen publiziert [zum Beispiel NIERO et al., 1999; CHALMERS et al., 2009; MANDA et al., 2011].

Die dokumentierten strahlensensibilisierenden Effekte von Etoposid sind je nach untersuchtem Zelltyp unterschiedlich ausgeprägt. Übereinstimmend mit unseren Ergebnissen, publizierte beispielsweise Hofstetter et al. für die humane Paclitaxel-resistente Kolonkarzinom-Zelllinie SW 480, dass eine supraadditive strahlensensibilisierende Wirkung *in vitro* beobachtet wurde sowie eine zumindest additive Wirkung *in vivo* [HOFSTETTER et al., 2005]. Dagegen konnte durch die Arbeitsgruppe um Bley, für die ebenfalls von uns untersuchte A549-Tumorzelllinie, *in vitro* nur ein additiver strahlensensibilisierender Effekt festgestellt werden; in Maus-Tumor-Xenograft-Modellen zeigte sich jedoch eine supraadditive Wirkung von Etoposid [ROHRER BLEY et al., 2009]. Die Ursachen für diese unterschiedlichen Ergebnisse lassen sich u.a. auf die Einwirkung der Tumormikroumgebung zurückführen, die zusätzlich strahlensensibilisierende Einflüsse aufweist. Bley und Kollegen veröffentlichten, dass Etoposid eine Hemmung der Angiogenese verursachte, welche einerseits in einem direkten Effekt durch die toxische Wirkung auf die Endothelzellen und andererseits in einem durch die Tumorzellen vermittelten indirekten Effekt begründet war. Dabei kam es zu einer Hemmung oder verminderten Expression bestimmter für die Angiogenese und Hypoxie-Adaption wichtiger Gene und Proteine. Oehler und Kollegen konnten für drei humane Medulloblastom-Zelllinien vergleichbare Ergebnisse demonstrieren, *in vitro* mindestens eine additive Strahlensensibilisierung und *in vivo* einen starken supraadditiven Effekt [OEHLER et al., 2011].

Desweiteren wurde für eine modifizierte Prostatakarzinom-Zelllinie, PC3 shDAB2IP, eine konzentrationsabhängige supraadditive Wirkung von Etoposid publiziert [KONG et al., 2010] und für die Fibrosarkom-Zelllinie HT1080 konnte ein additiver Effekt auf die Strahlensensibilisierung beschrieben werden [FURMANOVA-HOLLENSTEIN et al., 2013]. Die unterschiedlichen strahlensensibilisierenden Effekte von Wirkstoffen in den verschiedenen Zelllinien lassen sich mit den veränderten Mechanismen bzw. Signalkaskaden erklären, die je nach Tumorzelltyp mutiert sind. Diese Mechanismen bzw. Signalkaskaden sind unter anderem verantwortlich für eine veränderte Zellzyklusregulierung oder auch Defekte in der DNA-Reparatur [PETERSEN & DIKOMEY, 2011].

4.2.2 Zellzyklusveränderung

Ein Zellzyklusarrest in der strahlensensiblen G2/M-Zellzyklusphase wird in der Literatur als Hauptbegründung für eine wirkstoffinduzierte Radiosensibilisierung angeführt [PAWLIK & KEYOMARSI, 2004]. Deshalb wurde der Einfluss von Etoposid B und ionisierender Strahlung auf die Zellzyklusverteilung mittels Propidiumiodid-Färbung durchflusszytometrisch untersucht. Durch die Zellzyklusmessungen konnte ein signifikanter konzentrations- und zeitabhängiger G2/M-Zellzyklusarrest festgestellt werden [BAUMGART et al., 2012 (**Publikation 2**)]. Unsere Ergebnisse ergänzen andere Studien mit verschiedenen Zelllinien [beispielsweise SEPP-LORENZINO et al., 1999; ALTMANN et al., 2000; CHEN & HORWITZ, 2002; CHEN et al., 2003; KHABELE et al., 2004; OEHLER et al., 2011].

Traditionell werden Mikrotubuli-interagierende Substanzen zur Behandlung von Tumorerkrankungen in der maximal tolerierbaren Dosis eingesetzt [ROHRER BLEY et al., 2013]. Dementsprechend wurde für die Experimente der vorliegenden Arbeit eine Etoposid B-Konzentration von 10 nM verwendet, welches der maximal tolerierbaren Wirkstoffdosis im menschlichen Blutplasma entspricht [STALDER et al., 2011]. Interessanterweise wurde für niedrig dosierte Etoposid B-Konzentrationen ebenfalls eine Radiosensibilisierung publiziert, die aber G2/M-unabhängig auftrat und bei der die Kombination aus Wirkstoff und Bestrahlung einen vorübergehenden Zellzyklusarrest der Tumorzellen in der S-Phase hervorrief [HOFSTETTER et al., 2005]. Eine starke Akkumulation der Tumorzellen in der S-Phase des Zellzyklus konnte bei unseren Experimenten ebenfalls bei niedrigen Wirkstoffkonzentrationen von 2,5 nM und 5 nM Etoposid B beobachtet werden [BAUMGART et al., 2012 (**Publikation 2**)]. Allerdings wurden weiterführende Experimente mit einer Konzentration von 10 nM Etoposid B durchgeführt, da dort bei beiden Zelllinien der stärkste G2/M-Zellzyklusarrest gemessen wurde.

Unsere Experimente zeigten außerdem, dass bei den A549-Zellen der durch Etoposid B ausgelöste Zellzyklusarrest in der G2/M-Phase stärker und langanhaltender ausgeprägt war als bei den FaDu-Zellen. Überdies war in beiden Zelllinien der Zellzyklusstopp in der strahlensensiblen G2/M-Phase zum Zeitpunkt 24 Stunden nach Wirkstoffzugabe am stärksten ausgebildet. Somit wäre dieser Zeitpunkt zur Bestrahlung des Patienten in der klinischen Praxis günstig. Dem G2/M-Zellzyklusstopp folgten ein Anstieg der apoptotischen Zellen im SupG1-Peak (hypodiploide Zellen) sowie die Bildung einer hyperdiploiden Zellpopulation, welche besonders bei den FaDu-Zellen auffällig war [BAUMGART et al., 2012 (**Publikation 2**)].

4.2.3 Reduktion der DNA-Reparaturkapazität

Mit Hilfe von zwei Untersuchungsmethoden wurde die Bildung von strahleninduzierten DNA-Doppelstrangbrüchen sowie der Effekt von Etoposid B auf die DNA-Reparaturkapazität der Tumorzellen untersucht. Denn eine Beeinflussung der Reparaturfähigkeit von DNA-Schäden wird als ein weiterer Mechanismus der zellulären Strahlensensibilisierung angesehen [PÖTTER et al., 2012].

Der γ H2AX-Test dient als Nachweis für strahleninduzierte DNA-Doppelstrangbrüche, die durch eine Antikörpermarkierung von phosphorylierten γ H2AX-Histonen ausgewertet werden können, welche bei der enzymatischen Markierung der DNA-Schäden entstehen [REDON et al., 2009]. Die Experimente belegten, dass die kombinierte Behandlung der epithelialen Tumorzellen mit Etoposid B und ionisierender Strahlung einen konzentrationsabhängigen Anstieg von DNA-Schäden in den behandelten Zellen hervorrief. Dieser beobachtete Anstieg von residualen Doppelstrangbrüchen deutet auf eine durch Etoposid B induzierte Reduzierung der DNA-Reparaturkapazität der Tumorzellen hin [BAUMGART et al., 2012 (**Publikation 1**)].

Der Mikrokernstest gilt als einer der bevorzugten Untersuchungsmethoden, um Chromosomenschäden zu beurteilen und er erlaubt eine zuverlässige Messung von Chromosomenverlusten und -abbrüchen [FENECH, 2000]. Unsere Studien zeigten, dass die kombinierte Anwendung von Etoposid B und Bestrahlung die Mikrokernrate erhöht, verglichen mit den bestrahlten Kontrollproben. Somit wurde die Fähigkeit der Tumorzellen zur DNA-Reparatur nach Strahleneinwirkung durch die Etoposid B-Gabe signifikant eingeschränkt. Mittels des Mikrokerntests konnten damit die Ergebnisse vom γ H2AX-Test bekräftigt werden [BAUMGART et al., 2015 (**Publikation 3**)].

Die Zusammenhänge einer durch Etoposid B hervorgerufenen verminderten DNA-Reparaturfähigkeit sind noch nicht eindeutig geklärt. Allerdings wurde eine starke Anreicherung der Etoposid B-Moleküle im Zellkern bzw. in der Fraktion der nukleären Proteine publiziert und eine Interaktion mit diesen Proteinen, wie beispielsweise dem

nukleären Tubulin-Isotyp, könnte zu einer eingeschränkten Funktionsfähigkeit der Proteine im Zellkern führen [LICHTNER et al., 2001]. Daneben wurde eine weitere Hypothese veröffentlicht, dass die Wirkung von Mikrotubuli-stabilisierenden Substanzen auch auf eine Beeinflussung von Genen zurückzuführen ist, welche bei der DNA-Reparatur eine Rolle spielen [SWANTON et al, 2009]. Bei einer verringerten Expression dieser Gene, wie zum Beispiel BRCA1 oder H2AFX, könnten bestimmte DNA-Reparatursysteme (Mismatch-Reparatur oder Homologe Rekombination) nicht erfolgreich gestartet werden.

Neben unseren Untersuchungen zeigten ebenfalls Kong und Mitarbeiter für die modifizierte Prostatakarzinom-Zelllinie PC3 shDAB2IP, dass die Epothilon B-vermittelte Radiosensibilisierung der Tumorzellen assoziiert ist mit einer Hemmung der DNA-Doppelstrangbruch-Reparaturkinetik [KONG et al., 2010]. Sie vermuteten eine Ausschaltung der schnelleren Komponenten bei der Doppelstrangbruch-Reparatur, welche dem Reparatursystem Non-homologes end joining zugeschrieben werden.

4.3 Zelltod durch Apoptose

4.3.1 Expression von proapoptischen Proteinen

Anhand von mehreren Untersuchungsmethoden konnte unsere Arbeitsgruppe Anzeichen für eine durch Epothilon B, allein sowie kombiniert mit Bestrahlung, ausgelöste Apoptose dokumentieren [BAUMGART et al, 2012 (**Publikation 2**); BAUMGART et al., 2015 (**Publikation 3**)].

Zunächst wurden Messungen mit dem Durchflusszytometer durchgeführt. Erste Anzeichen für einen durch Epothilon B ausgelösten apoptotischen Zelltod konnten während der Zellzyklusmessungen als SubG1-Peak festgestellt werden. Während der Apoptose kommt es zum Abbau der DNA in den Zellen und somit zur Bildung einer hypodiploiden Zellpopulation (SubG1-Peak). Zur Bestätigung dieser Beobachtungen wurden anschließend AnnexinV-FITC/7AAD-Färbungen der Tumorzellen durchgeführt. Dabei zeigte sich, dass durch die Epothilon B-Inkubation die Detektion von externalisiertem Phosphatidylserin, als ein charakteristisches Anzeichen für eine frühe Apoptose, nachgewiesen werden konnte. Allerdings waren nur geringe Unterschiede bei der Apoptose-

Induktion zwischen den bestrahlten und nichtbestrahlten wirkstoffinkubierten Proben zu dokumentieren [BAUMGART et al., 2012 (**Publikation 2**)].

Interessanterweise war der Anteil an Zellen im apoptotischen SubG1-Peak während der Zellzyklusanalyse höher als der nachgewiesene prozentuale Anteil an Zellen während der AnnexinV/7AAD-Messung. Diese Beobachtungen veröffentlichten ebenfalls die Forscher Chen und Horwitz und vermuteten, dass nicht alle Zellen vom SubG1-Peak apoptotisch sind, sondern als hypodiploide Zellpopulation lebensfähig bleiben [CHEN & HORWITZ, 2002].

Western Blot Experimente wurden zur weiteren Analyse von apoptotischen Signalwegen genutzt. Basierend auf den Ergebnissen von Vorversuchen wurden die Apoptosemarker p53 für die A549-Zellen und Poly-(ADP)-Ribose-Polymerase 1 (PARP1) für die FaDu-Zellen ausgesucht, da bei diesen beiden Proteinen starke Veränderungen im Expressionsmuster zwischen den Kontrollen und den mit Etoposin B-inkubierten Proben vorlagen.

Die Anwendung von Etoposin B, allein und in Kombination mit Bestrahlung, induzierte eine zeitabhängige Expression von proapoptotischen Proteinen, 48 Stunden nach der Wirkstoffzugabe. In den A549-Zellen, welche den p53 Wildtyp aufweisen, konnte eine Etoposin B-induzierte Expression des Tumorsuppressors p53 nachgewiesen werden, wohingegen eine PARP1-Spaltung nicht dokumentiert werden konnte. In den FaDu-Zellen, welche nur eine mutierte Form des p53 Proteins bilden, konnte demgegenüber das große PARP1-Spaltprodukt nachgewiesen werden [BAUMGART et al., 2015 (**Publikation 3**)].

Da die Zelltod-Signalwege abhängig sind von der funktionsfähigen Expression des Tumorsuppressors p53 [PORTUGAL et al., 2009] und ein p53 Polymorphismus den Behandlungserfolg in der Klinik beeinflusst [PELLICCIOTTA et al., 2013], wurden die Untersuchungen unter Berücksichtigung des p53-Status der Tumorzellen durchgeführt. Während die A549-Zellen die Normalform des p53-Proteins bilden, weisen die FaDu-Zellen eine Mutation auf und exprimieren nur eine stark verringerte Menge des veränderten p53 Transkripts [REISS et al., 1992].

Bei der Einleitung des intrinsischen apoptotischen Signalweges spielt der Tumorsuppressor p53 eine wichtige Rolle. Durch das p53 Protein werden verschiedene Effektorcaspasen aktiviert, so dass es zur Freisetzung bestimmter apoptotischer Faktoren, wie zum Beispiel Cytochrom C aus den Mitochondrien kommt [RICCI & ZONG, 2006]. Die Aktivierung des Tumorsuppressors p53 kann nicht nur durch eine Schädigung der DNA erfolgen, sondern

auch durch eine Störung des Mikrotubuli-Spindelapparates [HA et al., 2007]. Das in dieser Arbeit ebenfalls untersuchte Protein PARP1 wird proteolytisch durch eine Caspase 3-Spaltung aktiviert und gilt deshalb ebenfalls als Apoptosemarker [OLIVER et al., 1998]. Allerdings kann eine Caspase 3-Spaltung sowohl im intrinsischen, durch eine Caspase 9 Aktivierung, als auch im extrinsischen Apoptose-Signalweg, durch eine Caspase 8 Spaltung, erfolgen [MANSILLA et al., 2012].

In der Literatur wurde ebenfalls für mehrere Zelllinien eine Etoposid-induzierte Apoptose beschrieben. Beispielsweise wurden für die Kolon-Tumorzelllinie SW620 eine durch Etoposid hervorgerufene Expression verschiedener proapoptotischer Proteine wie p53, Caspase 3 und Bax sowie die verminderte Expression des antiapoptotischen Proteins Bcl2 publiziert [LEE et al., 2007]. Für zwei verschiedene Myelom-Zelllinien veröffentlichten Lin und Kollegen ähnliche Untersuchungsergebnisse und zeigten, dass Etoposid eine Spaltung des Apoptosemarkers PARP1 hervorrief [LIN et al., 2005].

Abschließend ist den Untersuchungen zur Apoptose-Induktion durch Etoposid hinzuzufügen, dass apoptotische Signalwege durch Etoposid aktiviert werden, die aber Zelltyp-spezifisch ablaufen. Außerdem ist zu ergänzen, dass die relativ schwache Expression der proapoptotischen Proteine in den Western Blot Experimenten nicht den enormen Zellverlust nach 48-stündiger Wirkstoffinkubation erklärt, der in diversen Experimenten beobachtet werden konnte. Wir stimmen deshalb mit der Aussage von Bröker und Mitarbeiter überein, die vergleichbare Vermutungen über die untersuchten nicht-kleinzelligen Lungentumorzelllinien publizierten. Die Etoposid Inkubation der Tumorzellen führte zum Auftreten von verschiedenen apoptotischen Merkmalen, die sich aber erst relativ spät nach Wirkstoffzugabe zeigten und somit die Apoptose nicht als dominanter Zelltod-Mechanismus angesehen werden kann und alternative Zelltod-Wege für die zytotoxische Wirkung von Etoposid verantwortlich sind [BRÖKER et al., 2002]. Ähnliche Ergebnisse wurden von Oehler und Kollegen über die untersuchten Medulloblastom-Zelllinien veröffentlicht. Die Anwendung von Etoposid in Kombination mit Bestrahlung führte zu verschiedenen Zelltod-Mechanismen, die abhängig vom Zelltyp waren und die Anwendung von Caspase-Inhibitoren führte nicht zu einer Hemmung der Etoposid-beeinflussten Lebensfähigkeit der Tumorzellen. Diese Ergebnisse deuten darauf hin, dass die Apoptose als sekundärer Zelltod-Signalweg abläuft [OEHLER et al., 2011]. Für die Ovariatumorzelllinie SKOV-3 wurden Ergebnisse veröffentlicht, demzufolge die Etoposid-induzierte Apoptose durch den TRAIL (TNF-related apoptosis-inducing ligand)-vermittelten extrinsischen apoptotischen Signalweg

hervorgerufen wird [ROGALSKA et al., 2014]. Es lässt sich deshalb vermuten, dass der durch Epothilon B ausgelöste apoptotische Zelltod abhängig ist vom Tumortyp und sowohl auf dem intrinsischen als auch auf dem extrinsischen apoptotischen Signalweg ausgelöst werden kann.

4.3.2 Weitere apoptotische Anzeichen

Interessanterweise zeigten unsere Immunfluoreszenzfärbungen der behandelten epithelialen Tumorzelllinien mit anschließender lichtmikroskopischer Auswertung keine typischen Anzeichen einer Apoptose, was konträr zu anderen Veröffentlichungen ist, wie beispielsweise die publizierte Cytochrom C Freisetzung in zwei Neuroblastom-Zelllinien [KHAWAJA et al., 2008]. Typische Anzeichen einer Apoptose sind beispielweise die Freisetzung von Cytochrom C aus den Mitochondrien sowie eine Cytochrom C Konzentration im Zellkernbereich [NUR-E-KAMAL et al., 2004] oder auch eine reduzierte Fluoreszenzintensität der gefärbten Mitochondrien als Zeichen einer verminderten Membranintegrität [PENDERGRASS et al., 2004]. Die Antikörpermarkierung der Cytochrom C Proteine mit anschließender durchflusszytometrischer Messung bewies nur für die mit Nocodazol behandelten Positivkontrollen eine gesteigerte Fluoreszenzintensität im Gegensatz zu den mit Epothilon B inkubierten Proben, also den bestrahlten sowie den kombiniert behandelten Tumorzellen [BAUMGART et al., 2015 (**Publikation 3**)]. Als Ergebnis lässt sich zusammenfassen, dass in beiden Zelllinien durch die Positivkontrolle Nocodazol ein Cytochrom C Anstieg in den Zellen gemessen wurde, jedoch dieses Anzeichen einer Apoptose nicht durch Epothilon B ausgelöst werden konnte. Zu vermuten ist deshalb, dass durch Epothilon B apoptotische Signalwege ausgelöst werden, die jedoch nicht durch eine Cytochrom C-Freisetzung aus den Mitochondrien dokumentierbar sind.

4.4 Zelltod durch mitotische Katastrophe

4.4.1 Bildung von polyploiden Zellen

Zur genaueren Untersuchung der hyperdiploiden Zellpopulation, die während der Zellzyklusmessungen nachgewiesen werden konnte, erfolgte eine mikroskopische Bewertung der mit Bisbenzimid angefärbten Zellkerne. Nach einer 24-stündigen Inkubation mit Etoposin B konnte bei beiden Zelllinien ein hoher Prozentsatz an polyploiden bzw. multinukleären Zellen ausgezählt werden [BAUMGART et al., 2012 (**Publikation 2**)]. Die Bildung von polyploiden oder aneuploiden Zellen nach einem vorangegangenen Zellzyklusarrest ist ein typisches Zeichen für die mitotische Katastrophe, die durch bestimmte Wirkstoffe [RELO-VARONA et al., 2008] oder auch Strahlung ausgelöst werden kann [IANZINI et al., 2009].

Der zerstörerische Effekt von Etoposin B auf die Zellmorphologie und somit die Entstehung von polyploiden Zellen wurde ebenfalls für die Lungentumorzelllinie NCI-H460 nachgewiesen [BRÖKER et al., 2002] und ist auch für andere Mikrotubuli-stabilisierende Substanzen, wie Paclitaxel, bekannt [BLAGOSKLONNY et al., 2004].

4.4.2 Einleitung eines Zellzyklusarrestes

Zur Untersuchung weiterer Anzeichen für eine mitotische Katastrophe erfolgte die Anfärbung der Mitochondrien mit anschließender Messung im Durchflusszytometer. Dabei konnte ein Etoposin B- sowie ein strahlungsinduzierter Anstieg der mitochondrialen Expression dokumentiert werden [BAUMGART et al., 2015 (**Publikation 3**)]. Eine gesteigerte Menge an Mitochondrien in den Zellen wird als ein Anzeichen für einen Prometaphasen-Arrest gedeutet und das Auftreten eines langanhaltenden Zellzyklusarrest ist typisch bei einer mitotischen Katastrophe [GALLUZZI et al., 2012].

Zusätzlich konnte mittels durchflusszytometrischer Messungen eine Veränderung von Größe und Granularität der mit Etoposin B behandelten Zellen festgestellt werden [BAUMGART et al., 2015 (**Publikation 3**)]. Besonders eine erhöhte zelluläre Granularität deutet auf einen mitotischen Zellzyklusarrest hin, der durch einen Anstieg von intrazellulären Organellen sowie einer gesteigerten DNA-Menge begleitet wird [ZANET et

al., 2010]. Diese Ergebnisse zeigen, dass Etoposid B einen Zellzyklusarrest in den Tumorzellen hervorruft, der zur Entstehung einer mitotischen Katastrophe und somit zum Zelltod führen kann.

4.4.3 Expression von G2-Checkpointproteinen

Als abschließende Untersuchung der mitotischen Katastrophe wurden durchflusszytometrische Messungen von zwei fluoreszenzgefärbten G2-Checkpointproteinen durchgeführt. Die Proteine Cyclin B1 und Checkpoint Kinase 1 sind bedeutende Kontrollproteine beim G2-Checkpoint des Zellzyklus und dienen somit als Marker der mitotischen Katastrophe [WOLANIN et al., 2006; XIAO et al., 2005]. Durch unsere Messungen konnte ein Zelltypspezifischer Anstieg der Proteinexpression in den mit Etoposid B behandelten Zellen nachgewiesen werden, sowohl in den bestrahlten als auch in den nichtbestrahlten Proben. Bei den FaDu-Zellen war die Cyclin B1 Expression in den mit Etoposid B inkubierten Proben, besonders in der Kombination mit Bestrahlung, signifikant erhöht, wohingegen bei den A549-Zellen eine verminderte Cyclin B1 Expression festgestellt wurde. Die A549-Zellen zeigten eine gesteigerte Expression des Checkpoint Kinase 1 Proteins in den wirkstoffbehandelten bestrahlten und nichtbestrahlten Proben. Demgegenüber konnte bei den FaDu-Zellen kein veränderter Proteinlevel der Checkpoint Kinase 1 festgestellt werden [BAUMGART et al., 2015 (**Publikation 3**)]. Somit lässt sich zusammenfassen, dass die mitotische Katastrophe durch Etoposid B, alleine sowie in Kombination mit ionisierender Strahlung, ausgelöst wird, jedoch der zugrundeliegende Signalweg durch die unterschiedliche Expression der beiden G2-Checkpointproteine in den Zelllinien gekennzeichnet ist.

In der Literatur sind vergleichbare Ergebnisse mit anderen Untersuchungsmethoden zu finden. Beispielsweise wurde durch Western Blot Experimente mit dem synthetischen Etoposid-Derivat Sagoposid ebenfalls eine gesteigerte Cyclin B1 Expression in den A549-Zellen nachgewiesen [WINSEL et al., 2011]. Bekier und Kollegen untersuchten Aurora Kinasen als weitere Mediatoren des G2-Checkpoints. Durch die Hemmung der Kinasen in einer mit Etoposid B behandelten HeLa-Zelllinie und Auswertung mittels time-lapse Mikroskopie konnte demonstriert werden, dass ein durch Mikrotubuli-stabilisierende Substanzen herbeigeführter Zelltod mit einem verlängerten mitotischen Block einhergeht [BEKIER et al., 2009]. Die Expression von G2-Checkpointproteinen ist bei einem Zellzyklusarrest in der G2/M-Phase erhöht und kann somit, in Verbindung mit dem

Nachweis von polyploiden Zellen, als Zeichen einer mitotischen Katastrophe angesehen werden.

5 Abschließende Betrachtung

In der Behandlung von Tumorerkrankungen sind Tubulin-Filamente interessante Ziel-Moleküle, da sie während der Zellteilung eine wichtige Rolle spielen [PEREZ, 2009]. Eine Hemmung der dynamischen Instabilität der Mikrotubuli durch Chemotherapeutika führt zu einem veränderten Zellzyklusablauf, so dass Mikrotubuli-beeinflussende Substanzen zur möglichen Strahlensensibilisierung von Tumorzellen eingesetzt werden können [ROHRER BLEY et al., 2009].

In dieser Arbeit wurde die Wirkung von Etoposid B, allein und in Kombination mit ionisierender Strahlung, auf zwei Plattenepitheltumorzelllinien, die FaDu- und A549-Zellen, untersucht. Dabei konnte anhand verschiedener *in vitro* Experimente gezeigt werden, dass Etoposid B sowohl zytotoxische Eigenschaften aufweist als auch strahlensensibilisierend auf die untersuchten Tumorzelllinien wirkt. Der radiosensibilisierende Effekt von Etoposid B auf die Tumorzellen liegt hauptsächlich in dem herbeigeführten Zellzyklusarrest in der G2/M-Phase begründet [BAUMGART et al., 2012 (**Publikation 2**)], in der die Zellen besonders strahlenempfindlich reagieren. Ein zusätzlicher Grund der Strahlensensibilisierung von Etoposid B ist die verminderte DNA-Reparaturkapazität der Tumorzellen nach Wirkstoffgabe [BAUMGART et al., 2012 (**Publikation 1**); BAUMGART et al., 2015 (**Publikation 3**)].

Die Analyse ausgewählter Marker der Apoptose sowie Mediatoren der mitotischen Katastrophe zeigte, dass abhängig vom Zelltyp apoptotische Signalwege abliefen sowie ein Zellsterben über die mitotische Katastrophe durch Etoposid B eingeleitet wurde [BAUMGART et al., 2015 (**Publikation 3**)]. Neben der ebenfalls durch unsere Experimente nachgewiesenen Etoposid B-induzierten Nekrose als weiterer Zelltod in den epithelialen Tumorzellen [BAUMGART et al., 2012 (**Publikation 2**)], wurde durch Oehler und Kollegen eine durch Etoposid B hervorgerufene Autophagie als zusätzlicher Zelltod-Mechanismus beschrieben [OEHLER et al., 2011].

Für eine effektive Medikamenten-Bestrahlungsinteraktion wurden fünf spezielle Leitlinien eingeführt [STEEL & PECKHAM, 1979; BENTZEN et al., 2007]: die räumliche Kooperation, die Erhöhung der Zytotoxizität, die biologische Kooperation, die zeitliche Modulation und der Schutz des umliegenden normalen Gewebes. Die in dieser Arbeit dokumentierten Studien bestätigen für die Anwendung von Etoposid B in der simultanen Radiochemotherapie, die auf der *in vitro* Zytotoxizität basierenden Prinzipien; also die biologische

Kooperation, die Erhöhung der Zytotoxizität sowie die zeitliche Modulation der Anwendung. Durch verschiedene *in vivo* Studien anderer Forschergruppen konnten weitere Belege für eine geeignete Kombination von Epothilon B und Bestrahlung aufgeführt werden. Beispielweise führte die Anwendung von Epothilon B zu einer vaskulären Störung, wodurch ein vermindertes Blutvolumen im Tumor entstand [FERRETTI et al., 2005]. Desweiteren wurde eine durch Epothilon B reduzierte Metastasierungsfähigkeit von Tumorzellen beschrieben [FURMANOVA-HOLLENSTEIN et al., 2013]. Hierbei zeigte sich, dass Epothilon B der strahlungsbedingten erhöhten Sekretion von Matrix-Metalloproteinen entgegenwirkte und somit eine Zellinvasion hemmte.

Die Ergebnisse sind vielversprechend, jedoch sind weiterführende Experimente, wie Versuche an Tiermodellen nötig, um den klinischen Einsatz von Epothilon B in Kombination mit Bestrahlung bei der Behandlung von Plattenepithelkarzinomen zu ermöglichen.

6 Zusammenfassung

In der simultanen Radiochemotherapie von soliden Tumoren gilt die Anwendung von Mitosehemmstoffen wie den Taxanen bisher als Standardbehandlung. Allerdings wird der Einsatz der Taxane durch eine Vielzahl von Einschränkungen, wie die Bildung von Resistenzen begleitet. Die Suche nach alternativen Therapiemöglichkeiten führte zur Entdeckung der Epothilone, die eine taxan-ähnliche Wirkungsweise zeigen.

In dieser Dissertation wurde die Wirkung von Epothilon B, allein und kombiniert mit ionisierender Strahlung, auf die beiden Plattenepithelkarzinom-Zelllinien FaDu und A549 erforscht. Dabei wurden verschiedene Fragestellungen, im Hinblick auf den potentiellen Einsatz von Epothilon B in der simultanen Radiochemotherapie von solchen Plattenepithelkarzinomen, untersucht.

Es zeigte sich, dass Epothilon B bei beiden Zelllinien einen wachstumshemmenden Effekt auslöst. Die Mikrotubuli-stabilisierende Wirkung von Epothilon B konnte sowohl anhand einer Immunfluoreszenzfärbung der Mikrotubuli als auch durch einen Tubulin-Polymerisationsassay demonstriert werden. Zudem konnte eine konzentrationsabhängige Erniedrigung der metabolischen Aktivität durch Epothilon B mittels eines EZ4U-Proliferationsassays festgestellt werden.

Mit Hilfe der Koloniebildungstests wurde eine strahlensensibilisierende Wirkung von Epothilon B auf die FaDu- und die A549-Zellen nachgewiesen. Der radiosensibilisierende Effekt von Epothilon B auf die Tumorzellen basierte auf dem herbeigeführten Zellzyklusarrest in der strahlensensiblen G2/M-Phase sowie auf der verminderten Fähigkeit der Tumorzellen zur Reparatur von DNA-Schäden nach Epothilon B-Gabe.

Anhand verschiedener Untersuchungsmethoden, wie Western Blot und Durchflusszytometrie, konnte für beide Zelllinien der durch Epothilon B induzierte apoptotische Zelltod sowie der Zelltod während einer fehlerhaften Mitose, die sogenannte mitotische Katastrophe, als weiterer bedeutender Zelltod-Mechanismus nachgewiesen werden. Dabei zeigte sich durch molekulare Analysen, dass die eingeleiteten Zelltod-Signalwege durch die unterschiedliche Expression verschiedener Proteinmarker, beispielsweise p53 bei den A549-Zellen und PARP1 bei den FaDu-Zellen, Zelltyp-spezifisch abliefen.

Die Ergebnisse verdeutlichen, dass der Einsatz von Epothilon B als alleiniges Chemotherapeutikum sowie in der kombinierten Behandlung mit Bestrahlung ein

lohnendes Forschungsprojekt darstellt und zukünftig in der Therapie von Plattenepithelkarzinomen eingesetzt werden könnte.

Literaturverzeichnis

- Agrawal NR, Ganapathi R, Mekhail T. (2003) Tubulin interacting agents: novel taxanes and epothilones. *Curr Oncol Rep.* 5:89–98.
- Alberts B, Johnson A, Lewis J, Raff M, Roberts K, Walter P. (2004) *Molekularbiologie der Zelle.* 4. Auflage, WILEY-VCH Verlag GmbH & Co. KGaA, Weinheim.
- Allegra E, Trapasso S. (2012) Cancer stem cells in head and neck cancer. *Onco Targets Ther.* 5:375-383.
- Altmann KH, Wartmann M, O'Reilly T. (2000) Epothilones and related structures - a new class of microtubule inhibitors with potent in vivo antitumor activity. *Biochim Biophys Acta.* 1470(3):M79-91.
- Altmann KH, Pfeiffer B, Arseniyadis S, Pratt BA, Nicolaou KC. (2007) The chemistry and biology of epothilones - the wheel keeps turning. *Chem Med Chem.* 2(4):396-423.
- Argyriou AA, Marmioli P, Cavaletti G, Kalofonos HP. (2011) Epothilone-induced peripheral neuropathy: a review of current knowledge. *J Pain Symptom Manage.* 42:931–940.
- Baumgart T, Klautke G, Kriesen S, Kuznetsov SA, Weiss DG, Fietkau R, Hildebrandt G, Manda K. (2012) Radiosensitizing effect of epothilone B on human epithelial cancer cells. *Strahlenther Onkol.* 188(2):177-184.
- Baumgart T, Kriesen S, Hildebrandt G, Manda K. (2012) Effect of epothilone B on cell cycle, metabolic activity, and apoptosis induction on human epithelial cancer cells - under special attention of combined treatment with ionizing radiation. *Cancer Invest.* 30(8):593-603.
- Baumgart T, Kriesen S, Neels O, Hildebrandt G, Manda K. (2015) Investigation of Epothilone B-Induced Cell Death Mechanisms in Human Epithelial Cancer Cells -in Consideration of Combined Treatment With Ionizing Radiation. *Cancer Invest.* 33(6):213-224.
- Bekier ME, Fischbach R, Lee J, Taylor WR. (2009) Length of mitotic arrest induced by microtubule-stabilizing drugs determines cell death after mitotic exit. *Mol Cancer Ther.* 8(6):1646–1654.
- Bentzen SM, Harari PM, Bernier J. (2007) Exploitable mechanisms for combining drugs with radiation: concepts, achievements and future directions. *Nat Clin Pract Oncol.* 4(3):172–180.
- Blagosklonny MV, Darzynkiewicz Z, Halicka HD, Pozarowski P, Demidenko ZN, Barry JJ, Kamath KR, Herrmann RA. (2004) Paclitaxel induces primary and postmitotic G1 arrest in human arterial smooth muscle cells. *Cell Cycle.* 3:1050–1056.
- Bocci G, Nicolaou KC, Kerbel RS. (2002) Protracted low-dose effects on human endothelial cell proliferation and survival in vitro reveal a selective antiangiogenic window for various chemotherapeutic drugs. *Cancer Res.* 62:6938–6943.
- Bode CJ, Gupta ML Jr, Reiff EA, Suprenant KA, Georg GI, Himes RH. (2002) Epothilone and paclitaxel: unexpected differences in promoting the assembly and stabilization of yeast microtubules. *Biochemistry.* 41(12):3870-3874.

- Bollag DM, McQueney PA, Zhu J, Hensens O, Koupal L, Liesch J, Goetz M, Lazarides E, Woods CM. (1995) Epothilones, a new class of microtubule-stabilizing agents with a taxol-like mechanism of action. *Cancer Res.* 55(11):2325–2333.
- Bonnet D, Dick JE. (1997) Human acute myeloid leukemia is organized as a hierarchy that originates from a primitive hematopoietic cell. *Nat Med.* 3(7):730-737.
- Bröker LE, Huisman C, Ferreira CG, Rodriguez JA, Kruyt FA, Giaccone G. (2002) Late activation of apoptotic pathways plays a negligible role in mediating the cytotoxic effects of discodermolide and epothilone B in non-small cell lung cancer cells. *Cancer Res.* 62:4081–4088.
- Chalmers AJ, Ruff EM, Martindale C, Lovegrove N, Short SC. (2009) Cytotoxic effects of temozolomide and radiation are additive- and schedule-dependent. *Int J Radiat Oncol Biol Phys.* 75:1511–1519.
- Chen JG, Horwitz SB. (2002) Differential mitotic responses to microtubule-stabilizing and -destabilizing drugs. *Cancer Res.* 62:1935–1938.
- Chen JG, Yang CP, Cammer M, Horwitz SB. (2003) Gene expression and mitotic exit induced by microtubule-stabilizing drugs. *Cancer Res.* 63:7891–7899.
- Choe KS, Salama JK, Stenson KM, Blair EA, Witt ME, Cohen EE, Haraf DJ, Vokes EE. (2010) Adjuvant chemotherapy prior to postoperative concurrent chemoradiotherapy for locoregionally advanced head and neck cancer. *Radiation Oncol.* 97:318–321.
- Colombo N, Kutarska E, Dimopoulos M, Bae DS, Rzepka-Gorska I, Bidzinski M, Scambia G, Engelholm SA, Joly F, Weber D, El-Hashimy M, Li J, Souami F, Wing P, Engelholm S, Bamias A, Schwartz P. (2012) Randomized, open-label, phase III study comparing patupilone (EPO906) with pegylated liposomal doxorubicin in platinum-refractory or -resistant patients with recurrent epithelial ovarian, primary fallopian tube, or primary peritoneal cancer. *J Clin Oncol.* 30(31):3841-3847.
- Devi PU. (2004) Basics of carcinogenesis. *Health administrator.* 17(1), 16-24.
- Donehower RC, Rowinsky EK. (1993) An overview of experience with Taxol (paclitaxel) in the U.S.A. *Cancer Treat Rev.* 19(Suppl C):63–78.
- Downing KH, Nogales E. (1998) Tubulin and microtubule structure. *Curr Opin Cell Biol.* 10:16–22.
- Dunst J, Becker A, Fleig WE, Schmoll HJ. (1997) Simultane Radiochemotherapie. *Dt. Ärztebl.* 94:A-3277–3280 [Heft 48].
- Edelman MJ, Shvartsbeyn M. (2012) Epothilones in development for non-small-cell lung cancer: novel anti-tubulin agents with the potential to overcome taxane resistance. *Clin Lung Cancer.* 13(3):171-180.
- Eriksson D, Stigbrand T. (2010) Radiation-induced cell death mechanisms. *Tumour Biol.* 31(4):363-372.
- Fenech M. (2000) The in vitro micronucleus technique. *Mutat Res.* 455(1–2):81–95.
- Ferretti S, Allegrini PR, O'Reilly T, Schnell C, Stumm M, Wartmann M, Wood J, McSheehy PM. (2005) Patupilone induced vascular disruption in orthotopic rodent tumor models detected by magnetic resonance imaging and interstitial fluid pressure. *Clin Cancer Res.* 11(21):7773-7784.
- Fietkau R. (2012) Simultane Radiochemotherapie zur Behandlung solider Tumoren. *Strahlenther Onkol.* 188 Suppl 3:263-271.

- Flörsheimer A, Altmann KH. (2001) Epothilones and their analogues – a new class of promising microtubule inhibitors.
- Fogh S, Machtay M, Werner-Wasik M, Curran WJ Jr, Bonanni R, Axelrod R, Andrews D, Dicker AP. (2010) Phase I trial using patupilone (epothilone B) and concurrent radiotherapy for central nervous system malignancies. *Int J Radiat Oncol Biol Phys.* 77:1009–1016.
- Forli S. (2014) Epothilones: from discovery to clinical trials. *Curr Top Med Chem.* 14(20):2312-2321.
- Fumoleau P, Coudert B, Isambert N, Ferrant E. (2007) Novel tubulin-targeting agents: anticancer activity and pharmacologic profile of epothilones and related analogues. *Ann Oncol.* 18(Suppl):5:v9-15.
- Furmanova-Hollenstein P, Broggin-Tenzer A, Eggel M, Millard AL, Pruschy M. (2013) The micro tubule stabilizer patupilone counteracts ionizing radiation-induced matrix metalloproteinase activity and tumor cell invasion. *Radiat Oncol.* 8:105.
- Galluzzi L, Vitale I, Abrams JM, Alnemri ES, Baehrecke EH, Blagosklonny MV, Dawson TM, Dawson VL, El-Deiry WS, Fulda S, Gottlieb E, Green DR, Hengartner MO, Kepp O, Knight RA, Kumar S, Lipton SA, Lu X, Madeo F, Malorni W, Mehlen P, Nuñez G, Peter ME, Piacentini M, Rubinsztein DC, Shi Y, Simon HU, Vandenabeele P, White E, Yuan J, Zhivotovsky B, Melino G, Kroemer G. (2012) Molecular definitions of cell death subroutines: recommendations of the Nomenclature Committee on Cell Death 2012. *Cell Death Differ* 19(1):107–120.
- Galmarini CM, Dumontet C. (2003) EPO-906 (Novartis). *IDrugs.* 6(12):1182-1187.
- Gerth K, Bedorf N, Höfle G, Irschik H, Reichenbach H. (1996) Epothilons A and B: antifungal and cytotoxic compounds from *Sorangium cellulosum* (Myxobacteria). Production, physico-chemical and biological properties. *J Antibiot (Tokyo).* 49:560–563.
- Ha GH, Baek KH, Kim HS, Jeong SJ, Kim CM, McKeon F, Lee CW. (2007) p53 activation in response to mitotic spindle damage requires signaling via BubR1-mediated phosphorylation. *Cancer Res.* 67(15):7155–7164.
- Hanahan D, Weinberg RA. (2000) The hallmarks of cancer. *Cell.* 100(1):57-70.
- Hanahan D, Weinberg RA. (2011) Hallmarks of cancer: the next generation. *Cell.* 144(5):646-674.
- Hofstetter B, Vuong V, Broggin-Tenzer A, Bodis S, Ciernik IF, Fabbro D, Wartmann M, Folkers G, Pruschy M. (2005) Patupilone acts as radiosensitizing agent in multidrug-resistant cancer cells in vitro and in vivo. *Clin Cancer Res.* 11:1588–1596.
- Ianzini F, Kosmacek EA, Nelson ES, Napoli E, Erenpreisa J, Kalejs M, Mackey MA. (2009) Activation of meiosis-specific genes is associated with depolyploidization of human tumor cells following radiation-induced mitotic catastrophe. *Cancer Res.* 69:2296–2304.
- Khabele D, Lopez-Jones M, Yang W, Arango D, Gross SJ, Augenlicht LH, Goldberg GL. (2004) Tumor necrosis factor-alpha related gene response to epothilone B in ovarian cancer. *Gynecol Oncol.* 93:19–26.
- Khawaja NR, Carré M, Kovacic H, Estève MA, Braguer D. (2008) Patupilone-induced apoptosis is mediated by mitochondrial reactive oxygen species through Bim relocalization to mitochondria. *Mol Pharmacol.* 74(4):1072–1083.

- Kim JC, Kim JS, Saha D, Cao Q, Shyr Y, Choy H. (2003) Potential radiation-sensitizing effect of semisynthetic epothilone B in human lung cancer cells. *Radiother Oncol.* 68:305–313.
- Kingston DG. (2009) Tubulin-interactive natural products as anticancer agents. *J Nat Prod* 72:507–515.
- Kong Z, Raghavan P, Xie D, Boike T, Burma S, Chen D, Chakraborty A, Hsieh JT, Saha D. (2010) Epothilone B confers radiation dose enhancement in DAB2IP gene knock-down radioresistant prostate cancer cells. *Int J Radiat Oncol Biol Phys.* 78:1210–1218.
- Kowalski RJ, Giannakakou P, Hamel E. (1997) Activities of the microtubule-stabilizing agents epothilones A and B with purified tubulin and in cells resistant to paclitaxel (Taxol®). *J Biol Chem.* 272:2534–2541.
- Kriesen S. (2013) Wirkung von Celecoxib und Cetuximab auf die Strahlensensibilität der Tumorzelllinien A549 und FaDu *in vitro*. Inauguraldissertation, Universitätsmedizin Rostock.
- Larkin JMG. (2007) Patupilone. Antimitotic drug, microtubule-stabilizing agent, oncolytic. *Drugs Future.* 32:323–336.
- Lauber K, Ernst A, Orth M, Herrmann M, Belka C. (2012) Dying cell clearance and its impact on the outcome of tumor radiotherapy. *Front Oncol.* 11;2:116.
- Lee FY, Borzilleri R, Fairchild CR, Kim SH, Long BH, Reventos-Suarez C, Vite GD, Rose WC, Kramer RA. (2001) BMS-247550: a novel epothilone analog with a mode of action similar to paclitaxel but possessing superior antitumor efficacy. *Clin Cancer Res.* 7:1429–1437.
- Lee SH, Son SM, Son DJ, Kim SM, Kim TJ, Song S, Moon DC, Lee HW, Ryu JC, Yoon DY, Hong JT. (2007) Epothilones induce human colon cancer SW620 cell apoptosis via the tubulin polymerization independent activation of the nuclear factor-kappaB/IkappaB kinase signal pathway. *Mol Cancer Ther.* 6(10):2786–2797.
- Lichtner RB, Rotgeri A, Bunte T, Buchmann B, Hoffmann J, Schwede W, Skuballa W, Klar U. (2001) Subcellular distribution of epothilones in human tumor cells. *Proc Natl Acad Sci USA.* 98:11743–11748.
- Liebmann J, Cook JA, Fisher J, Feague D, Mitchell JB. (1994) In vitro studies of taxol as a radiation sensitizer in human tumor cells. *J Natl Cancer Inst.* 86:441–446.
- Lin B, Catley L, LeBlanc R, Mitsiades C, Burger R, Tai YT, Podar K, Wartmann M, Chauhan D, Griffin JD, Anderson KC. (2005) Patupilone (epothilone B) inhibits growth and survival of multiple myeloma cells *in vitro* and *in vivo*. *Blood.* 105:350–357.
- Manda K, Kriesen S, Hildebrandt G, Fietkau R, Klautke G. (2011) Omega-3 fatty acid supplementation in cancer therapy: does eicosapentanoic acid influence the radiosensitivity of tumor cells? *Strahlenther Onkol.* 187:127–134.
- Mansilla S, Llovera L, Portugal J. (2012) Chemotherapeutic targeting of cell death pathways. *Anticancer Agents Med Chem.* 12(3):226–238.
- May P, May E (1999) Twenty years of p53 research: structural and functional aspects of the p53 protein. *Oncogene.* 18(53):7621–7636.
- Melichar B, Casado E, Bridgewater J, Bennouna J, Campone M, Vitek P, Delord JP, Cerman J Jr, Salazar R, Dvorak J, Sguotti C, Urban P, Viraswami-Appanna K, Tan E, Tabernero J. (2011) Clinical activity of patupilone in patients with pretreated ad-

- vanced/metastatic colon cancer: results of a phase I dose escalation trial. *Br J Cancer*. 105(11):1646-1653.
- Nettles JH, Li H, Cornett B, Krahn JM, Snyder JP, Downing KH. (2004) The binding mode of epothilone A on alpha, beta-tubulin by electron crystallography. *Science*. 305:866–869.
- Niero A, Emiliani E, Monti G, Pironi F, Turci L, Valenti AM, Marangolo M. (1999) Paclitaxel and radiotherapy: sequence-dependent efficacy – a preclinical model. *Clin Cancer Res*. 5:2213–2222.
- Nur-E-Kamal A, Gross SR, Pan Z, Balklava Z, Ma J, Liu LF. (2004) Nuclear translocation of cytochrome c during apoptosis. *J Biol Chem*. 279(24):24911–24914.
- Oehler C, von Bueren AO, Furmanova P, Broggini-Tenzer A, Orłowski K, Rutkowski S, Frei K, Grotzer MA, Pruschy M. (2011) The microtubule stabilizer patupilone (epothilone B) is a potent radiosensitizer in medulloblastoma cells. *Neuro Oncol*. 13(9):1000-1010.
- Oehler C, Frei K, Rushing EJ, McSheehy PM, Weber D, Allegrini PR, Weniger D, Lütolf UM, Knuth A, Yonekawa Y, Barath K, Broggini-Tenzer A, Pruschy M, Hofer S. (2012) Patupilone (epothilone B) for recurrent glioblastoma: clinical outcome and translational analysis of a single-institution phase I/II trial. *Oncology*. 83(1):1-9.
- Oliveira PA, Colaço A, Chaves R, Guedes-Pinto H, De-La-Cruz P LF, Lopes C. (2007) Chemical carcinogenesis. *An Acad Bras Cienc*. 79(4):593-616.
- Oliver FJ, de la Rubia G, Rolli V, Ruiz-Ruiz MC, de Murcia G, Murcia JM. (1998) Importance of poly(ADPribose) polymerase and its cleavage in apoptosis. Lesson from an uncleavable mutant. *J Biol Chem*. 273:33533–33539.
- Pawlik TM, Keyomarsi K. (2004) Role of cell cycle in mediating sensitivity to radiotherapy. *Int J Radiat Oncol Biol Phys*. 59(4):928-942.
- Pellicciotta I, Yang CP, Venditti CA, Goldberg GL, Shahabi S. (2013) Response to microtubule-interacting agents in primary epithelial ovarian cancer cells. *Cancer Cell Int*. 10;13(1):33.
- Pendergrass W, Wolf N, Poot M. (2004) Efficacy of MitoTracker Green and CMXRosamine to measure changes in mitochondrial membrane potentials in living cells and tissues. *Cytometry A*. 61(2):162–169.
- Perez EA. (2009) Microtubule inhibitors: differentiating tubulin inhibiting agents based on mechanisms of action, clinical activity, and resistance. *Mol Cancer Ther*. 8:2086–2095.
- Petersen C, Dikomey E. (2011) Strahlenresistenzforschung. In „Forum“. Springer Verlag, Berlin.
- Piccart M. (2003) The role of taxanes in the adjuvant treatment of early stage breast cancer. *Breast Cancer Res Treat*. 79(Suppl 1):S25–S34.
- Pötter R, D. Georg, L. Handl-Zeller, A. Kranz, E. Selzer (2012) Strahlentherapie. In „Die Onkologie“. Springer Verlag, Berlin.
- Portugal J, Bataller M, Mansilla S. (2009) Cell death pathways in response to antitumor therapy. *Tumori*. 95:409–421.
- Redon CE, Dickey JS, Bonner WM, Sedelnikova OA. (2009) γ -H2AX as a biomarker of DNA damage induced by ionizing radiation in human peripheral blood lymphocytes and artificial skin. *Adv Space Res*. 43(8):1171-1178.

- Reiss M, Brash DE, Muñoz-Antonia T, Simon JA, Ziegler A, Vellucci VF, Zhou ZL. (1992) Status of the p53 tumor suppressor gene in human squamous carcinoma cell lines. *Oncology Res.* 4:349–357.
- Rello-Varona S, Stockert JC, Canete M, Acedo P, Villanueva A. (2008) Mitotic catastrophe induced in HeLa cells by photodynamic treatment with Zn(II)-phthalocyanine. *Int J Oncol.* 32:1189–1196.
- Ricci MS, Zong WX. (2006) Chemotherapeutic approaches for targeting cell death pathways. *Oncologist.* 11(4):342–357.
- Rogalska A, Gajek A, Marczak A. (2014) Etoposide B induces extrinsic pathway of apoptosis in human SKOV-3 ovarian cancer cells. *Toxicol In Vitro.* 28(4):675–683.
- Rohrer Bley C, Jochum W, Orłowski K, Furmanova P, Vuong V, McSheehy PM, Pruschy M. (2009) Role of the microenvironment for radiosensitization by paclitaxel. *Clin Cancer Res.* 15(4):1335-1342.
- Rohrer Bley C, Furmanova P, Orłowski K, Grosse N, Broggini-Tenzer A, McSheehy PM, Pruschy M. (2013) Microtubule stabilising agents and ionising radiation: multiple exploitable mechanisms for combined treatment. *Eur J Cancer.* 49(1):245-253.
- Rothermel J, Wartmann M, Chen T, Hohnaker J. (2003) EPO906 (etoposide B): a promising novel microtubule stabilizer. *Semin Oncol.* 30(Suppl 6):51–55.
- Sauer R. (2010) *Strahlentherapie-Radiotherapie-Radioonkologie in Strahlentherapie und Onkologie.* Elsevier, Urban & Fischer Verlag, München.
- Schiff PB, Fant J, Horwitz SB. (1979) Promotion of microtubule assembly *in vitro* by taxol. *Nature.* 277(5698):665-667.
- Schiff PB, Horwitz SB. (1980) Taxol stabilizes microtubules in mouse fibroblast cells. *Proc Natl Acad Sci USA.* 77(3): 1561-1565.
- Schulte-Hermann R, Parzefall W. (2010) Mehrstufenprozess der Kanzerogenese und chemische Kanzerogenese. In „Die Onkologie“. Springer Verlag, Berlin.
- Sepp-Lorenzino L, Balog A, Su DS, Meng D, Timaul N, Scher HI, Danishefsky SJ, Rosen N. (1999) The microtubule-stabilizing agents etoposides A and B and their desoxyderivates induce mitotic arrest and apoptosis in human prostate cancer cells. *Prostate Cancer Prostatic Dis* 2:41–52.
- Stalder MW, Anthony CT, Woltering EA (2011) Metronomic dosing enhances the anti-angiogenic effect of etoposide B. *J Surg Res.* 169:247–256.
- Steel GG, Peckham MJ. (1979) Exploitable mechanisms in combined radiotherapy-chemotherapy: The concept of additivity. *Int J Radiat Oncol Biol Phys.* 5(1):85–91.
- Swanton C, Nicke B, Schuett M, Eklund AC, Ng C, Li Q, Hardcastle T, Lee A, Roy R, East P, Kschischo M, Endesfelder D, Wylie P, Kim SN, Chen JG, Howell M, Ried T, Habermann JK, Auer G, Brenton JD, Szallasi Z, Downward J. (2009) Chromosomal instability determines taxane response. *Proc Natl Acad Sci USA.* 106(21):8671–8676.
- Tishler RB, Busse PM, Norris CM Jr, Rossi R, Poulin M, Thornhill L, Costello R, Peters ES, Colevas AD, Posner MR. (1999) An initial experience using concurrent paclitaxel and radiation in the treatment of head and neck malignancies. *Int J Radiat Oncol Biol Phys.* 43(5) 1001-1008.
- Torre LA, Bray F, Siegel RL, Ferlay J, Lortet-Tieulent J, Jemal A. (2015) Global cancer statistics, 2012. *CA Cancer J Clin.* 65(2):87-108.

- Twentyman PR. (2012) Experimental chemotherapy studies: intercomparison of assays. *Br J Cancer Suppl.* 4:279-287.
- Wani MC, Taylor HL, Wall ME, Coggon P, McPhail AT. (1971) Plant antitumor agents. VI. The isolation and structure of taxol, a novel antileukemic and antitumor agent from *Taxus brevifolia*. *J Am Chem Soc.* 93(9):2325-2327.
- Wartmann M, Altmann KH. (2002) The biology and medicinal chemistry of epothilones. *Curr Med Chem - Anticancer Agents.* 2(1): 123-148.
- Weller M. (1989) Predicting response to cancer chemotherapy: the role of p53. *Cell Tissue Res.* 292(3):435-445.
- Wessjohann L. (1997). Epothilones: Promising Natural Products with Taxol-Like Activity. *Angew Chem Int Ed Engl.* 36(7):715-718.
- Wilson GD, Bentzen SM, Harari PM. (2006) Biologic basis for combining drugs with radiation. *Semin Radiat Oncol.* 16(1):2-9.
- Winsel S, Sommer A, Eschenbrenner J, Mittelstaedt K, Klar U, Hammer S, Hoffmann J. (2011) Molecular mode of action and role of TP53 in the sensitivity to the novel epothilone sagopilone (ZK-EPO) in A549 non-small cell lung cancer cells. *PLoS One.* 6(4):e19273.
- Wolanin K, Magalska A, Mosieniak G, Klinger R, McKenna S, Vejda S, Sikora E, Piwocka K. (2006) Curcumin affects components of the chromosomal passenger complex and induces mitotic catastrophe in apoptosis-resistant Bcr-Abl-Expressing cells. *Mol Cancer Res.* 4(7):457-469.
- Xiao Z, Xue J, Semizarov D, Sowin TJ, Rosenberg SH, Zhang H. (2005) Novel indication for cancer therapy: Chk1 inhibition sensitizes tumor cells to antimetotics. *Int J Cancer.* 115(4):528-538.
- Yu D, Pessino V, Kuei S, Valentine MT. (2013) Mechanical and functional properties of epothilone-stabilized microtubules. *Cytoskeleton (Hoboken).* 70(2):74-84.
- Zanet J, Freije A, Ruiz M, Coulon V, Sanz JR, Chiesa J, Gandarillas A. (2010) A mitosis block links active cell cycle with human epidermal differentiation and results in endoreplication. *PLoS One.* 5(12):e15701.

Publikationen und Kongressbeiträge

Publikationen

Baumgart T, Kriesen S, Neels O, Hildebrandt G, Manda K. (2015) Investigation of Etoposide B-Induced Cell Death Mechanisms in Human Epithelial Cancer Cells -in Consideration of Combined Treatment With Ionizing Radiation. *Cancer Invest.* 33(6):213-224. IF: 2,218.

Baumgart T, Kriesen S, Hildebrandt G, Manda K. (2012) Effect of etoposide B on cell cycle, metabolic activity, and apoptosis induction on human epithelial cancer cells - under special attention of combined treatment with ionizing radiation. *Cancer Invest.* 30(8):593-603. IF: 1,85.

Baumgart T, Klautke G, Kriesen S, Kuznetsov SA, Weiss DG, Fietkau R, Hildebrandt G, Manda K. (2012) Radiosensitizing effect of etoposide B on human epithelial cancer cells. *Strahlenther Onkol.* 188(2):177-184. IF: 3,56.

Kongressbeiträge

Manda K, Baumgart T, Hildebrandt G. Etoposide B influences cell cycle and metabolic activity and induces apoptosis in human epithelial cancer cells - in consideration of combined treatment with ionising radiation. *Strahlenther Onkol* 2013; 189: Suppl. 1, 134-135. 19th Annual Conference of the Deutschen-Gesellschaft-für-Radioonkologie (DEGRO) Berlin, Germany, 09.-12. Mai 2013; Typ: Poster Präsentation.

Baumgart T, Hildebrandt G, Manda K. Untersuchungen zur Wirkungsweise von Etoposide B in Kombination mit ionisierender Strahlung - Einfluss auf Zellzyklus, metabolische Aktivität, Apoptose-Induktion und Kernmorphologie. 22. Symposium Experimentelle Strahlentherapie und klinische Strahlenbiologie 21.-23. Februar 2013, Dresden, Deutschland, Typ: Poster Präsentation.

Baumgart T, Hildebrandt G, Manda K. Effect of radiation and etoposide B on human epithelial cancer cells. 1. Forschungscamp der Universität Rostock, 20. Juni 2012 Rostock, Deutschland, Typ: Poster Präsentation.

Baumgart T, Kriesen S, Hildebrandt G, Manda K. Einfluss von Strahlenexposition und Etoposide B auf humane Tumorzellen. 20. Symposium Experimentelle Strahlentherapie und Klinische Strahlenbiologie 10.-12. Februar 2011 Dresden, Deutschland, Typ: Oral Präsentation.

Manda K, Baumgart T, Weiss DG, Fietkau R, Klautke G. Does Etoposide B remove Paclitaxel in the radio-oncology? *Strahlenther Onkol* 2009; 185: 145-146, Suppl. 1; 15th

Annual Conference of the Deutschen-Gesellschaft-für-Radioonkologie (DEGRO) Bremen, Deutschland, 11.-14. Juni 2009; Typ: Oral Präsentation.

Baumgart T, Manda K, Klautke G. Einfluss von Epthilon B und Bestrahlung auf humane Tumorzellen. 11. Jahrestagung der Gesellschaft für Biologische Strahlenforschung Tübingen, Deutschland, 6.-8. Oktober 2008; Typ: Poster Präsentation.

Danksagung

An dieser Stelle möchte ich mich bei allen bedanken, die zur Entstehung dieser Dissertation beigetragen haben.

- Bei Frau Dr. Katrin Manda für die freundliche und intensive Betreuung während der Dissertation und die vielen hilfreichen Anregungen.
- Bei Herrn Prof. Dr. Guido Hildebrandt für das Ermöglichen dieser Arbeit und der guten interdisziplinären Zusammenarbeit.
- Bei Herrn Dr. Sergei Kuznetsov und Dr. Oliver Neels sowie deren Arbeitsgruppen für die produktive Zusammenarbeit bei den Veröffentlichungen.
- Bei Herrn Stephan Kriesen und seinen Kollegen für die Bestrahlung der Zellen, die guten Ratschläge sowie das Korrekturlesen der Manuskripte.
- Bei den Mitarbeitern des Strahlenbiologischen Labors für die gute Zusammenarbeit.
- Besonderer Dank gebührt meiner Familie für die stetige Unterstützung und den Rückhalt.